Ph.D. in Electronic and Computer Engineering
Dept. of Electrical and Electronic Engineering
University of Cagliari

Algorithms and Systems for Home Telemonitoring in Biomedical Applications

Alessia Dessì

Advisor: Eng. Danilo Pani, Ph.D.
PhD Coordinator: Prof. Fabio Roli, Ph.D.
Curriculum: ING-INF/06 Bioingegneria elettronica e informatica

XXVII Cycle
February 2015

Ph.D. in Electronic and Computer Engineering
Dept. of Electrical and Electronic Engineering
University of Cagliari

Algorithms and Systems for Home Telemonitoring in Biomedical Applications

Alessia Dessì

Advisor: Eng. Danilo Pani, Ph.D.
PhD Coordinator: Prof. Fabio Roli, Ph.D.
Curriculum: ING-INF/06 Bioingegneria elettronica e informatica

XXVII Cycle
February 2015

Dedicato ai miei nonni

Acknowledgements

I would like to express my deepest gratitude to my advisor, Danilo Pani, for guiding my research, for his patience, motivation and caring. I wish to thank my colleague, Gianluca Barabino, for his strong contribution to the development of the telerehabilitation device presented in the second part of this thesis, but especially for his friendship.

I would also like to thank Prof. Annalisa Bonfiglio and Eng. Jose Saenz-Cogollo, for giving me the opportunity to work in the research field of textile electrodes.

I want to thank Prof. Alessandro Mathieu and Dr. Matteo Piga for their collaboration to the development of the telerehabilitation system and for taking care of the experimental clinical trial. Moreover, I would like to thank Dr. Roberto Tumbarello and all the staff of the Pediatric Cardiology Unit of the Sardinian Hospital G. Brotzu in Cagliari, for their support in the acquisition of the fetal electrocardiographic signals.

I gratefully acknowledge Sardinia Regional Government for the financial support of mine PhD scholarship (P.O.R. Sardegna F.S.E. Operational Programme of the Autonomous Region of Sardinia, European Social Fund 2007-2013 - Axis IV Human Resources, Objective l.3, Line of Activity l.3.1).

Contents

List of Figures

List of Tables

Introduction

The improvement of the population health condition requires to increase screening and monitoring procedures, but the National Health Systems cannot afford the related growth of the public health costs, limiting the diagnostic and maintenance controls to the bare essentials. Patients can take advantage of a closer medical assistance exploiting telemonitoring, which involves remotely monitoring their conditions when they are not at the same location as the health care provider. Home-based assistance allows both cost reduction and patient comfort improvement, also enabling long-term monitoring controls which would be infeasible in hospitals, thus improving the quality of the therapy. Nevertheless, the exploitation of this technology requires strong effort in terms of research in both the acquisition and algorithmic sides, because of the measurement environment and setup which are completely unsupervised. Many clinical studies in different applications demonstrated the positive effect of home telemonitoring on clinical outcomes, for example in patients with chronic heart failure [1].

In this work the telemonitoring approach is investigated in two different bioengineering applications: non-invasive fetal electrocardiography (FECG) and hand rehabilitation for rheu-matic patients (telerehabilitation).

Non-invasive FECG is based on the recording of the fetal heart electrical activity during pregnancy using surface skin electrodes placed on the maternal abdomen. The fetal heart can be externally monitored by ultrasound techniques from the seventh/ninth week of gestation, but the cardiac waveforms and beat-to-beat variability of the heart rate are not measurable by ultrasound imaging. Also, ultrasound techniques are not suitable for long term monitoring application, requiring skilled professionals and being potentially dangerous for fetal health. Nevertheless, these techniques are the most common approach in fetal surveillance. FECG can be invasively acquired by using a scalp electrode during delivery [2]. Obviously, this approach cannot be performed in early pregnancy for diagnostic purposes and is seldom used in clinical practice during labour because of the risk of infection. Non-invasive FECG can provide Fetal Heart Rate (FHR) and ECG morphological information, being potentially able to detect fetal arrhythmias in early pregnancy. A variety of FHR patterns have also been related to placenta abruption. However this technique is still considered inadequate for congenital cardiac defect diagnosis. The lack in reliability of the obtained FECG recordings is both due to the signal acquisition, with the signal contaminated by many other electrical sources (e.g., maternal ECG, electromyographic interferences), and to the signal processing techniques, which are still inadequate for these weak sources and can compromise signal morphology [3]. Also, signal detection is strongly affected by the influence of the *vernix caseosa*, a dielectric protective film surrounding the fetus with thickness and homo-

geneity dependent on the gestational age [4].

Beyond the diagnostic importance provided by the electrical trace of the fetal heart activity, the absence of any side-effects and the remarkable patient comfort during the acquisition, make this technique suitable for long-term monitoring. Prolonged home telemonitoring requires a deep investigation to improve both the signal acquisition setup and processing techniques, which should be able to work with different acquisition setup (e.g., the electrodes positioning can be inaccurate and the number of recordings can be reduced to guarantee patients' comfort). The aim of the first part of this work is the investigation of both these aspects, which need to be studied before designing the whole monitoring system. Two processing algorithms are presented for the extraction of the FECG from maternal abdomen recordings together with the evaluation of different acquisition setup which can help in improving the quality of the acquired signals.

The second telemonitoring application regards the design of a hand rehabilitation system for rheumatic patients. Motor functional deficits are usually treated through long-term rehabilitation [5]. Due to the high-cost requirements, after an acute rehabilitation needing in-person interactions, patients are asked to perform some adapted physical exercises at their home. Here, the poor compliance and the lack of a monitoring strategy enabling supervision on the exercises execution, lead to progressive drop-outs with negative consequences on the functional recovery. Telerehabilitation permits to deliver rehabilitation services over distance, allowing the therapists to assess the compliance of the patients to the rehabilitation protocol and to correct their wrong behaviours in the exercise execution. The greatest part of the works in the field deals with post-stroke rehabilitations [6, 7].

The second part of this thesis describes the development of a low-cost portable system for hand telerehabilitation of rheumatic patients at their home, in particular for Rheumatoid Arthritis (RA) and Systemic Sclerosis (SSc) diseases. RA is a systemic chronic inflammatory disease primarily affecting synovial joints, causing joint and tendon restrictions and adhesions due to fibrosis. SSc is an autoimmune disease that targets the vascular tissues ultimately leading to fibrosis in the skin, the musculoskeletal system and internal organs. These diseases are particularly invalidating, especially when they compromise hand functionality, limiting patients daily life activities. In this work the conception of a device for the execution and objective monitoring of therapeutic active exercises adapted to the patient's specific needs and the design of the telemedicine infrastructure to give the physicians the opportunity of monitoring patients' progresses and their compliance to the prescribed rehabilitation protocol are presented. The system, patent pending in the United States, underwent a clinical trial,approved by the Italian Public Health Department, in the University Hospital of Cagliari involving 40 rheumatic patients enrolled for 12 weeks in a home rehabilitation program with the proposed device. Subjective (hand algofunctional Dreiser's index) and objective (ROM, strength, dexterity) indexes have been used for patients evaluation. Also, the usability of the telemonitoring system has been evaluated by medical personnel not involved in the study using questionnaires and interviews.

With respect to the hand telerehabilitation system development, which involves the monitoring of the exercises execution through a set of sensorized tools, the research in the field of non-invasive FECG required a deeper investigation from the signal processing point of view. In fact, the conception of a home-monitoring device needs a reliable extraction algorithm to guarantee the clinical usability of the acquired data, that is the most critical aspect

in non-invasive FECG, especially in an unsupervised scenario.

Thesis structure

This thesis is structured in two main sections, the first one related to fetal electrocardiography (FECG), the latter to hand rehabilitation of rheumatic patients.

In the first chapter, the motivations for non-invasive fetal electrocardiography are reported. The diagnostic tests currently used in clinical practice during pregnancy and the birth are described, highlighting their advantages and limitations. Then, the main obstacles to the introduction of non-invasive FECG are explained, together with the description of first clinical studies which emphasized its potential benefits.

In the second chapter, two algorithms for the analysis of non-invasive FECG are presented, both of them tested on real and synthetic dataset. The first one is a real-time post-processing stage of on-line blind source separation algorithms, that allows the automatic identification of the fetal sources permutations, of the fetal heart rate and of an average fetal QRS complex on which the evaluation of the characteristic electrical intervals can be performed. It could be useful for providing the instantaneous fetal heart rate when monitoring is performed with a high number of electrodes. The latter is a signal processing algorithm for the extraction of the fetal heart rate from a reduced number of signals recorded from the maternal abdomen, that would be advantageous for long-term monitoring applications, both during pregnancy or the labour.

In the third chapter, the main problems related to the non-invasive acquisition of abdominal recordings are investigated. This chapter includes both the evaluation of commercial disposable electrodes with different skin treatments and the evaluation of innovative textile electrodes which could be exploited for the design of a sensorized abdominal band for the acquisition of the surface potentials. Also, a prototypical system for the acquisition of these signals exploiting different configuration setup is described.

The second part, as already said, presents the design and clinical evaluation of a telerehabilitation system. Then, in the fourth chapter, the motivations for the development of such a kinesiotheraphy device for active rehabilitation of rheumatic patients and the state of the art in the field of telerehabilitation are presented.

The fifth chapter describes the design and conception of a hand telerehabilitation device, developed taking into account the specific needs of rheumatic patients, and of the external telemonitoring infrastructure, which allows the physicians to monitor patients progress during the rehabilitation sessions and promotes the collaboration among different specialized figures involved in the rehabilitation program and int he patient's follow up.

The last chapter reports the results of a clinical trial involving rheumatic patients. In order to evaluate the whole telerehabilitation system both objective (measurement of the performance) and subjective (tests, interviews) measures are presented, taking into account both the patient and the physician opinions.

Then the conclusions are reported, highlighting the obtained advances in FECG and hand telerehabilitation monitoring and showing the current direction of the research in both these fields.

Part I

FECG SIGNAL ACQUISITION AND PROCESSING

Chapter 1

Motivations for Fetal Electrocardiography

Fetal Heart Monitoring can provide significant information about the fetal condition during pregnancy and labour, allowing the evaluation of fetal development and the existence of fetal distress or congenital heart disease. Fetal heart rate (FHR) is considered an indicator of a correctly functioning nervous system and its monitoring is currently recommended as a routine physiological measurement, particularly for high-risk pregnancies [8]. Despite the technological advancement, Fetal Heart Monitoring is still an open research issue.

The fetal heart begins beating by the third week of life and pumps its own blood through a separate closed circulatory system. Fetal heart rate is around 120/160 beats per minute (BPM) at 20 weeks of gestation. Although fetal circulatory system is different from that of the infant, their electrical activity is believed to be really similar.

Currently, many diagnostic tests are carried out in the hospitals to recognize fetal distress during the birth or to identify cardiac diseases and congenital malformations during pregnancy. These tests are mainly based on ultrasound devices and allow the estimation of the fetal heart contractile activity from a mechanical perspective, but they can not provide a fetal electrocardiographic (FECG) signal which would be useful for the identification of many cardiac diseases. Also, the quality of ecographic tests is strongly affected by the ability of the examiner, often providing non objective results.

Diagnostic electrocardiography (ECG) is a consolidated clinical practice in adults and children. The widely used 12-lead configuration allows discovering pathological conditions even before structural changes in the heart can be diagnosed by other methods [9]. From a clinical perspective, there are recognized differences in the ECG waveforms between adults and children due to the progressive changes in anatomy and physiology occurring between birth and adolescence [10]. Such changes descend from the evolution of the fetal circulation mechanisms and stabilize during the childhood [11]. An example of adult ECG morphology is shown in Figure 1.1, in which it is possible to recognize the P-wave (atrial depolarization or contraction), the QRS complex (ventricular depolarization or contraction) and the T-wave (ventricular repolarization or relaxation), whereas the atrial repolarization is hidden by the ventricular depolarization. With respect to adults, in fetal and neonatal ECG the T-waves are really weak.

The only way to directly acquire the FECG is by using an invasive electrode which can

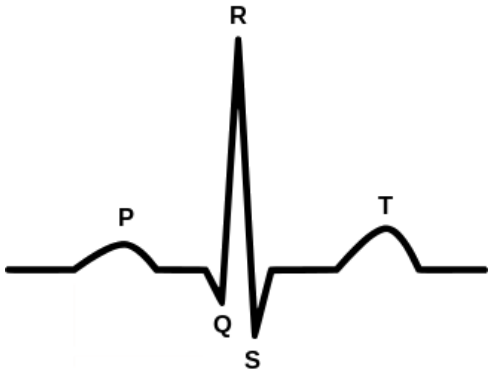

Figure 1.1: Typical adult ECG morphology. In fetal and neonatal ECG the T-wave is rather weak.

be placed on the fetal scalp during birth. The invasive nature of this exam limited its introduction in the clinical practice. Also, it can not be used for diagnostic purposes during pregnancy. Many studies in the field investigate the possibility of obtaining the FECG with non invasive procedures, i.e., by placing a number of electrodes on the skin of the maternal abdomen. This approach is strongly limited by the intrinsic difficulty in acquiring and processing weak fetal signals which are hidden by many interference sources, particularly the maternal ECG signal. The research in this field is currently directed towards the improvement of both acquisition and signal processing techniques for non-invasive FECG, which need to be deeply investigated before a monitoring system could be developed.

In the following sections the main fetal heart monitoring systems in clinical practice are described, deepening the systems and signal processing techniques which are currently used for non-invasive FECG.

1.1 Fetal Heart Monitoring in Clinical Practice

The fetal heart can be externally monitored by ultrasound imaging from the seventh/ninth week of gestation, but the cardiac waveform that is altered by most of the cardiac defects and the beat-to-beat variability of the heart rate are not measurable by ultrasound imaging [3]. Nevertheless, ecocardiography is considered the gold standard for the identification of congenital heart diseases during pregnancy (which are the leading cause of birth defect-related deaths), whereas cardiotocography (CTG) represents the most common approach in fetal surveillance during labour. Alternative approaches for fetal heart monitoring are phonocardiography, based on the registration of the heart sounds and murmurus, pulse oximetry, that can be used only after the rupture of the membranes and allows the estimation of oxygen in the blood of the fetus, and fetal magnetocardiography (FMCG), that is is based on the registration of the cardiac magnetic fields. These antepartum and intrapartum diagnostic tests are described below.

1.1.1 Intrapartum fetal heart rate monitoring

Fetal heart monitoring techniques developed as intrapartum tests in order to reduce the mortality rate during birth. Intrapartum fetal asphyxia is an important cause of stillbirth and neonatal death, and has also been implicated as a cause of cerebral palsy. The first intrapartum monitoring system, called the Pinard horn, a type of stethoscope for the auscultation of the valves closure during heart beats, was introduced during the 19th century to detect fetal heart rate (FHR).

Electronic fetal monitoring (EFM) developed in the 1960's with the commercialization of the first ultrasound monitoring device based on Doppler effect for the identification of the FHR and of the maternal uterine contractios, called cardiotocograph (CTG) [12, 13]. Despite it can be in principle used from the 24th week of gestation, in clinical practice it is exploited in the last weeks of gestation only (from the 35th week) at the hospitals. CTG system includes an ultrasound sensor which measures the frequency shift of sound waves from the heart moving chambers producing the FHR trace, and a pressure sensor (toco) that records the maternal uterine contractions. Cardiotocography represents the most widely used intrapartum monitoring system. From the FHR trace the following features are analysed to evaluate fetal distress: baseline rate, variability, periodic changes and dysrhythmias. In normal conditions the baseline rate ranges from 120 to 160 beats per minute (bpm). HR variability reflects neurological modulation and is classified as short-term variability (beat-to-beat irregularity) and long term variability (variations occurring 3-5 times per minute). Abnormal decelerations in fetal heart rate and decreased beat-to-beat variability during uterine contractions are considered to be suggestive of fetal distress. Nevertheless, some controlled trials have demonstrated critical aspects of CTG systems because of the difficulty in interpreting its results (a significant intra- and interobserver variation in assessing cardiotocograms has been reported). Most fetuses tolerate intrauterine hypoxia during labour and are delivered without complications, but assessments suggesting fetal distress are associated with an increased likelihood of cesarean delivery. In addition, normal heart rate patterns do not exclude the diagnosis of fetal distress. In the study presented in [14], 12 randomized, controlled trials with more than 37,000 women, randomly assigned to either receive continuous EFM or intermittent auscultation, have been analysed. The results show that compared to intermittent auscultation, continuous CTG is associated with a reduction in neonatal seizures, but no significant differences in cerebral palsy, infant mortality or other standard measures of neonatal well-being were reported. However, continuous CTG was associated with an increase in caesarean sections and instrumental vaginal births. Moreover, despite frequent FHR monitoring is recommend especially in risky pregnancies, it has not been proven that long term expositions to ultrasound irradiation are absolutely safe for the foetus [15, 16]. For this reason the prolonged use of Doppler fetal heartbeat monitor should be avoided. Its use for home monitoring is also prevented by the difficulty in the positioning procedure of the directional ultrasound beam towards a small target (the fetal heart), requiring continuous repositioning for long periods applications.

The only clinically accepted way to access the FECG is by using a scalp electrode during labour as in the $STAN^{TM}$ (www.neoventa.com) monitor [2] from Neoventa Medical (Figure 1.2), thus enabling the FECG waveform analysis [17]. FECG morphology, particularly the ratio between the amplitude of the fetal T and R waves and the presence or absence of a biphasic ST segment, allows to evaluate hypoxia and other fetal distress affections, suggesting an instrumental obstetric intervention [18]. This approach is seldom used in clinical practice

Figure 1.2: The Stan S31^{TM} CTG monitor and the Goldtrace^{TM} scalp electrode for ST analysis by Neoventa Medical AB.

because it presents a risk for fetal safety. Also it provides only one projection of the fetal heart electrical activity, which could be insufficient for a morphological evaluation. In [19] the Swedish randomized controlled trial showed the reduction of both the rates of operative deliveries for fetal distress and of metabolic acidosis at birth when the intrapartum monitoring is performed with CTG combined with ST analysis of invasive FECG, with respect to the use of CTG alone. This reduction highlights the possibility of improvement in intrapartum fetal surveillance.

Other approaches have been developed to improve the evaluation of the fetal distress during birth, such as the fetal scalp blood sampling (FBS) or the pulse oximetry, to estimate the level of oxygen in the blood of the fetus. Both these methods can be used only after the rupture of the membranes and represent invasive procedures associated with occasional complications.

1.1.2 Antepartum fetal heart monitoring

Apart from the FHR, the atrial contraction rate, the duration of the PR-interval, QRS-complex, and QT-interval represent important parameters for the diagnosis of many fetal cardiac diseases. Fetal arrhythmias have an incidence of $0.2-1.3\%$ and extrasystoles (supraventricular, ventricular, blocked or missed beats) are the most common cause of fetal arrhythmia. Their identification in the early phase of pregnancy would allow their treatment by transplacentar drugs administration or the scheduling of the delivery through caesarean section. While for paediatric and adult patients the classification of arrhythmias is based on the analysis of the ECG, for fetus is currently based on ultrasound evaluation of cardiac anatomy and M-mode analysis of atrial and ventricular contraction patterns [20]. A variety of fetal heart rate patterns have also been described in association with placenta abruption.

Ultrasound M-mode analysis allows the visualization of the heart movement versus time (in fact, M stands for Motion), thus allowing an indirect estimation of the cardiac time inter-

vals. In M modulation, the brightness is controlled by the amplitude of the echoes, the vertical position shows the depth of echo-producing interfaces and the horizontal axis the time. So, the obtained signal is proportional to the motion of the interfaces towards and away from the transducer. For example, atrial contraction is recognizable by the movement of the atrial wall towards the atrial septum, whereas the ventricular contraction can be recognized by the opening of an arterial valve or the start of the ventricular wall movement towards the ventricular septum. M-mode analysis can provide an estimation of the PR intervals and represents the gold standard in clinical practice for the assessment of fetal arrhythmias. However this diagnostic test is costly, time-consuming, requires highly-skilled operators [21] and is not able to directly provide the electrophysiological information [20].

Non-invasive fetal electrocardiography (FECG), based on the acquisition of the electrical signals from the maternal abdomen using surface electrodes, has the potential to provide both the FHR data with beat-to-beat accuracy and the cardiac waveforms containing diagnostic information. FECG can provide long-term monitoring in both clinic and domiciliary settings. However, the quality of the measurement can not be guaranteed during all the pregnancy. Further details on this technique are presented in Section 1.2.

Fetal magnetocardiogram (MCG) is the recording of the magnetic fields generated by the current flowing within the fetal heart. These fields are extremely weak (10^{-12} tesla), so highly sensitive sensors, called SQUID (Superconductive Quantum Interference Device) need to be used. FMCG can be recorded from the 20^{th} week of gestation and can be used to classify arrhythmias such as heart blocks and atrial flutter, and to diagnose a prolonged QT-syndrome. FMCG represents one of the most promising alternatives to fetal ECG because of the higher SNR. However, the high costs, the size, the need of skilled personnel and the impossibility of continuous monitoring prevent its introduction in the clinical practice.

For both FECG and FMCG, the amplitudes of the waves depend on the distance between the fetal heart and the sensors and on the electrical properties of the tissues. For this reason the amplitudes of the waves can not be used for diagnostic purposes.

1.2 Non-Invasive Fetal Electrocardiography

Fetal ECG (FECG) can be non-invasively recorded from the maternal abdomen as early as the eighteenth to twentieth week of gestation [3]. Even if the first attempts to observe the FECG through non-invasive biopotential measurements can be dated at the beginning of the 20th century [22], the non-invasive FECG extraction is still an open research issue [23], mainly because there is no low-cost, reliable method to measure the actual ECG of the fetus in early pregnancy [24].

Non-invasive FECG can provide Fetal Heart Rate (FHR), ECG morphological information such as PR, ST, QT intervals, contraction monitoring (as in [25]), fetal movement (as suggested in [26]) and fetal position. It would be potentially able to detect fetal arrhythmias in early pregnancy [27], when it is either possible to treat them by transplacentar drugs administration, such as for heart blocks [28], or to closely follow the gestation, possibly pre-scheduling the delivery through caesarean section. Late or variable decelerations, reduced variability, bradycardia, or a sinusoidal FHR pattern have also been related to placental abruption [29]. However this technique has not been proved to be an effective tool for congenital cardiac defect diagnosis, and the studies in the field are limited to the identification of fetal heart rate to recognize conditions as general ischemia. The main reason for

this limitation is that FECG is contaminated by many other electrical sources with overlapping time and frequency content, such as the maternal ECG (stronger because of the bigger dimension of the heart), myographic (muscle) signals, movement artifacts and the presence of a number of dielectric layers through which the fetal electrical signals must pass. Both the signal to noise ratio (SNR) and the signal to interference ratio (SIR) are generally low, meaning that the FECG is typically lower than all the noise contributions [30].

The lack in reliability is both due to the signal processing techniques, which are still inadequate for these weak sources, and to the signal acquisition, with detection not guaranteed at any particular instant [31] or strongly affected by the influence of the *vernix caseosa*, a dielectric protective film surrounding the fetus with thickness and homogeneity dependent on the gestational age [32]. The study presented in [4] confirms this limitation, showing how signal quality is significantly poorer between 27 ad 36 weeks of gestation. The acquisition quality is also influenced by the skin and subcutaneous fat, that have a poor conductivity, because they represent the interface of the non-invasive electrodes [3]. Moreover, fetal presentation changes during pregnancy particularly during the fist two trimesters, strongly influencing the acquired signals, whereas at the half of the last trimester the vertex presentation (head-down position) is typically observed.

Apart from the maternal ECG main interference, FECG is contaminated by other noise and artefacts that are commonly present in standard ECG acquisition and that can be within the frequency band of interest, manifesting with similar morphologies [33], which are particularly critical in this application because of the low amplitude of the fetal signal. These interferences are typically classified as:

- Power line interference (50 or 60 Hz);
- Electrode pop or contact noise, manifesting with signal sharp changes due to loss of contact;
- Patient-electrode motion artefacts that cause baseline jumps because of the movement of the electrode with respect to the skin;
- Electromyographic (EMG) noise, due to muscle contraction especially of the uterus with a frequency band from dc to 10 kHz;
- Baseline drift, usually caused by maternal respiration;
- Hardware noise of the acquisition device;
- Noise generated by other medical equipment present in the patient care environment;
- Quantization noise and aliasing;
- Signal processing artefacts.

The suppression of these sources of interference using different signal processing techniques can strongly compromise the signal morphology, making the FECG useless for clinical purposes. From this viewpoint, the lack of common databases and of a ground truth for the fetal cardiac electrical activity during pregnancy, due to the inaccessibility of the fetus, hamper the progresses in the field and the comparison of the different algorithmic approaches at the state of the art. Also, some unclear aspects, for instance related to the validity

of the FECG morphology throughout the gestational period [34, 35] or to the mathematical properties behind the supposed physiological mixing model of the involved sources [36, 37], hamper its introduction in the clinical practice.

Beyond the diagnostic importance provided by the electrical trace of the fetal heart activity, non-invasive FECG has the following advantages:

- the non-invasive nature allows the use of this test both antepartum for diagnosing and monitoring cardiac diseases and intrapartum for the identification of fetal distress, not providing any risk of infection for the fetus and being comfortable for the mother;
- the acquisition device is similar to a common commercial electrocardiograph, both for the dimensions and easy of use;
- the absence of side-effects and the preserved freedom of movement make this technique adequate for long term monitoring, even for the use at home.

These aspects are particularly important when prolonged monitoring is required for fetal health assessment.

Many studies in the literature have been carried out about the possibility of obtaining clinical usable FECG signals with non-invasive electrodes during pregnancy. In [4] a study on singleton and multiple pregnancy FECG on 304 pregnant woman from 15 to 41 weeks of gestation is described. The results show that for singleton, the FECG was observable in 85% of the recordings (250), highlighting a poorer success rate between 27 and 36 weeks of gestation probably caused by the formation of the *vernix caseosa* with isolating properties over the fetal skin, whose effect decreases as the fetal dimension increases in later gestation. They acquired 5 minute signals using at least 12 electrodes placed over the whole of the abdominal wall, exploiting unipolar recordings, and preparing the skin to reduce the skin-electrode impedance above 5 $k\Omega$ by using a gentle excoriation of the skin cells (3M Skinprep 2236), and then analysed only one minute chosen by visual inspection with reduced movement artefacts. Maternal muscular noise from abdomen was reduced by suggesting the mother to assume a semi-recumbent position. To estimate the PR, QRS, QT and QTc (heart rate corrected QT) intervals, a simple coherent averaging was performed by time aligning of successive QRS complexes on the R peaks. The results show that the probability of the T wave detection increased with age (probably the poor T waves detection are due to their small amplitude which increases as the fetus grows).

Since the only way to directly access the FECG is during the birth with a scalp electrode, many of these studies are focused on intrapartum analysis, in order to obtain a validation of the non-invasive procedure. In [35] a comparative study between invasive (fetal scalp electrode, FSE) and non-invasive FECG has been carried out. They compared both the FHR ad the ST-segment changes in signals contemporary acquired from 32 women during labour with ruptured membranes and a dilatated cervix. Signals have been acquired using the E-TROLZ (North Andover, MA) physiological monitoring platform using 32 channels at 1kHz and gelled adhesive ECG electrodes in standard configuration without any skin treatment. Electrodes were positioned according to anatomic landmarks, and so their distances depend on the physical characteristic of the patient. Signal processing was based on a modified version of the Kalman Filtering that uses a priori information such as the pseudoperiodic structure of the cardiac signal. They always used the complete set of electrodes and then exploited a series of signal quality measures to choose the sensors with more information. The results

demonstrates the possibility of non-invasively extracting the FECG without distortion of the morphology, but it should be taken into account the presence of the epidural anesthesia in all the subjects (which can reduce patient activity and consequently the interferences) and the limited number of subjects.

1.2.1 Open-access databases of non-invasive FECG

There are a few open databases of non-invasive FECG and this represent a substantial obstacle to the development of new signal processing techniques.

The Daisy dataset [38] includes one dataset of 8 channels acquired at 250 Hz, with 5 abdominal and 3 thoracic signals. It is probably the most popular non-invasive FECG data, but it includes only 1 signal of 10 seconds with high SNR.

The "Non-Invasive Fetal Electrocardiogram Database" (NIFECGDB) includes 55 multichannel signals acquired weekly with Ag-AgCl electrodes from the same patient between 21 to 40 weeks of pregnancy and it is available on Physiobank [39]. The records have variable durations and are composed by 2 thoracic signals and 3 or 4 abdominal signals acquired at 1kHz (bandwidth 0.01-100 Hz and analog 50Hz notch filter) with 16 bits resolution. Some of these signals present a very low SNR.

Another database is provided with The Open Source Electrophysiological Toolbox [40] by the University of Shiraz, Iran, consisting of both real and synthetic FECG signals recorded from 8 maternal abdominal sensors. The real recordings have been provided by Dr. A. Tokarev from the Biomedical Signal Processing Laboratory of National Aerospace University, Kharkov, with different quality level and sampling rate (bandwidth 0.05-100Hz).

The "Abdominal and Direct Fetal Electrocardiogram Database"(ADFECGDB), available on PhysioNet[39], provides 5 signals with 4 channels acquired during labour (between 38 and 41 weeks of gestation) at 1kHz (Bandwidth: 1Hz - 150Hz) together with the scalp ECG for reference. The recordings were acquired in the Department of Obstetrics at the Medical University of Silesia, by means of the KOMPOREL system for acquisition and analysis of fetal electrocardiogram (ITAM Institute, Zabrze, Poland). Each recording comprises four differential signals acquired from maternal abdomen and the reference direct fetal electrocardiogram registered from the fetal head. The configuration of the abdominal electrodes comprised four electrodes placed around the navel, a reference electrode placed above the pubic symphysis and a common mode reference electrode (with active-ground signal) placed on the left leg. To reduce the skin impedance, the areas under the Ag-AgCl electrodes were abraded.

Recently the scientific community welcomed the publication of a new database of 4 channels signals on Physiobank which included both the previously published NIFECGDB and ADFECGDB databases, one artificial database and two new databases. All the data are presented at a sampling frequency of 1kHz but they have been acquired with different instruments, resolution and configuration, with the annotations of the fetal R peaks usually using a scalp electrode. It should be noted the low dimension of the databases (4 channels) with unknown positioning setup and the absence of correlated clinical information about the gestation. The big dimension of the dataset, the provision of a test and validation sets and the poor knowledge of the acquisition setup and conditions make this dataset the best choice for the evaluation of low density algorithms, with the aim of identifying the most generic algorithmic solution which can ideally fit the acquisition in non-controlled environment, such as for home telemonitoring applications.

Commercial devices for the acquisition of non-invasive FECG

There are only two FDA approved commercial devices for non-invasive FECG acquisition: the Monica AN24 monitor (Monica Healthcare, Nottingham, UK) and the MERIDIAN monitor (MindChild Medical, North Andover, MA).

Monica AN24 monitor [41], shown in Fig.1.3a, includes 4 acquisition channels (5 abdominal electrodes, Blue SensorVLC-00S, Ambu, St. Ives, UK) to record 3 signal at 300 Hz and one at 900 Hz. It provides to the user the fetal ECG morphology, beat to beat (RR) fetal heart rate and the possibility to obtain raw abdominal signals from a continuous 20 hr recording. The study described in[42], funded by Monica Healthcare Ltd, compares the accuracy and reliability of fetal heart rate identification from the Monica AN24 monitor and Doppler ultrasound with a fetal scalp electrode during the birth in 75 women, showing that, compared with the fetal scalp electrode, fetal heart rate detection using abdominal fetal ECG was more reliable and accurate than ultrasound, and that Monica was less likely than ultrasound to display the maternal heart rate instead of the fetal one. In [43] a comparison of the ST segment analysis (STAN) on 6 patients using simultaneous traditional fetal scalp electrode and non-invasive FECG acquired with Monica AN24 monitor is described, reporting the feasibility of the non invasive technique. However, this study includes only a limited number of subjects and results show the T waves (that need to be identified for the ST analysis) were visible in only 50% of the patients.

The MERIDIAN Monitor, shown in 1.3b, is an intrapartum fetal monitor that measures FHR from abdominal surface electrodes, or alternatively, by using direct ECG (DECG) with a fetal scalp electrode. It is indicated for use on women who are at term (>36 completed weeks), in labour, with singleton pregnancies, using surface electrodes on the maternal abdomen. This system has been developed starting from the research presented in [35] and described above in section 1.2 on page 13.

1.3 Non-Invasive FECG Signal Processing

Signal processing of noninvasively acquired FECG signals remains one of the main obstacles to its introduction in clinical practice. As mentioned above, the presence of a number of sources of interference with overlapping spectral content and comparable signal amplitude, makes the extraction of the fetal cardiac information extremely difficult.

Depending on the signal acquisition setup, different signal processing algorithm can be used for FECG extraction. The number of acquisition channels depends on the application. When long-term monitoring is required, a reduced set of electrodes is preferred to improve patient comfort and electrodes positioning, whereas diagnostic tests can take advantage from the use of high density recordings.

Linear and nonlinear decomposition methods are based on the decomposition of the signals in components by using some basis functions, such as wavelet decomposition, or data driven approaches (SVD, blind or semi-blind source separation). These techniques are able to separate overlapping maternal and fetal beats without any a-priori information, but they are based on the assumption of independence of the sources we want to estimate and the absence of Gaussian sources. Linear methods are based on the assumption of a linear and stationary mixing problem of the sources, that is not always a good approximation because of the presence of both fetal and maternal movements. Also, there are many issues such as

(a) The Monica AN24 monitor

(b) The MERIDIAN Monitor

Figure 1.3: Commercial systems for non-invasive FECG acquisition, The Monica AN24 monitor by *Monica Healthcare (Nottingham, UK)* and the MERIDIAN Monitor by *MindChild Medical Inc (North Andover, MA)*.

the interpretation, stability, robustness, and noise-sensitivity of the extracted components. Despite all this problem, decomposition methods represent probably the most effective algorithms for fetal ECG signal extraction [44, 45]. When high density recordings are used [46, 47], it is possible to apply Blind Source Separation (BSS) techniques or to select the best subset of channels, disregarding the others. In fact, BSS algorithms requires at least as many channels as the independent components generating the observed signals, thus enabling the exploitation of Independent Component Analysis (ICA) algorithms [45]. A rough computation of the independent components can be made assuming 3 components for the maternal ECG, 2-3 for the fetal one, at least the instrumental noise and the EMG. Some studies reveal that it is possible to achieve a good separation with only 8 electrodes in singleton pregnancies [36] and 12-16 in multiple pregnancies [4], even if some results could be achieved even with a reduced electrodes set [48] or with a single channel [49]. The adoption of less than 8 electrodes, leading to low-density recordings, would hamper the adoption of ICA algorithms unless a substantial preprocessing is performed [50].

Adaptive filters, based on the adjustment of the filter taps according to an optimization algorithm, have been successfully used for the suppression of the maternal ECG source.

Their adaptive nature make them suitable for many time-varying applications. They require the acquisition of at least one maternal source of reference (that is the component we want to remove) to adjust the filter coefficients in order to minimize a cost function. The main problems of these techniques are the need of at least one reference signal with a marked morphological similarity to obtain good performance and the difficulty to extract fetal and maternal beats with temporal overlap. One of the most famous algorithms for the maternal ECG suppression has been developed by Widrow in the 1970's [51]. It is based on the application of the LMS (Last Mean Square) adaptive filter using some references signals acquired from the maternal chest (in order to have only maternal ECG source) to remove the maternal component from the abdominal channels. However, this technique results too much sensitive to noise sources, not being able to preserve fetal ECG morphology after filtering. More recently, Martens et al. tried to improve the quality of the maternal subtraction, [52], using an upsampling stage to improve the subtraction quality of an average maternal QRS complex from the abdominal sources. This algorithm requires a heavy preprocessing (the baseline wandering is removed using a FIR filter with a cutoff frequency of 3Hz at a sampling frequency of 400 Hz, while the power-line interference is reduced by using an adaptive noise cancelling technique) and shows good performance only when the maternal frequency is lower than 86 bpm or if the heart rate is stable during average.

Chapter 2

Algorithms for Non-Invasive Fetal ECG Analysis

Depending on the specific gestational age and on the disease we want to investigate, different requirements can arise, from the evaluation of the fetal heart rate (HR) to the analysis of the FECG waveform morphology.

The choice of both the number of acquisition signals and the displacement of the electrodes on the body of the pregnant woman depend on the kind of analysis required and strongly influence the signal processing techniques that can be used for fetal ECG identification (e.g., Blind Source Separation, BSS, algorithms require a minimum number of acquisition channels properly applied on the maternal abdomen). When diagnostic features are required, we can expect that the highest number of acquisition channels would provide more clinical information with respect to a reduced recording configuration (possibly enabling the choice of the best quality channels only), whereas long term monitoring requires a comfortable setup for fetal well-being assessment both at home or intrapartum.

This chapter includes the description of two processing algorithms that have been developed for the analysis of fetal ECG signals.

The first algorithm has been developed for the real-time post-processing of on-line BSS algorithms and allows the automatic identification of the fetal source, the fetal heart rate (FHR) and an average fetal QRS complex. It is suitable for both diagnostic and monitoring applications, where the real-time feature allows to provide the instantaneous HR. As discussed in section 1.2.1, only a reduced number of open real dataset are available and they typically present a limited number of recordings, not being adequate for the application of BSS algorithms. For this reason, the algorithm has been tested on both real signals, acquired with the collaboration of the Pediatric Cardiology Unit of the Sardinian Hospital G. Brotzu in Cagliari, and synthetic signals generated with the The Open-Source Electrophysiological Toolbox (OSET) [40].

The second algorithm has been conceived for the identification of the FHR in low-density non-invasive FECG recordings, that is the typical setup of long-term monitoring applications, both at home or during the birth. To this aim, the algorithm has been tested on the non-invasive FECG database recently published on Physiobank, which includes both a training set and two validation sets (one open and one hidden). This dataset includes signals acquired at different gestational epochs and with different setup/resolution, representing a

good benchmark for the evaluation of a telemonitoring algorithm that needs to be applied on a wide variety of signals and electrodes configurations.

2.1 A Tracking Algorithm for Fetal ECG Sources Extracted by BSS Techniques

When the number of ECG signals is equal to (or higher than) the number of sources we want to estimate (at least eight sources are expected for FECG applications [36]), algorithms based on Independent Component Analysis can be used for the FECG signal extraction with satisfying results [3]. If these algorithms are used for real-time applications, one of the main problems is the identification of the fetal sources because of the permutation ambiguity of on-line Blind Source Separation (BSS) methods [53, 54].

Starting from this consideration and taking into account the previous implementation of an on-line version of the JADE algorithm (OL-JADE [55]) at the EOLAB (Microelectronics and Bioengineering Lab) of the University of Cagliari, a block-on-line tracking algorithm of the fetal source has been developed. It includes a tracking stage and an unsupervised morphological stage able to create an average FECG beat. The tracking stage is based on the creation of a feature signal for each estimated source on which the turning point count is performed to identify the noise sources; the remaining sources are then classified as maternal or fetal sources using a single linkage hierarchical clustering. After the fetal sources have been identified, the morphological stage is performed in order to recognize possible permutations among the fetal channels and to obtain an average PQRST complex to evaluate FECG morphology. The creation of the average beats is based on the Pearson's correlation coefficient and is completely unsupervised.

The developed algorithm, described in [56], has been tested on both real and synthetic mixtures processed by the OL-JADE algorithm and is presented in detail in the following sections. It can work with any on-line FECG extraction technique and can aid other processing stages. An example of the integration of the proposed algorithm in the real-time FECG processing is shown in Fig. 2.1. The stage for the real-time back projection and Body Surface Map creation [57, 4] requires the identification of the fetal sources in order to estimate their power contribution at the electrodes. This information can be used to iteratively move some of the electrodes during the acquisition in order to maximise the FECG contribution in at least 2 signals.

The automatic FECG channels classification without any clinician intervention is seldom addressed in literature. In [58] a Fast Fourier Transform (FFT) technique is used to identify which of the Independent Component Analysis (ICA) output waveforms include the foetal beats. The system proposed in [59] computes for each channel its probability of being maternal or foetal using a modified Pan Tompkins QRS detection algorithm and the autocorrelation function to find the heart rate in the estimated FECG and MECG. Conversely, many systems integrate a stage to enhance signal morphology highlighting the characteristic waves. For instance, the BSS system described in [36] computes the average FECG beat by maximizing the correlation between consecutive pulses. Also the ICA system described in [60] exploits an average waveform to measure the characteristic ECG intervals using the autocorrelation to align approximately 50 consecutive foetal complexes.

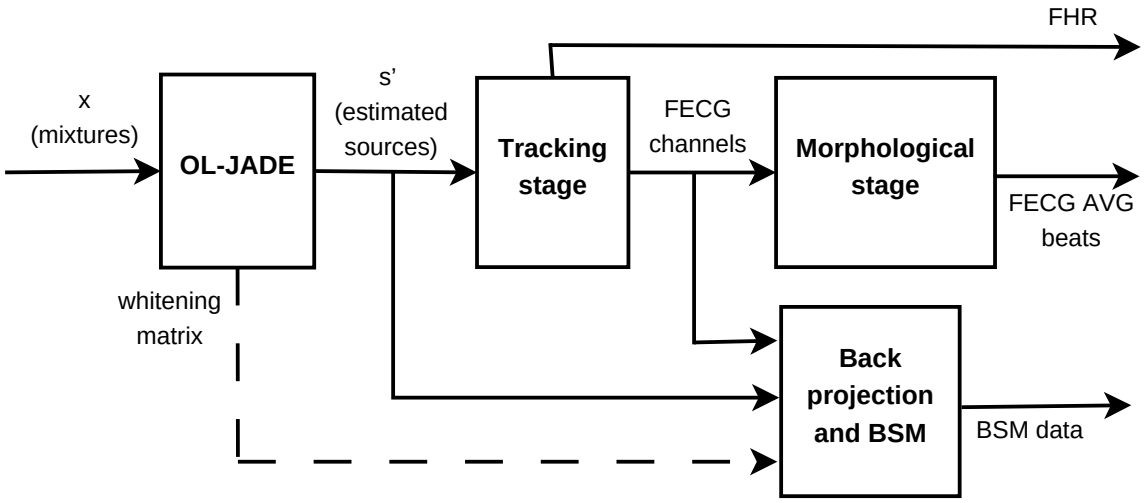

Figure 2.1: Block diagram of all the block-on-line processing system

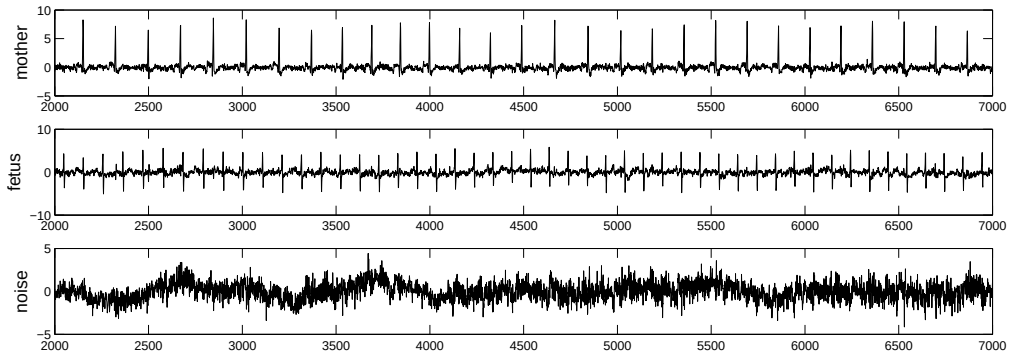

Figure 2.2: An example of maternal, fetal and noise sources estimated by OL-JADE from real mixtures by courtesy of Prof. L. De Lathauwer

2.1.1 Algorithm structure

The proposed tracking algorithm can be used with any FECG extraction technique. Nevertheless, the OL-JADE one [55] has been chosen because of the particularly critic slow permutations (compared to other approaches [61]). OL-JADE is a real-time BSS technique which allows the extraction of FECG from non-invasive recordings. Considering the linear instantaneous model $\mathbf{x} = \mathbf{As}$, it allows the estimation of the sources $\mathbf{s}$ from the observed signals $\mathbf{x}$, exploiting an approximated orthogonal 2-stage algorithm to find an unmixing matrix $\mathbf{A}^{-1}$=$\mathbf{R}$·$\mathbf{W}$, where $\mathbf{W}$ is a whitening matrix and $\mathbf{R}$ a rotation one. An example of three different OL-JADE estimated signals (maternal, foetal and noise sources) is shown in Fig. 2.2. They have been obtained from eight real mixtures (by courtesy of Prof. L. De Lathauwer [38]) consisting of five abdominal leads and three thoracic ones, 60s long, sampled at 250 Hz.

Even though scalable, the original algorithm works with 8 input channels, with a sliding window with length $L = 1024$ samples and an overlap of $L - T$ samples, where T is set to be 256 at a sampling rate of 250 Hz. The proposed tracking algorithm has been sized accordingly. The algorithm, whose block diagram is shown in Fig. 2.3, includes 2 main stages, the tracking and the morphological ones. The former is further divided in 3 steps, namely:

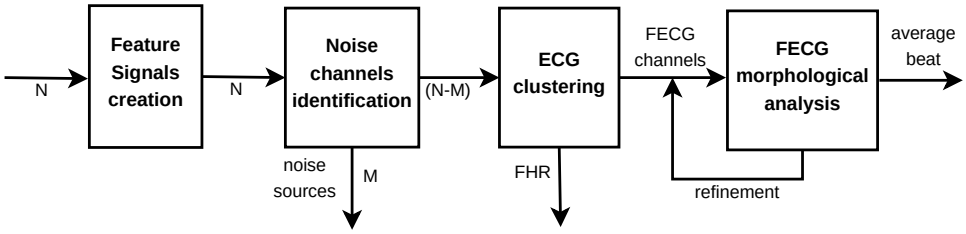

Figure 2.3: Block diagram of the proposed algorithm

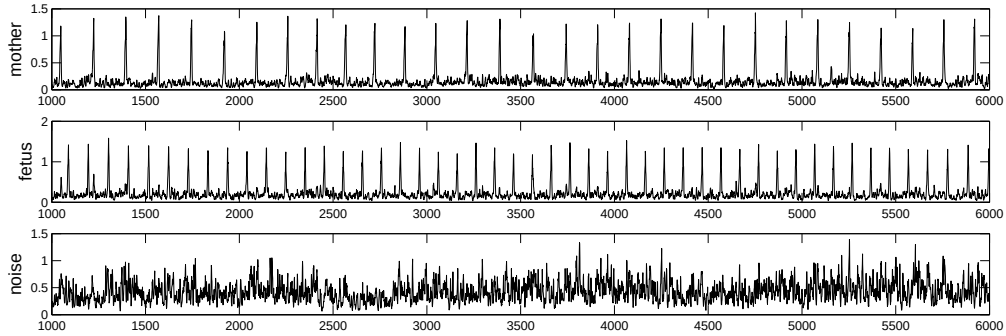

Figure 2.4: 7-tap matched filter applied on the first derivative of the signals of Fig. 2.2

feature signals creation, noise channel identification, ECG clustering.

The tracking algorithm: identification of the fetal sources

At first, the tracking algorithm creates Feature Signals (FS) for all the OL-JADE estimated Source Signals (SS_i with $i = 1,2,...,N$ where N is the number of input signals). SS_i are created as follows (n spans from 1 to 256):

- rectified first order derivative of the SS_i:

$$x_i[n] = \frac{1}{2}(|SS_i[n] - SS_i[n-1]|) \tag{2.1}$$

- rectified second order derivative of the SS_i:

$$w_i[n] = \frac{1}{4}(|S_i[n] - 2SS_i[n-2] + SS_i[n-4]|) \tag{2.2}$$

- a 7-tap matched filter to emphasize the presence of QRS waves, applied on the rectified first derivative:

$$\begin{aligned} y_i[n] = &\frac{1}{44}(2x_i[n+3] + 4x_i[n+2] + 8x_i[n+1] + \\ &+ 16x_i[n] + 8x_i[n-1] + \\ &+ 4x_i[n-2] + 2x_i[n-3]); \end{aligned} \tag{2.3}$$

  the result of this filtering on different type of sources is shown in Fig. 2.4;

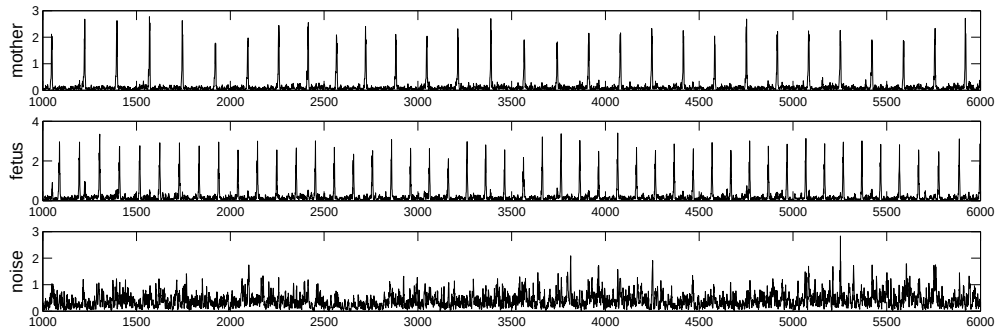

Figure 2.5: Linear combination of the first and second derivative filters applied on the signals of Fig. 2.2.

- $y_i[n]$ is used to compute $z_i[n]$ through a multiplication operation between two adjacent samples, using an approach described in MOBD QRS detection algorithms [62], for magnification of high peaks:

$$z_i[n] = y_i[n] * y_i[n-1] \tag{2.4}$$

- a linear combination of z_i and w_i, inspired to the Balda QRS detector [63], emphasizes the highest signal peaks, as shown in 2.5:

$$f_i[n] = z_i[n] + 0.5\, w_i[n] \tag{2.5}$$

- the f_i signals are then smoothed exploiting an 8 tap moving average filter in order to merge bicuspid peaks in FECG and MECG FS related to the same QRS event.

At this point, the noise channel identification step finds the M noise sources among the N channels. The FS are soft thresholded to remove the baseline information in the ECG signals (the threshold th_{tp} is equal to 45% of the average between the maximum in the analysed block and the maximum in the previous one). Then the first derivative operator of equation (2.1) is applied to FS_i and the transitions from positive to negative and vice versa are counted (turning point count). As shown in Fig. 2.6, slope inversions in noise are significantly more than those in ECG FSs so it can be identified adopting a threshold on the turn count.

Then the ECG clustering step occurs, with the aim of identifying two clusters among the $N-M$ remaining FS which represent MECG and FECG sources. Single Linkage Hierarchical Clustering is an agglomerative clustering method which, starting from considering each object as a separate cluster, tries to merge the closest pair of clusters according to a chosen metric distance, such as the Euclidean distance, until certain termination conditions are satisfied (e.g., a distance threshold or the number of clusters). In this clustering method, the proximity of two clusters is defined as the shortest distance between all the elements of the clusters. We chose as metric for clustering a distance defined as $d = 1 - |\rho|$, where ρ is the Pearson's correlation coefficient. Every FS is standardized subtracting the mean value and dividing by the standard deviation, block wise. Then they are soft thresholded to remove the lowest 20%. The actual clustering stage can be described as follows:

1. creation of the $(N-M) \times (N-M)$ proximity matrix $\mathbf{D}$, which contains the minimum distance for each pair of clusters;

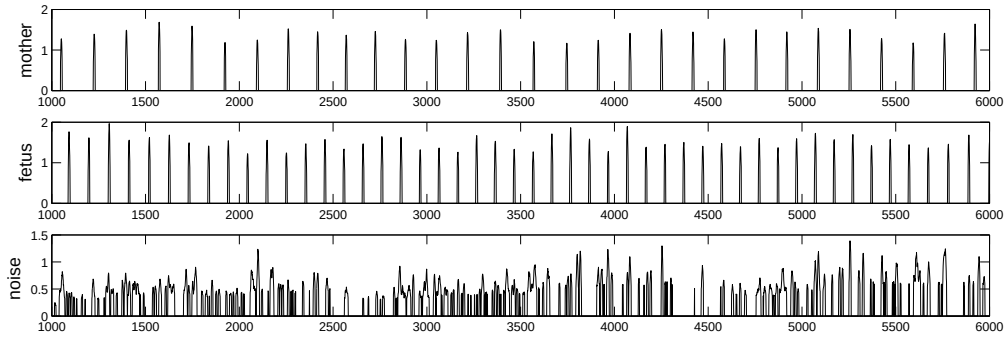

Figure 2.6: Final processed signals of Fig. 2.2 on which the turning points are evaluated

2. research of the most similar pair of clusters *(r,c)* by searching for the minimum value of **D**:

$$d(r,c) = min\,\mathbf{D}(i,j), \quad with\ i \neq j \tag{2.6}$$

3. comparison of the minimum distance with a fixed threshold th_d (0.2, which corresponds to a $|\rho|$ of 0.8, an empirical value which allows the discrimination between maternal and foetal sources). If $d(r,c) < th_d$ the clustering proceeds, otherwise it is stopped;

4. merge of the clusters r and c and update of the proximity matrix according to the single linkage method. All the information about the position of channels composing a cluster is preserved;

5. if the number of clusters is greater than 2 (which is the ideal situation where MECG and FECG are identified) the analysis goes to the step 2 to complete the clustering, otherwise the clustering is finished.

If the number of clusters is greater than 2, the algorithm tries to merge them according to their R-peaks positions. If unsuccessful, a tracking error occurs and the FECG and MECG cannot be properly identified, otherwise the 2 clusters are classified as MECG or FECG according to the heart rate. Chosen one signal per cluster, any sample exceeding the 50% of the maximum in a block is marked as belonging to a QRS complex. Then a refractory period of 30 samples is used to clear multiple occurrences belonging the same complex. Since $FHR > MHR$, if the number of QRS complexes in the two clusters is different, the highest one indicates the FECG, otherwise the RR intervals are computed and the minimum used to identify the FECG.

The morphological algorithm: average fetal beat identification

The tracking stage sends to the morphological one the FECG channels number and their R-peaks positions. This stage allows to identify possible foetal signals permutations and to enhance the signal to remove noise by synchronized averaging based on a cross-correlation analysis between the foetal source and a proper template. In the proposed approach, rather than using a synthetic template, for up to 2 FECG channels a template of 80 samples per channel (320 ms @250 Hz) centred on the R peak of the first identified beat is extracted.

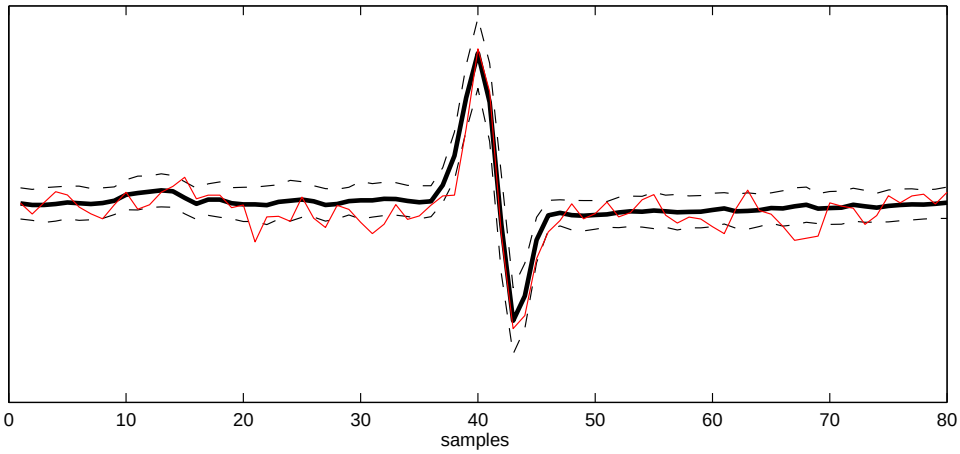

Figure 2.7: Bold line shows an average FECG beat obtained from a one minute signal. Dashed lines represent the standard deviation. A single beat from the ensemble average is also shown.

At first, the morphology of every new beat is evaluated according to its QRS balance (polarity). Then a cross-correlation, based on the Pearson's index, between every template and a window around the R peak is applied. In this way, if the algorithm identifies in one of the foetal channels some consecutive QRS complexes whose morphology belongs to the other foetal channel, it reports a permutation between the two channels. Every time a QRS complex is found, it is also evaluated for updating a template by synchronized averaging. Because of the limited memory resource, an incremental averaging is preferred, without any precision loss. The necessary updating conditions are:

- the correlation index has to exceed a specific empirical threshold, which is 0.8 at the steady state (it slowly grows from a first value of 0.6);
- the QRS complex polarity has to be coherent with that of the related template.

Since the correlation index is obtained for every sample around the R peak, its value allows the individuation of the exact R-peak position which reflects the better alignment between the template and the beat. If the template is not updated within 25 consecutive beats found by the tracking stage, the algorithm selects a new template to be representative of the channel morphology. Also, since the FECG channels permutation can cause a polarity inversion, the algorithm takes into account this possible inversion when aligning the QRS complexes before updating the mean beat. In this way, a real-time updated template represents the average beat until then: Fig. 2.7 shows the average FECG beat after the analysis of a one minute signal, compared to a single real beat.

2.1.2 Test on real and synthetic signals

To evaluate the performance of the proposed tracking algorithm, we performed tests on both real and synthetic mixtures processed by the OL-JADE algorithm [55].

The real signals were acquired non-invasively by an ADI PowerLab16/30 (Fig. 2.8a) and a *g.tec* GT201 16 channels Bioamp (Fig. 2.8b) from voluntary pregnant patients with the col-

(a) ADI PowerLab16/30

(b) *g.tec* GT201 16 channels Bioamp

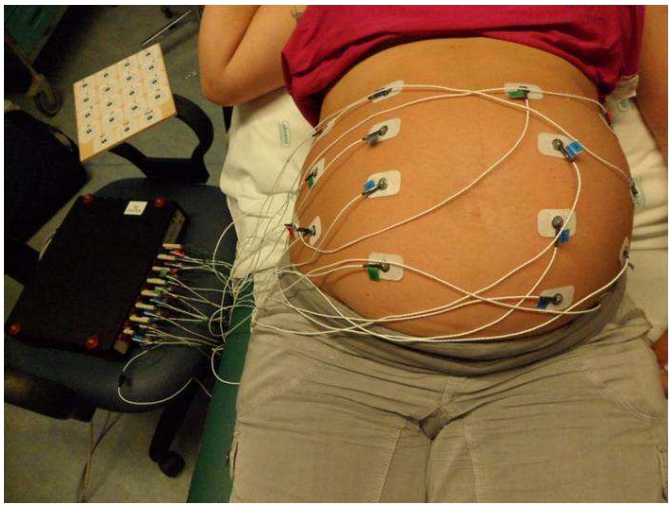

(c) The electrodes positioning on the maternal abdomen

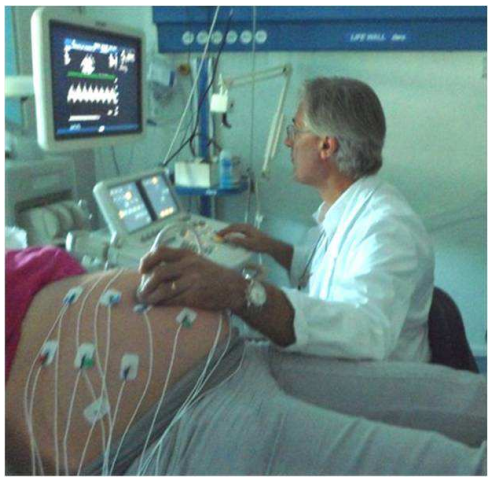

(d) An example of acquisition setup

Figure 2.8: The acquisition modules and setup for real non-invasive FECG acquisition at the Pediatric Cardiology Unit of the Hospital G. Brotzu of Cagliari

laboration of the pediatric cardiology unit of the Hospital G. Brotzu of Cagliari. The measurement setup is shown in Fig. 2.8c and 2.8d. The Bioamp includes 16 differential channels for true bipolar recordings and non bypassable low and high pass analog filters. Since the greatest part of the studies in the field underline the need of unipolar recordings with respect to a reference electrode, and taking into account that bipolar signals can be easily obtained in a digital processing stage differentiating the unipolar channels, we used the *0223 Shortcut Jumper* cables to obtain a unique reference. The data of two voluntary subjects respectively at the 36^{th} and the 20^{th} week of pregnancy have been used for the algorithm testing. These data have been chosen because their SNR was enough high to allow the sources separation. In fact, the greatest part of the acquired signals are too noisy for providing clinically usable information. This is manly due to the acquisition devices and to the unshielded wires.

An example of on-line tracking of the FECG traces produced by OL-JADE is shown in Fig. 2.9, where the identified foetal R-peaks are marked. It is possible to see how the quality of the extracted MECG is higher than that of the FECG, which in turn has reverberations on the permutation aspects.

For the synthetic signals generation, the OSET tool [40] described in [64], which enables the creation of two rotating dipoles with selectable parameters (including position) for both mother and foetus, was used. It allows to add to the clean sources also some parameterized time variant noise, weighting 3 different contributions of baseline wandering (BW), electrodes movements (EM) and muscle artefacts (MA). Since on real signals it is difficult to recover all the 3 foetal components, we decided to constrain the foetal dipole to a planar rotation. With this choice, for every single kind of noise and for the composite one (CN,

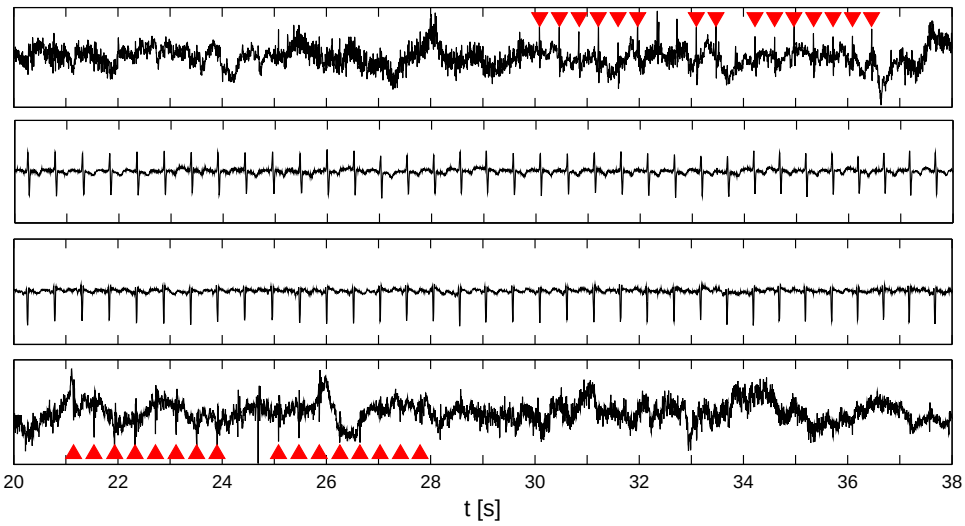

Figure 2.9: An example of tracking on real extracted ECG sources, acquired on a 20-week pregnant woman.

	FECG source 1		**FECG source 2**	
	% TP	# perm	%TP	# perm
real signal (36^{th})	66.7	5	64.9	3
real signal (20^{th})	69.7	4	-	-
CN, SNR=5	79.2	1	51.9	1
CN, SNR=10	78.4	3	65.8	1
CN, SNR=15	83.3	0	78.8	2
CN, SNR=20	90.3	0	89.8	0
CN, SNR=20‡	62.7	1	52.5	1
CN, SNR=20†	93.4	0	93.4	1
MA, SNR=15	89.6	0	83.9	2
EM, SNR=15	86.9	0	52.2	2
BW, SNR=15	90.2	0	70.2	2

‡: with abrupt translation of the foetal dipole

†: with abrupt rototranslation of the foetal dipole

Table 2.1: Tracking algorithm performance

with the same weight for the individual noises) we created segments of 30 seconds with a different SNR, with or without expressly introduced foetal movements (position and 3D rotation of the foetal dipole abruptly changed at second 15), passed to OL-JADE to estimate the independent sources on which the tracking algorithm is applied.

The tracking results are shown in Tab.2.1 in terms of percentage of True Positive (TP) revealed peaks, obtained considering the number of the FECG peaks correctly identified by the tracking algorithm, with respect to the total amount identifiable by visual inspection. All the permutations in the FECG sources have been detected and their number is also indicated

in the same table. The results are affected by the noise level, which influences the separation quality. The performance does not grow monotonically with the SNR because of the stochastic nature of the process used to create the noise in OSET. Since the FECG sources identification works block-wise, some errors lead to the misdetection of more than one consecutive FECG beat (as clearly visible in Fig. 2.9) but such isolated errors can be easily filtered out. The poor signal quality influences the noise sources identification step, which has been identified as the weakest step of the algorithm because of the high variability of the turning point count. Wrong noise sources identification produces wrong ECG clustering, preventing the identification of the FECG sources. From this viewpoint, the tuning of th_{tp} can be beneficial and, thanks to the real-time capabilities of the proposed solution, this can be performed at run time. It should be noted that the th_{tp} tuning is mainly required when changing acquisition setup (e.g., we changed its value from 0.45 to 0.15 for all the synthetic signals).

In order to assess the capability of the algorithm of properly operating in real-time along with the main FECG extraction algorithm, it has been coded in C and optimized to run on the C6747 floating point DSP core of the OMAP L137 embedded processor by Texas Instruments. When the processor is clocked at 300MHz and the sampling rate is 250Hz, the proposed tracking algorithm requires only 3.7ms (1.6ms for the morphological stage), which is a short time compared to the worst-case 158ms required by the main separation algorithm [65]. Even though the algorithm can be improved, its performance is compatible with the needs of an embedded system implementation and for this reason it has been integrated with OL-JADE on a prototypical embedded platform based on the dual core OMAP L137 processor for advanced studies in the field of FECG extraction.

2.2 Identification of Fetal QRS Complexes in Low Electrode Density Recordings

One of the main obstacles in FECG study is the lack of annotated databases that could be used to develop and evaluate the quality of new processing algorithms. In fact, it is difficult to understand the clinical effectiveness of the extracted parameters. In 2013, a new annotated non-invasive fetal ECG database has been published on Physionet [66] and an international competition has been organized [67]. The data have been organized into a training set (set A, 75 signals), a test set (set B, 100 signals) and a validation set (not public, set C, 272 signals) to obtain an objective evaluation of the algorithms. Each signal includes four channels of one minute acquired from the maternal abdomen using different instruments and unknown setup with various resolution and sampling rate but presented at 1000Hz; the corresponding annotations of the fetal R peaks locations have been provided for the training set only.

When few channels are provided (for example for long term monitoring applications at home or during birth) different approaches have to be used, aiming at removing the maternal main components. The proposed algorithm for the identification of fetal QRS complexes is mainly based on the subtraction of the maternal QRS complexes in every lead, obtained by synchronized averaging of morphologically similar complexes, the filtering of the maternal P and T waves and the enhancement of the fetal QRS through Independent Component Analysis (ICA) applied on the processed signals before a final fetal QRS detection stage. It also includes the RR time series analysis of both the mother and the fetus to enhance pseudope-

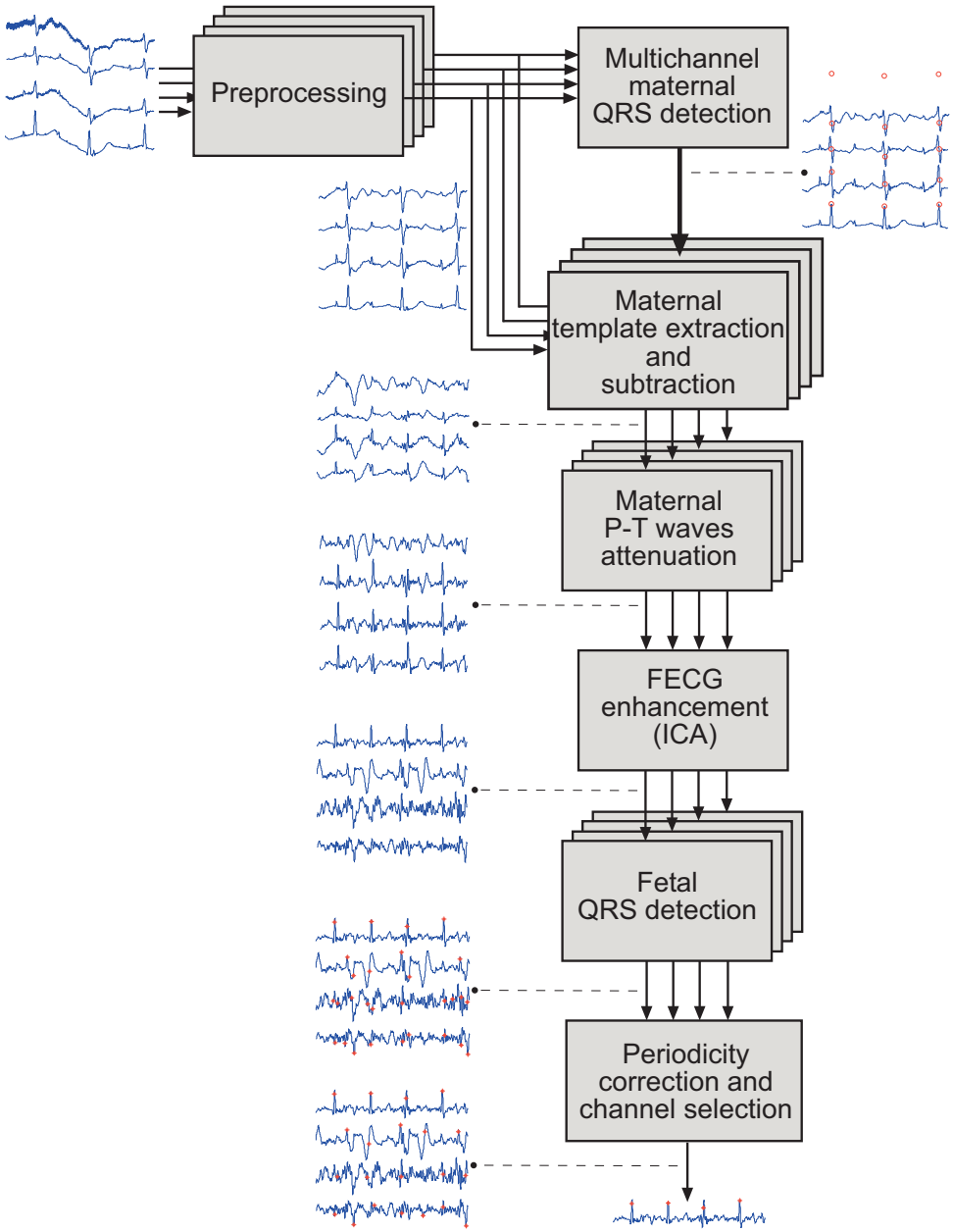

Figure 2.10: Block diagram of the proposed algorithm for fetal RR time series estimation.

riodicity with the aim of correcting wrong annotations. It has been developed and tested on the provided database, in order to obtain an objective evaluation of the results.

2.2.1 Algorithm description

The proposed algorithm, presented in [68], has been developed in Matlab and released under the GNU GPL-2.0 open-source license [69]. It is parametric in the number of channels so that in principle it can be used to process datasets acquired using any number of electrodes. The block diagram of the algorithm is shown in Figure 2.10 and its processing stage are described in details in the following sections.

Preprocessing

The available dataset includes saturated and invalid data in several signals, due to wrong outputs of the A/D converter. For this reason, a first preprocessing stage has been included to find these values and replace the invalid segments with a cubic spline interpolation. In order to remove the fundamental noise sources in ECG signals, i.e. baseline drift and artificial noise interference, a band-pass FIR filter between 2 and 46 Hz cascading a low-pass (order 459) and an high-pass (order 2234) filters have been designed using the windowed linear-phase design method with a Kaiser window. Since the algorithm has been conceived and tested on one minute signals, zero-phase digital filtering has been used to minimize start-up and ending transients, preserving at the most the ECG morphology for the sake of the following detection stages, taking into account that maternal morphological alterations that do not produce any side effect on the template creation are not troubling for the final fetal detection. Bidirectional filtering leads to multiply by 2 the order of the filters; intrinsic non-causality, along with the considerable delay, is without consequences in this case, since the algorithm is thought to work off-line. At the same time, the choice of adopting FIR filtering is aimed at minimizing recursion errors that could affect the successive ICA processing and the ringing effects typical of IIR filtering. Taking into account the open-source nature of the developed code, the use of bidirectional filtering would also allow the introduction of IIR filters in a safe way in the algorithm getting rid of the phase distortion problems.

Maternal Multi-Channel QRS detection

Since the algorithm is based on the subtraction of the maternal QRS complexes, the first main stage aims at identifying their position with good selectivity with respect to the fetal ones. In fact, the quality of all the subsequent processing stages is strongly affected by the quality of the maternal subtraction. There are many approaches in literature for the identification of the QRS complexes in adult's ECGs. The main difficulty of this stage is the discrimination of the maternal QRS complexes from the fetal ones, since their spectra overlap and the amplitude of the fetal R peaks is strongly variable, in some signals of the test database being almost comparable with the maternal one and in some others being barely visible. At the same time, the algorithms conceived to work on adult's signals do not have to face these problems. This leads to unsatisfactory results even with top algorithm such as [70]. In order to identify a good solution with enhanced selectivity, several algorithm from the scientific literature in the field have been implemented and tested [63, 71, 72, 73, 74, 75]. From a comparison of these algorithms, we noticed that the Pan-Tompkins one [75], is more sensitive to the maternal QRS complexes than to the fetal ones. The algorithm includes a preprocessing stage consisting of a band-pass filter followed by a differentiator; the output of the differentiator is squared and then integrated by means of a moving-average filter. The band-pass filter is composed of a low-pass filter:

$$H_L(z) = \frac{1}{32}\frac{(1-z^{-6})^2}{(1-z^{-1})^2} \tag{2.7}$$

which, at the sampling frequency used by the authors (200Hz), leads to a cut-off frequency of 11Hz, and a high-pass filter:

$$H_H(z) = z^{-16} - \frac{1}{32}H_l p(z) \tag{2.8}$$

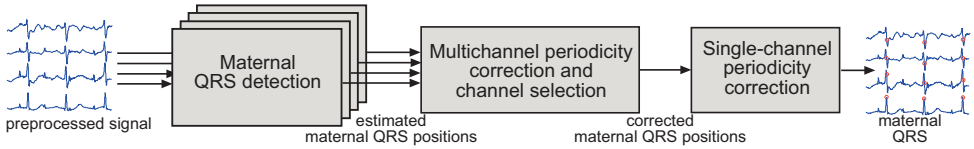

Figure 2.11: Block diagram of the maternal QRS complexes detection stage.

where:

$$H_{lp}(z) = \frac{(1-z^{-32})}{(1-z^{-1})} \tag{2.9}$$

which, at the same sampling frequency, leads to a cut-off frequency of 5Hz. This is in contrast with the common knowledge about the QRS complex bandwidth, ranging from about 10Hz to about 25Hz [76]. Originally the filters were chosen for their simple transfer functions to avoid multiplication and to work in real-time on the old microcontrollers. We exploited the algorithm at a sampling rate of 250Hz without altering the filters coefficients, thus obtaining a band-pass filter between 6 and 14 Hz, which is still adequate, even better, for QRS complexes detection. Spectral transformations of the filters to meet the original specifications did not produced better results.

The derivative operator is implemented as:

$$H_D(z) = \frac{1}{10}(-2z^{-2} - z^{-1} + z + 2z^2) \tag{2.10}$$

and its output is simply squared and integrated through a 37-tap moving-average filter (rather than the 30-tap original one [75], in order to respect the idea of the authors of having a window fitting the size of a typical QRS complex). Compared to the original algorithm, no search-back strategy has been implemented, using only an adaptive threshold system to follow the changes in the signal amplitude. The threshold is computed every second as 40% of the 6th highest value of the signal in that window. A sample is then identified as a maternal QRS if it is above such a threshold along with the 8 neighbouring samples. This solution reduced the detections of noise peaks.

A refinement of the time series of R peaks created by such an algorithm is performed by a separate stage implementing a double strategy to improve pseudoperiodicity[1], as shown in Figure 2.11. The multichannel periodicity correction allows to take advantage of the information coming from all the available sources by correcting both redundant and missing beats when the noise interferences causing the errors are not present in all the channels at the same time. The algorithm takes as reference the time series of the channel with the lowest number of RR intervals deviating from their median value RR_m more than 60 samples at 250Hz (pseudoperiodicity criterion). It tries to correct the outliers replacing the corresponding QRS annotations with those found in other channels when this improves the pseudoperiodicity of the final time series. An example is shown in Figure 2.12, where the algorithm chooses the third channel as reference because of the better pseudoperiodicity (due to the lower noise in the middle of the signal) but corrects the position of two peaks identified by the QRS detector with those obtained from the fourth channel (the second best one). This modifies the original annotation (red asterisks) leading to the final one (blue triangles) and to a new RR_m over a single time series.

[1] In this case, pseudoperiodicity is not meant in strict mathematical sense but only as a way to highlight the repetitive pattern of the cardiac cycle in absence of severe arrhythmias.

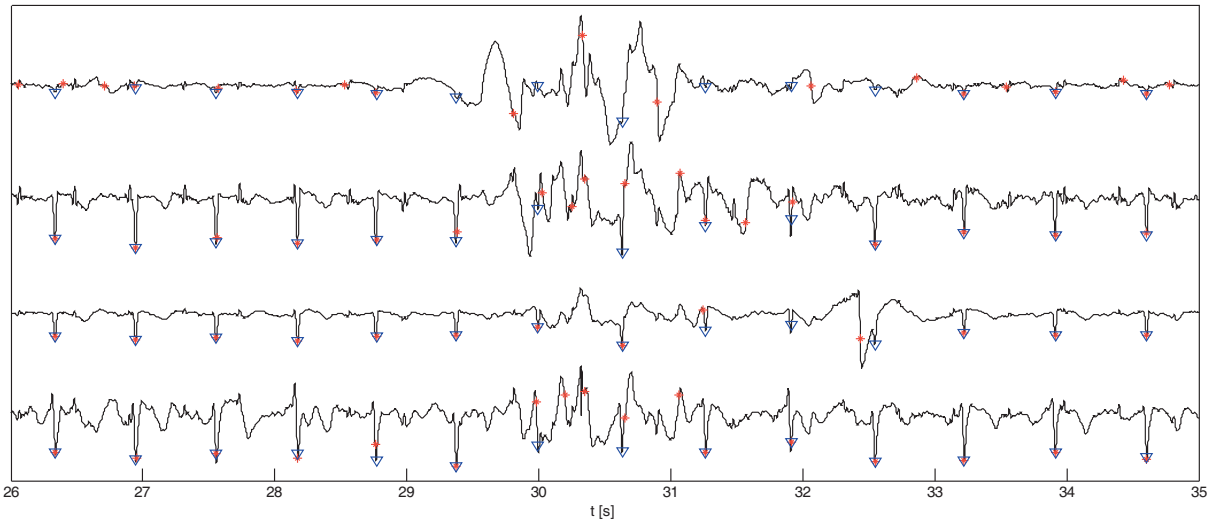

Figure 2.12: An example of multi-channel periodicity correction on *signal 30* of *dataset A*, where the red asterisks represent the peaks identified by the QRS detector and the blue triangles represent the corrections.

Since some artefacts can be simultaneously present in all the channel, a second strategy to enforce pseudoperiodicity has been implemented. Starting from the longest sequence of R peaks defining RR intervals respecting the pseudoperiodicity criterion, RR_m is used to forecast and correct, point by point, the occurrence of the next QRS, exploiting as tolerance the threshold of the pseudoperiodicity criterion, iteratively adapting its value as:

$$RR_m[n+1] = (1-\gamma)RR_m[n] + \gamma RR[n] \tag{2.11}$$

with $\gamma = 0.25$. An example of this strategy is shown in Figure 2.13, in which a noise peak affecting all the channels is at first identified by the maternal QRS detector (red asterisks) in every channel and finally corrected according to the *RRm*. In the zoom it is possible to observe the noise peak and the applied correction.

Extraction and subtraction of maternal average QRS template

Time position of the maternal QRS complexes can be used to extract one or more average templates from each channel to be subtracted. In fact, maternal morphology is different in every channel due to the different projections on the maternal abdomen. This is also the reason because an algorithm completely blinded to the electrodes positioning is necessarily suboptimal and must include additional features, otherwise redundant. The block diagram related to the maternal QRS subtraction is shown in Figure 2.14.

The quality of the subtraction is strongly affected by the alignment of the signals. When the alignment is performed looking at the cross-correlation of the template with the candidate part of the signal, one possibility to improve the alignment is to pursue a more detailed waveform in terms of time resolution. This means that the original signal could be upsampled and low-pass filtered in order to increase its sampling rate even though obviously no information is added. Such an approach has been also described in [52] and is common to other biomedical signal processing problems such as neural spike sorting [77]. We chose to upsample the signal to 8 kHz before extracting and subtracting the average templates. In

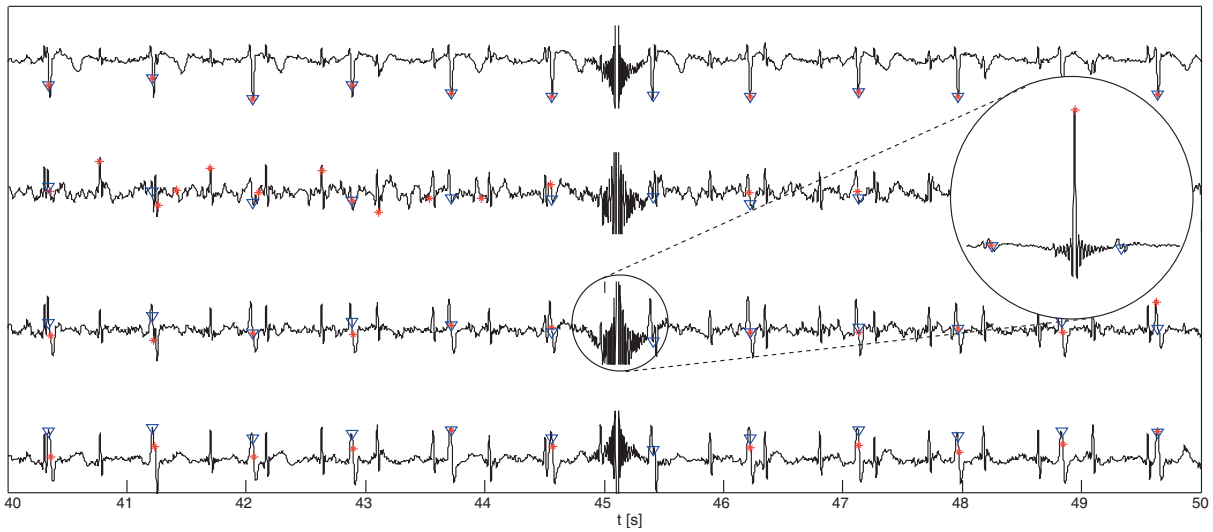

Figure 2.13: An example of the final periodicity correction on *signal 15* of *dataset A*, where the red asterisks represent the peaks identified by the QRS detector and the blue triangles represent the corrections. In the circle, a zoom of an artefact.

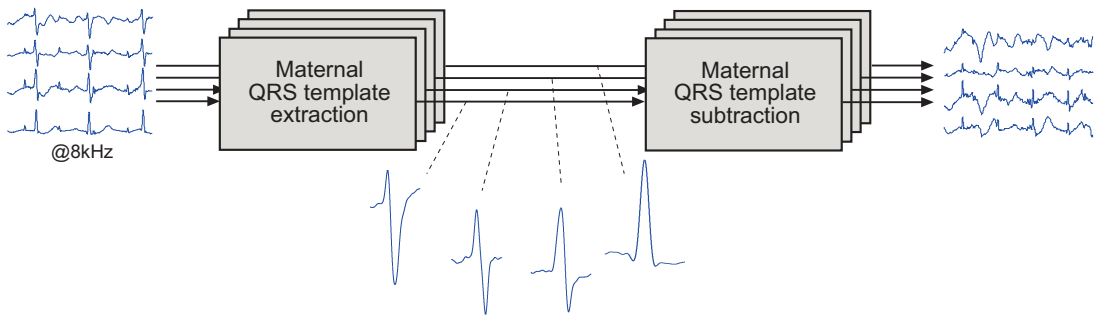

Figure 2.14: Block diagram of the extraction and subtraction of maternal average QRS template.

every signal, for each identified maternal QRS, a window of $N = 1600$ samples is extracted around the R peak. If it represents the first QRS complex extracted from that signal, it is assumed as a template, otherwise the normalized cross-correlation of the extracted complex with the previously acquired templates is evaluated to identify the best match. The length of the cross-correlation sequence is 2.5% of N: if its maximum exceeds a threshold of 0.85, the extracted QRS complex undergoes a weighted synchronized averaging with the best-matching template to refine it, smoothing over the random noise components, otherwise it becomes a new template because its morphology can be considered different. The threshold of 0.85, in a possible interval [0, 1], has been empirically chosen to maximize the performance on the *dataset A*. Negative values of the correlation can be a priori excluded because polarity matching is relevant in this context.

At the end of the analysis, only the templates coming from the averaging of at least 20 QRS complexes per minute of the signal are considered for subtraction, in order to avoid the presence of residual noise or fetal R peaks. For the maternal QRS cancellation, the conventional cross-correlation beat alignment technique is used to align the best matching average template with each candidate QRS complex. The average template with the highest corre-

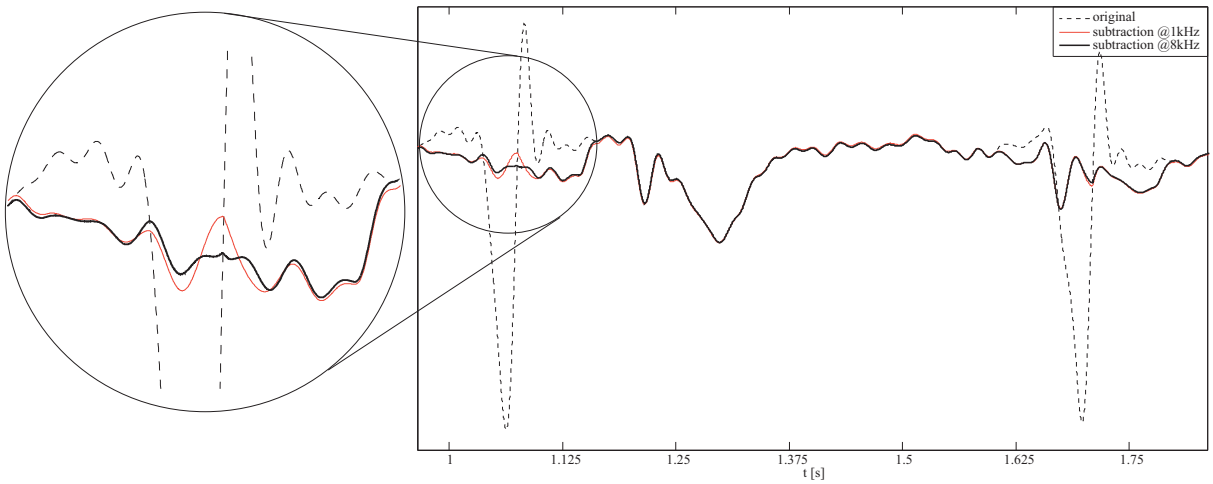

Figure 2.15: An example of subtraction of the maternal average template on signal 39 of *Dataset A* @1000Hz and @8000Hz.

lation is then multiplied by a Tukey cosine-tapered window [78] (with the ratio of taper to constant sections fixed to 0.2) before subtracting, to avoid the generation of artificial peaks on the borders of the subtraction window. This could still leave depressed areas in case the isoelectric line would be different from zero but the following stages are not affected by such an artefact. Furthermore, a corrective gain is applied to the template before subtraction, according to the maximum and minimum amplitude of the signal, in order to improve the subtraction quality. An example of subtraction of the average maternal template is shown in Figure 2.15. The zoom allows evaluating the impact of the upsampling on the subtraction quality, whereas the second beat on the right shows the effect of the subtraction when maternal and fetal QRS complexes overlap. The computation of a template by synchronized averaging of repetitive noisy events is well known in literature for its ability in reducing random components of the signal emphasizing the deterministic ones [52]. The use of this strategy allows to remove the main maternal deterministic components, while leaving unchanged both the fetal and the noise sources, where the latter can hide the first or be comparable to its amplitude.

FECG enhancement

After subtracting maternal QRS complexes, the signal is downsampled back to 250Hz to reduce the computational cost. Then, it is band-pass filtered between 6 and 45 Hz, to attenuate maternal P and T waves, through a cascade of a low-pass filter (order 112) and a high-pass one (order 140), designed as those in the preprocessing stage and applied in a forward-backward mode. The low-pass filtering is performed to smooth over the signal after the subtraction, thus not being redundant with respect to the preprocessing. The high-pass filtering, which allows the reduction of the maternal P-T residual components, is performed as a post-processing stage which can in principle be replaced by a subtractive stage similar to the one presented for the QRS components.

The output signal could still hide the small FECG contribution, unless it was clearly visible since the beginning. Due to the short time support of the fetal QRS complexes and the similarity with the residual noise, the previous attempt to identify the fetal QRSs with

a template matching strategy led to unsatisfactory performance performance. In such a noisy contest, Blind Source Separation (BSS) algorithms have been proved to be effective in estimating sources even when they are not recognizable to the naked eye. For this reason, having removed the highest maternal interferences, the application of BSS algorithm as (not-underdetermined) ICA become more respectful of their fundamental assumptions. We chose to apply the JADE algorithm [79] to the whole signal avoiding the possible permutation risks of on-line ICA algorithms for this application [55].

Fetal QRS detector

The final step of the algorithm involves the identification of the fetal QRS complexes in the estimated sources. As for the maternal QRS detection, in principle it is possible to use a QRS detection algorithm from the literature, but these algorithms have not been specifically designed for the FECG, which usually presents higher HR compared to an adult's ECG, lower SNR and, at the output of an ICA algorithm in particular, relevant morphological alterations. Moreover, due to the ICA permutation ambiguity, an algorithm which supports the final identification of the fetal channel among the extracted sources is required. To this aim, a QRS detector partially taken from the FECG tracking algorithm described in 2.1 has been used. In fact, this method has been developed for the autonomous tracking of the output permutations of on-line ICA algorithms for fetal ECG extraction, showing better performance in tracking the fetal source of interest with respect to other simple detection algorithms. The main characteristic of the chosen approach is its ability in emphasizing the difference between noisy channels (that exhibit a large number of peaks) and ECG signals (that exhibit some psudo-periodicity). It includes digital filters to create *feature signals* for the different channels and a decisional stage, which has not been used here. This approach allows preserving small fetal R peaks when they are comparable to the noise ones, also taking into account the small temporal support of the fetal QRS.

At this point, an adaptive threshold similar to the maternal stage (but with 60% of the 6th highest value in a 1-second window, and an interval of only 6 samples around the candidate sample) is used to detect the fetal QRS complexes. This algorithm is applied to all the four estimated sources. Then, the periodicity corrector is applied to each RR series without any possibility of exploiting the information from the other channels to perform the correction of single beats. The FECG channel is supposed to be the one with the minimum number of corrections, since the noise channels don't have any pseudoperiodicity. The information coming from the pseudoperiodicity corrector can also be used as an index of reliability of the obtained results in a real clinical scenario. In fact, if several corrections are required to improve the psudo-periodicity of the RR sequence, the obtained results will probably be inadequate, coming from the attempt of the corrector to estimate the missing peaks positions. Furthermore, in order to avoid the risk of detecting residual maternal components after the subtraction, the median RR interval of each channel is compared to the median maternal one. An example of detection of the fetal QRS complexes is shown in Figure 2.16.

2.2.2 Algorithm evaluation

As described in [80, 81], the entries of the competition were scored using functions implemented in the WFDB software package [82] for the fetal HR (FHR) and the fetal RR time series. The first score is obtained as the mean square error between the fetal heart rate time

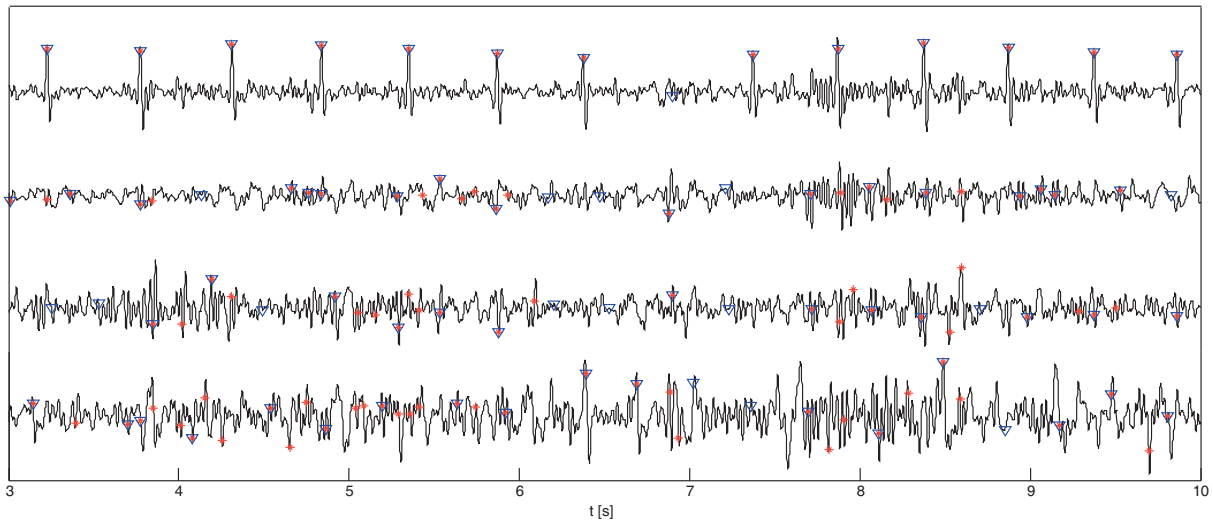

Figure 2.16: An example of the identification of the fetal source after ICA in the first channel and the effect of the periodicity corrector on *signal 3* of *dataset A*, where the red asterisks represent the peaks identified by the QRS detector and the blue triangles represent the corrections.

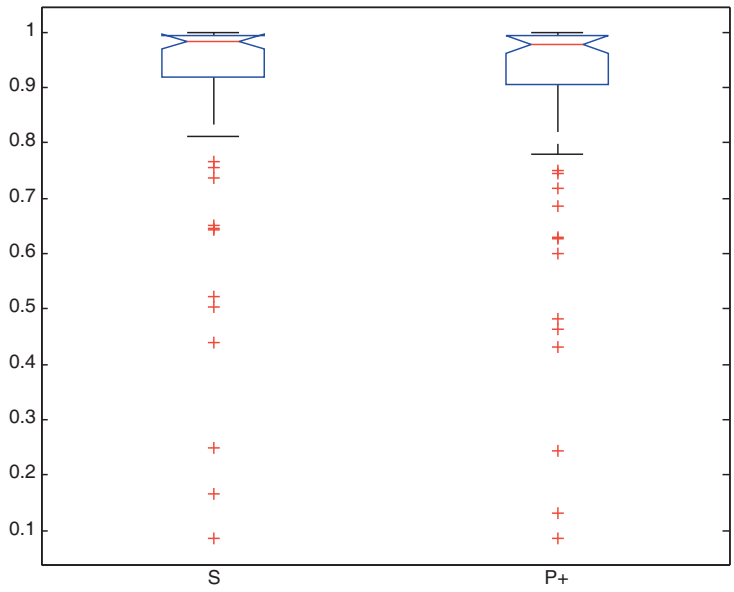

Figure 2.17: Boxplot of the sensitivity S and positive predictivity P+ for dataset A.

	Dataset A	**Dataset B**	**Dataset C**
Score 1 (bpm^2)	91.38	134.49	281.11
Score 2 (ms)	10.18	12.38	25.93

Table 2.2: Table of average results (events 1 and 2) on Dataset A (N=75), B (N=100) and C(N=272)

data	#ann	#det	S	P+	Sc1	Sc2	*data*	#ann	#det	S	P+	Sc1	Sc2
1	150	140•••	0.99	0.99	0.0029	0.98	39	140	130•••	0.99	0.99	0.0007	1.2
2◇	160	100•◦◦	0.64	0.63	13	20	40	150	140•••	0.96	0.95	0.011	2.6
3	130	130•••	0.98	0.98	0.16	1.1	41	140	130•••	0.99	0.99	0.00035	1.2
4	130	130•••	1	0.98	22	0.84	42	150	150•••	0.98	0.98	0.0014	1.3
5	130	130•••	0.99	0.99	0.00094	1	43	160	160•••	0.99	0.99	0.0044	1.1
6◇	160	120•◦◦	0.74	0.69	370	27	44	160	160•••	0.98	0.98	0.0025	1
7◇	130	84•◦◦	0.65	0.6	51	20	45	140	140•••	0.99	0.97	0.013	2.9
8	130	130•••	1	1	0.0016	0.86	46	130	130•••	0.96	0.96	0.005	1.2
9◇	130	11•◦◦	0.085	0.087	120	27	47	140	130••◦	0.88	0.92	100	17
10◇	180	130•◦◦	0.75	0.75	36	19	48	130	130••◦	0.97	0.95	0.0052	1.5
11◇	140	91•◦◦	0.65	0.63	110	17	49	150	140•••	0.93	0.93	5.7	5
12	140	140•••	0.99	0.99	0.21	1.3	50	140	140•••	0.98	0.97	0.0025	3.5
13	130	130•••	1	1	0.0026	0.9	51	140	130•◦◦	0.92	0.9	7.7	8
14	120	120•••	0.98	0.98	0.3	6.2	52	130	110••◦	0.84	0.78	160	14
15	130	130•••	1	0.99	3.7	1.1	53	150	150•••	1	1	0.0059	1.3
16◇	130	68•◦◦	0.52	0.46	340	31	54◇	37	30••◦	0.81	0.24	3800	130
17	130	130•••	0.99	0.99	0.0031	1.3	55	140	140•••	0.99	0.99	0.17	1.5
18◇	150	66•◦◦	0.44	0.43	210	29	56◇	130	100•••	0.77	0.72	6.1	23
19	130	130•••	1	1	0.00098	0.66	57	150	150•••	0.99	0.99	0.0012	0.69
20	130	130•••	1	0.98	0.0013	0.82	58	140	140•••	1	1	0.0018	0.57
21◇	150	110•◦◦	0.77	0.74	21	20	59	150	150•••	0.99	0.99	0.001	1.2
22	130	130•••	1	1	0.00074	1	60	150	140••◦	0.92	0.91	0.019	10
23	130	130•••	1	1	0.00064	0.7	61	140	140•••	0.99	0.98	29	1.3
24	120	120•••	1	1	0.0024	0.81	62	140	140•••	0.99	0.99	0.0028	1.4
25	130	130•••	1	1	0.0072	0.82	63	140	140••◦	1	0.99	0.002	1.2
26	140	140•◦◦	0.99	0.99	0.0034	2.7	64	140	130•••	0.97	0.97	0.00071	4.6
27	140	120•◦◦	0.87	0.87	20	14	65	140	140•••	0.99	0.99	0.014	0.97
28	170	160•••	0.98	0.98	22	1.1	66	130	130•••	0.97	0.97	0.071	5.3
29◇	130	21•◦◦	0.17	0.13	680	27	67	150	150•••	0.97	0.97	0.0052	6.6
30	140	120••◦	0.84	0.84	13	17	68	140	140•••	1	0.99	0.0056	1.5
31	140	140•••	0.99	0.99	0.0054	3.1	69	150	150•••	0.97	0.97	0.024	7.7
32	150	150•••	1	1	0.0011	1	70	140	140•••	0.99	0.99	0.0011	0.82
33	140	130•••	0.94	0.9	260	120	71◇	150	77•◦◦	0.5	0.48	92	27
34	130	130•••	0.98	0.96	0.0053	1.6	72	170	170•••	0.99	0.99	0.014	1.5
35	160	160•••	0.96	0.95	0.0069	2.6	73	140	130••◦	0.93	0.91	0.0039	7.7
36	170	170•••	0.99	0.99	0.0035	1.5	74	140	130•••	0.94	0.93	16	13
37	140	140•••	0.99	0.99	0.0039	1.1	75	130	130•••	0.99	0.99	0.0017	1.6
38◇	160	39•◦◦	0.25	0.24	340	32	-	-	-	-	-	-	-

Table 2.3: Results achieved on *dataset A*: *data* is the identification number of the signal, *#ann* is the number of annotated fetal QRSs in the dataset, *#det* is the number of fetal beats detected by this algorithm, *S* is the Sensitivity, *P+* is the Positive Predictivity, *Sc1* is the first score referred to the FHR time series in bpm^2, *Sc2* is the second score referred to the FRR time series in ms. On the *data* column, a ◇ identifies the outliers represented in the boxplot in Figure 2.17. The symbols near to the value of *#det* refer to the trustworthy of the obtained results, computed considering the sum of the removed peaks and the double of the added peaks(••• trustworthy result, index ≤ 30; ••◦ reasonably trustworthy result, index >30 & ≤ 50; •◦◦ not trustworthy result, index >50)).

series estimated from both the test and reference annotation according to the WFDB TACH function [83]. The second one is obtained comparing the RR series using the MXM function [84] which calculates the scores by picking the closest RR pair between both time series and measuring the mean square error distance. For *dataset B* (N=100) and *dataset C* (N=272), only the mean scores are produced and, for the proposed algorithm, they are reported in Tab. 2.2 whereas for *dataset A* (N=75) is possible to better analyse the algorithm performance according to the signals characteristics. In order to provide a comparable assessment of the proposed algorithm, a full evaluation of the algorithm on each signal of the *dataset A* has been reported in Tab. 2.3. It includes the number of annotations provided with the dataset, the number of fetal QRSs detected by this algorithm, the sensitivity, the positive predictivity, and the two scores used in the challenge. The sensitivity *S* is defined as TP/(TP+FN) whereas the positive predictivity *P*+ is defined as TP/(TP+FP), where TP is the number of true positive detections, FN is the number of false negative detections, and FP is the number of false positive detections. A reliability index, computed as the sum of the number of removed peaks and the double of the number of the added ones, which could be not trustworthy, has been added to the Tab. 2.3 with a different symbol for different range that have been empirically derived on dataset A (≤ 30, >30 & ≤ 50, >50) to provide an evaluation metrics for the user. The distribution of the results is inhomogeneous in the dataset so that, beyond the mean, it is more interesting to analyse the actual distribution of such parameters. To this aim, in Figure 2.17 is reported the boxplot for the sensitivity and the positive predictivity to allow a quick evaluation of the global performance on *dataset A*. As we can observe, the median values for sensitivity and positive predictivity are respectively 0.982 and 0.976, but there are some outliers which affect the results of the algorithm. The outliers are marked in Tab. 2.3 with a $\diamond$ symbol in the $data$ column. Due to the huge distance of some outliers from the median values, the boxplot for the other scores has not been included because of its little readability.

The algorithm globally shows good performance in the identification of the fetal peaks position,comparable to those of the top 3-4 algorithms in the Challenge, as from the official results. From a morphological viewpoint, beyond possible distortions caused by the maternal QRS template subtraction, the tight bandwidth imposed in the preprocessing stage, and the P and T wave cancelling, prevents the exploitation of the signal with attenuated maternal ECG interference for the FECG waveform analysis, which was not the aim of the algorithm, all the more so for the signals coming out from the ICA stage. Nevertheless, for overlapping peaks, the proposed template subtraction is usually able to preserve the fetal QRS shape (when it is distinguishable), as results from a fetal template matching study.

The analysis of the *dataset A* enables the study of the behaviour in specific situations. On signals 29 and 38 , for instance, the low maternal signal quality hampers the identification of the maternal QRS templates and consequently is not possible to identify any fetal beat, obtaining a very bad score. This information (any maternal average template found) can be used as an index to forecast the bad quality of the fetal estimation. More generally, a low intensity of the FECG despite the maternal QRS subtraction and filtering affects the BSS output quality, compromising the final detection (e.g., signals 7 and 11).

A unique behaviour is observed on signal 9, where the maternal heart rate suddenly changes in the middle of the signal from a mean value of 80 bpm to 110 bpm. In this really clean signal, the correlation level is low enough to prevent the identification of 2 different maternal QRS templates, even though the support of the QRS complexes changes over time. This reduces the quality of the subtraction of the average template leading to a bad

global performance. Another problem can be related to the residual presence of maternal P and T waves after the last band-pass filtering, which probably could benefit from a specific subtraction technique (e.g., signals 18 and 71). To this aim the open-source code has been implemented as a framework in which every single stage (including P-T waves filtering) can be easily replaced by a different approach.

A more detailed analysis of the annotations provided for *dataset A* highlights some further problems. In fact, usually the provided annotations are not well centred on the fetal R peaks whereas in literature they are usually identified as the median of the positions provided by a panel of experts manually annotating the dataset, and then the results of a detection algorithm are evaluated with a tolerance related to the standard deviation of these data [85]. However, in the field of the fetal ECG research, it is really difficult to provide such an estimation, and in the best case the annotations are provided thanks to a reference signal from a scalp electrode. Starting from these considerations, no strategy for centering the final annotations on the R peak positions has been included, necessary in a real scenario to improve the quality of the provided estimation. Moreover, in some signals (e.g., signal 54) the annotations are provided only for a small part because of the presence of some sporadic noise waves, although the fetal beats remain visible. For this signal, the results in Tab. 2.3 show how the algorithm correctly identifies the largest part of the fetal R peaks, obtaining a good sensitivity score and a bad positive predictivity score because of the high number of annotations considered as false positive in comparison with the provided ones.

Moreover, it should be taken into account that the scoring criteria of the challenge imply that a bad detection is better than a missing estimation. It is worth to note that such approach is unsuitable for a real clinical application, where an uncertain estimation of the fetal HR should not be used for any evaluation. In a real scenario, the algorithm should not provide any estimation of the frequency every time the periodicity corrector needs to heavily intervene on the RR sequence to enforce a pseudoperiodicity, which is still acceptable for the maternal QRS detection. To this aim in Tab. 2.3 an evaluation index in the form of a 3-values range of the obtained results based on the information extracted by the pseudoperiodicity corrector has been added. Such evaluation index could be useful in a clinical context to evaluate the trustworthiness of the detection. A full evaluation of the algorithm would require an autonomous clinical study apart from this work. In fact, beyond the data of the contest, no clinical information is provided about how and when the signals have been acquired. Also, the evaluation of the clinical utility of the results produced by an algorithm cannot only rely on numerical performance figures without a deeper analysis including the important step of signal acquisition and clinical needs.

Despite the algorithm has been developed apart from the real-time requirements according to the contest evaluation criteria, it can be in principle adapted to work on-line (as for a real clinical scenario) by implementing the algorithm in the form of block on-line processing, using causal FIR filtering, on-line ICA algorithms as [55] and providing both the template matching algorithm and the periodicity corrector with a set-up stage.

2.2.3 An alternative approach: Wavelet Denoising instead of ICA stage

Since the main problem of the identification of the fetal QRSs is related to the high noise level still present after the subtraction of the maternal components, a different strategy that

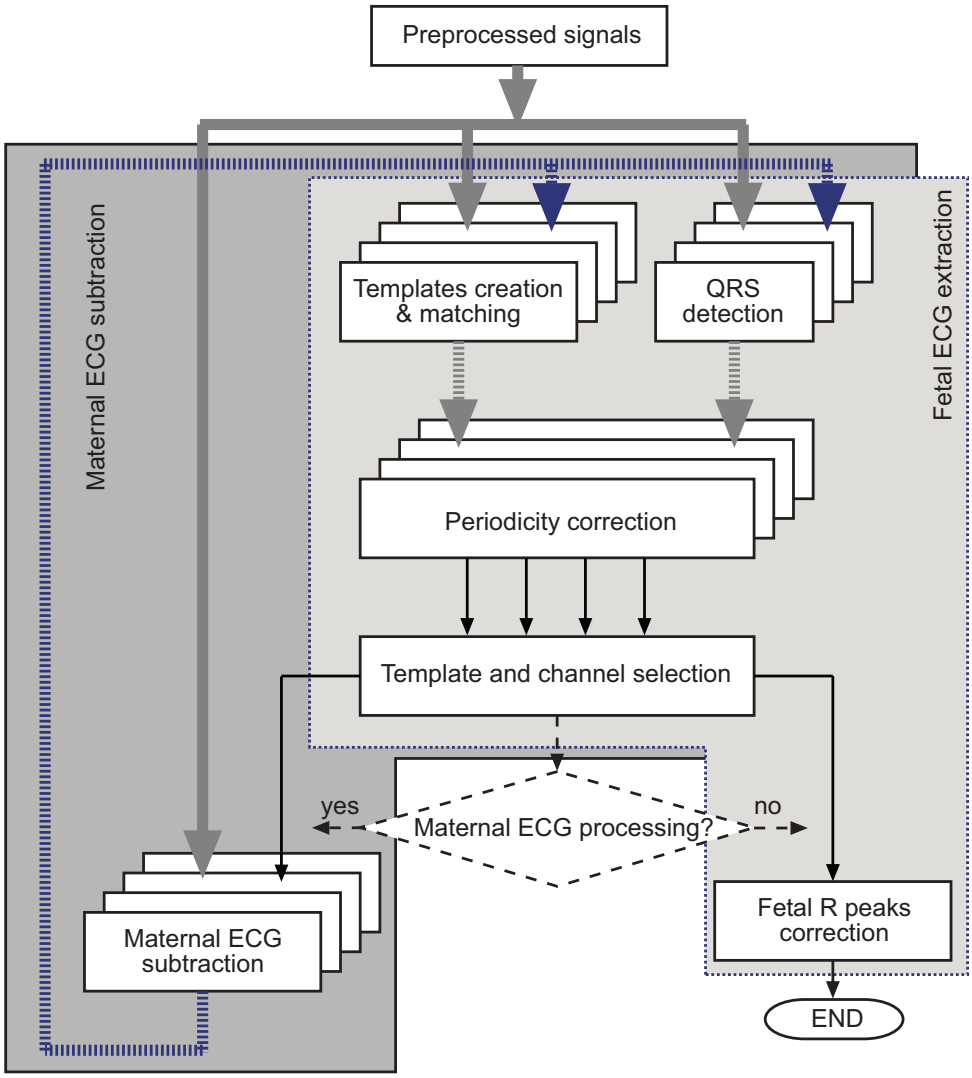

Figure 2.18: The block diagram of an alternative approach based on wavelet denoising for the identification of the fetal QRS complexes in low-electrode dentity recordings

has been tested and described in [86], alternatively to the BSS, is a wavelet denoising stage applied to all the four channels both before and after subtraction, in order to highlight the QRSs and improve the quality of a multi-channel QRS detector. The block diagram of this alternative algorithm is shown in Fig. 2.18.

As the one described in the previous section 2.2.1, this algorithm is mainly based on the subtraction of a maternal QRS average template exploiting correlation but wavelet denoising is applied on each channel to improve peak detection. The *bior6.8* mother wavelet, with 3 decomposition levels, has been used, clearing the approximation signal and hard thresholding the details exploiting a minimax scaling for the median absolute deviation of the signal, computed at each scale. The resulting signal undergoes a peak detection based on a modified version of the Balda QRS detector [63]. For every peak identified in the WD processed signal (which can belong to the mother or to the fetus), a 200ms window at 1000 Hz centred on the maximum of the feature signal is extracted and cross-correlated with the templates present at the moment. If the correlation is below a threshold of 0.8, the extracted window creates a new template, otherwise it undergoes a weighted synchronized averaging with the

best-matching template. At the end, the similar templates are merged and the two most frequent ones used for a global cross-correlation. The points where the cross-correlation exceeds 0.85 are marked, defining a temporal series. Similarly to the algorithm in section 2.2.1, a periodicity corrector is applied in each channel, but taking into account the possible presence of two temporal series belonging to maternal and fetal beats. Maternal temporal series is then identified taking into account the lower heart rate and the extracted template is used for subtraction. The same approach is then used for the fetal QRS complexes detection, with adapted thresholds, including the periodicity corrector with an higher tolerance as an higher heart rate variability is expected for fetal heart rate.

The algorithm has been evaluated according to the same scoring criteria described in 2.2.2 at page 35, achieving a score of 639.465 bpm^2 and 23.821 ms on dataset B and of 684.158 bpm^2 and 47.990 ms on dataset C. The score related to the fetal heart rate is quite high, suggesting that the algorithm produces more false negatives than false positives, underestimating the fetal heart rate whenever the maternal ECG is erroneously assumed to be representative of the fetal one. The algorithm tends to identify in any case the fetal R peaks, even where they cannot be detected, producing a large number of false positives if no fetal R peaks are present, and of false negatives when it tracks the residual maternal ECG rather than the fetal ECG. The algorithm took part to the *PhysioNet/Computing in Cardiology Challenge 2013* [87], entering into the top ten best-performing open-source algorithms presented at the challenge.

Chapter 3

Non-Invasive fetal ECG Signal Acquisition

Since FECG signal processing is strongly affected by the acquisition quality, the research work was also focused on improving the SNR at the recording stage. In fact, non-invasive FECG signals have a magnitude comparable to, or are even smaller than the noise levels commonly found in biopotential recordings, and the maternal QRS might be even 10 times bigger than fetal QRS. This problem is emphasized when dealing with a telemonitoring setup with respect to a standard acquisition in a clinical setting, because both the acquisition setup (e.g., electrodes positioning) and patient's environment considerably influence the quality of the results.

One of the main problem in physiological signals acquisition is the high impedance due to the skin-electrode contact. This high value causes the reduction of the signal strength because of the loading effect and the decrease of the common-mode rejection capability of the acquisition system, causing the introduction of more noise in the signals. In order to reduce the skin-electrode contact impedance in FECG, different electrode models have been tested, taking into account the specific needs of the application on the maternal abdomen, treating the skin with mechanical or chemical scrubs to remove the stratum corneum and testing conductive gels typically used for electroencephalographic applications.

Furthermore, a study on textile conductive electrodes has been started with the *DEALAB Innovative Devices and Materials laboratory* of the University of Cagliari to evaluate the effect of this new technology in FECG acquisition. In fact, the conception of a wearable band for the maternal abdomen providing low skin-electrode impedance without any skin treatment and without adhesive, would improve the acquisition quality and setup, both for the use at home or in a clinical setting.

Driven by the need of investigating specific aspects connected to the signal acquisition setup and of developing a telemonitoring system, a custom portable biopotential acquisition module has been evaluated.

All these aspects are discussed in the following sections.

3.1 Evaluation of Body Surface Electrodes for Non-Invasive FECG Acquisition

The major acquisition problems when using body surface recording electrodes to acquire low amplitude signals such as non-invasive fetal ECG are:

- how to attach these electrodes to the patient's skin;
- how to reduce the impact of patient's movements on the acquired signals;
- how to reduce the high impedance of the skin, especially when it is dry or hairy;
- how to choose the best skin surface area for connection.

All these problems are emphasized in home telemonitoring applications because it would probably requires the patient to autonomously position the electrodes. Also, patient's movements are typically present in long term monitoring applications.

High skin-electrode impedance values cause the reduction of the signal strength and have been correlated to signal distortion, making the recorded ECG unusable from a clinical point of view. Despite the greatest part of the modern biomedical signal acquisition systems are based on MOSFET amplifiers which present high input impedance, when small biopotentials like FECG are recorded, noise generation (that is proportional to the impedance) becomes more important and need to be minimized.

Every resistor exhibits a certain amount of thermal noise, but the noise originating from the electrode-skin interface is higher than the thermal noise corresponding with the resistance of electrodes and tissues. For this reason some effort has been put on different strategies to reduce the skin-electrode contact impedance in non-invasive FECG, by testing different electrode models (chosen taking into account the specific needs of the application on the maternal abdomen), treating the skin with mechanical or chemical scrubs to remove the stratum corneum and using conductive gel typically adopted in electroencephalographic applications.

3.1.1 Electrodes for biopotential acquisition

Biopotential electrodes are transducers that convert the ion currents in the body into a current carried by moving electrons, allowing the acquisition of the potentials generated by the human body [88, 89]. A negatively charged ion is an anion and a positively charged ion is a cation. At the interface between an electrode and an ionic solution, redox (oxidation-reduction) reactions need to occur for a charge to be transferred between the electrode and the solution. These reactions can be represented in general by the following equations:

$$C \leftrightarrows C^{n+} + ne^{-} \tag{3.1}$$

$$A^{m-} \leftrightarrows A + me^{-} \tag{3.2}$$

where n is the valence of cation material C, and m is the valence of anion material, A. The cations in solution and the metal of the electrodes are assumed to be the same, so the atoms C are oxidized when they give up electrons and go into solution as positively charged ions. These ions are reduced when the process occurs in the reverse direction. In the case

of the anion reaction the directions for oxidation and reduction are reversed. So, the flow of ions in the electrolyte give rise to a flow of electrons in the electrode due to a redox reaction occurring at the interface. By this way, the anions in the electrolyte will flow to the interface boundary. Cations in the electrolyte will flow away from the interface boundary. To counteract this, electrons in the electrode will flow away from the interface boundary creating a current in the electrode. This process is called oxidation of the metal.

The interaction between a metal in contact with a solution of its ions produces a local change in the concentration of the ions in solution near the metal surface. This causes charge neutrality not to be maintained in this region, causing the electrolyte surrounding the metal to be at a different electrical potential from the rest of the solution. Thus, a potential difference known as the half-cell potential is established between the metal and the bulk of the electrolyte. Different characteristic potentials occur for different materials. These half-cell potentials can be important when using electrodes for low frequency or dc measurements. They are usually measured with respect to the standard hydrogen electrode.

When two ionic solutions of different activity are separated by an ion-selective semipermeable membrane that allows one type of ion to pass freely through the membrane, an electric potential E will exist between the solutions on either side of the membrane, based upon the relative activity of the permeable ions in each of these solutions. This relationship is known as the *Nernst equation*:

$$E = -\frac{RT}{nF} \ln \frac{a_1}{a_2} \tag{3.3}$$

where a_1 and a_2 are the activities of the ions on either side of the membrane, R is the universal gas constant, T is the absolute temperature, n is the valence of the ions, and F is the Faraday constant. The half-cell potential or the Nernst potential appears when no electric current flows between an electrode and the solution of its ions. If there is a current the potential changes and the difference between this potential and the half-cell potential is known as over voltage. It is caused by an alteration in the charge distribution in the solution in contact with the electrode. There are two main categories of electrodes:

- Perfectly polarizable electrodes: no actual charge crosses the electrode-electrolyte interface when a current is applied (the electrode behaves as a capacitor);
- Perfectly nonpolarizable electrodes: the current passes freely across the electrode-electrolyte interface, so there is not any overpotential.

The polarization effect can result in diminished electrode performance, especially under conditions of motion. These types of electrodes can not be fabricated in practice, but there are electrode structures that closely approximate their characteristics. Electrodes made from noble metals such as platinum are often highly polarizable. These electrodes can create serious limitations when movement is present and the measurement involves low frequency or even dc signals. In fact, when the electrode moves the change in charge distribution in the solution adjacent to the electrode surface produces a voltage change in the electrode that will appear as motion artefact in the measurement. For this reason nonpolarizable electrodes are usually preferred for most biomedical measurements.

The Ag-AgCl electrode has characteristics similar to a perfectly nonpolarizable electrode and is practical for use in many biomedical applications. It consists of a silver base structure that is coated with a layer of the ionic compound silver chloride. Since there is a minimal

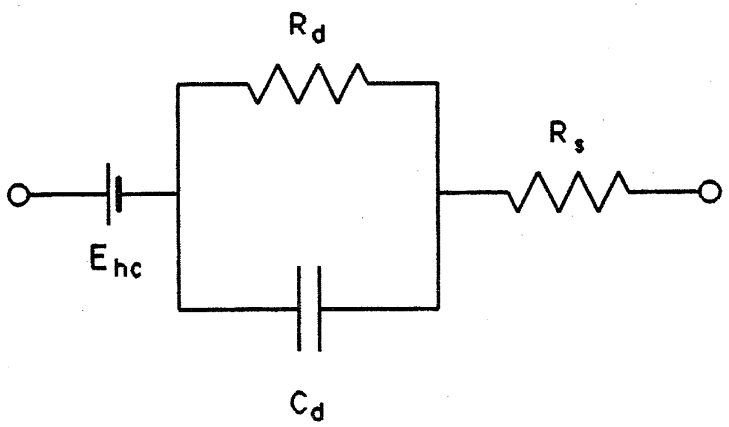

Figure 3.1: Equivalent circuit for a biopotential electrode in contact with an electrolyte, figure taken from [89].

polarization associated with this electrode, motion artefact is reduced and there is also a smaller effect of frequency on electrode impedance, especially at low frequencies.

The electric characteristics of biopotential electrodes are generally nonlinear. Under idealized conditions, electrodes can be represented by an equivalent circuit of the form shown in Fig. 3.1. In this circuit E_{hc} is the half-cell potential, R_d and C_d represent the impedance associated with the electrode-electrolyte interface and polarization effects, R_s is the series resistance associated with interface effects and is due to resistance in the electrolyte. The capacitance in the model takes into account the polarization effects. The equivalent circuit shows the frequency dependence of the electrode impedance. In fact, at high frequencies ($1/wC \ll R_d$) the impedance is constant at R_s. At low frequencies ($1/wC \gg R_d$) the impedance is constant but larger ($R_s + R_d$). At frequencies between these extremes, the electrode impedance depends on frequency.

When using body surface electrodes to acquire biopotentials from the surface of the skin we have to take into account the additional interface between the electrode-electrolyte and the skin. In clinical practice, an electrolyte gel or cream containing Cl^- is used to maintain good contact. The skin consists of three layers and the outermost one (epidermis), representing the interface with the electrolyte, is a constantly changing layer because of the cellular renewing. This process causes the formation of the stratum corneum, a layer of dead material that has different electrical characteristics from live tissues. The electrical model that takes into account also the interface between the electrolyte and the skin is shown in Fig. 3.2. R_s is the resistance associated with interface effects of the gel between the electrode and the skin. The epidermis is considered as a membrane semipermeable to ions, causing a potential difference E_{se} when there is a difference in ionic concentration. The epidermal layer is considered as a parallel RC circuit, whereas the dermis and the subcutaneous layer behave as a pure resistance. As we can observe from the figure, if the effect of the stratum corneum is removed or reduced (for example by vigorous rubbing using a pad soaked in acetone or alcohol or abrading with sandpaper) we can reduce E_{se}, C_e and R_e, improving the stability of the signal. Nevertheless the stratum corneum can regenerate in 24h. In the circuital model we have also the contribution of the sweat glands and ducts, shown by the broken lines, to take into account the potential difference between the lumen of the sweat duct and the dermis and subcutaneous layers and the wall of the sweat gland and duct (parallel R_pC_p).

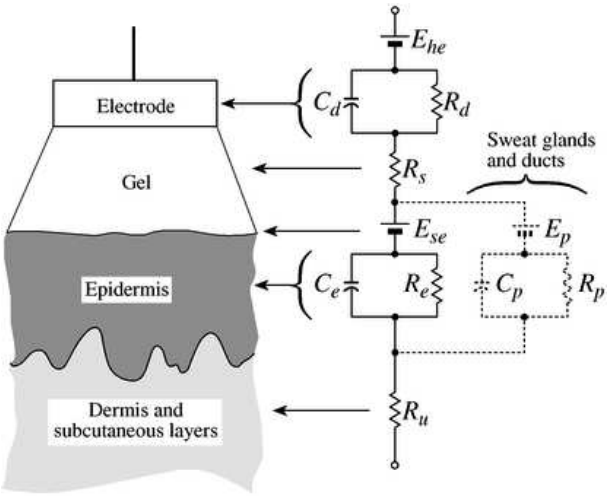

Figure 3.2: The total equivalent circuit for a biopotential electrode in contact with an electrolyte and the skin, figure taken from [88]

3.1.2 Electrodes classification

Many different forms of electrodes are available for different types of biomedical measurements [88]. Since we are mainly interested in investigating electrodes for non-invasive fetal ECG acquisition, we will focus our attention on body-surface recording electrodes.

Metal-plate electrodes

These electrodes are among the most used in biopotential acquisition. In their simplest form they consist of metallic conductor plate in contact with the skin. A terminal is placed on its outside surface near one end in order to attach the lead wire. They are usually made of German silver (a nickel-silver alloy) and require the use of electrolyte soaked pad or gel to maintain the contact. A more common variety of metal-plate electrodes are the metal disks, that have a lead wire soldered and are typically made of a disk of Ag with an electrolytically deposited layer of AgCl. They are usually secured to the patient chest wall by a strip of surgical tape or a plastic foam disk with a layer of adhesive tack on one surface. More commonly, pregelled disposable electrodes with the adhesive already in place are used in electrocardiographic monitoring systems. They usually consist of a relatively large disk of plastic foam material with a silver-plated disk on one side and a snap in the center of the other side to connect the acquisition system. These electrode are the most used in ECG because they are very easy to position, not requiring particular skill. They are usually stored in a foil envelope in order to prevent evaporation of the water component. Fig. 3.3 shows the structure of typical metal-plate and metal-disk electrodes.

Suction electrodes

These electrodes are similar to the metal-plates ones but do not require straps or adhesive to be secured on the patient skin. They consist of a hallow metallic cylindrical electrode that makes contact with the skin (Fig. 3.4). After the electrolyte gel is placed over the containing surface, the rubber suction bulb is squeezed and then released to apply suction against the skin, holding the electrode in place. They are frequently used for precordial leads ECG

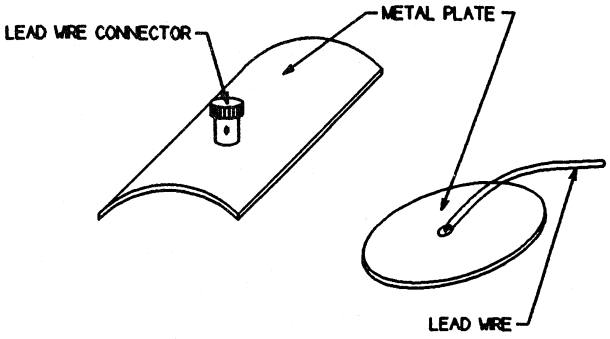

Figure 3.3: Examples of typical metal-plate and metal-disk electrodes, figure taken from [88]

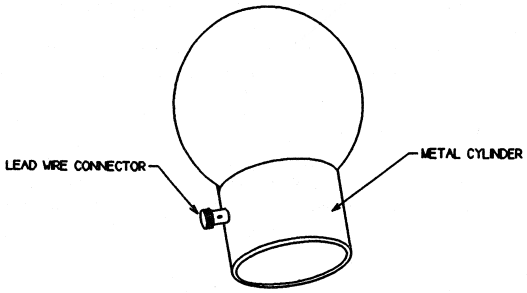

Figure 3.4: Metallic suction electrode, figure taken from [88]

acquisition for short periods of time to avoid irritation, but are not easily suitable for FECG acquisition. Fig. 3.3 shows the structure of typical metal-plate and metal-disk electrodes.

Floating electrodes

Since the motion artefact are mainly caused by the double layer of charge at the electrode-electrolyte interface, floating electrodes are used to stabilize the interface mechanically to reduce this problem. An example of floating electrode, called top-hat electrode, is shown in Fig. 3.5. In this structure the metal disk (typically made of silver coated with AgCl) is recessed in a cavity, so it is not in contact with the skin. Electrolyte gel is inserted in the cavity; the cavity and hence the gel does not move with respect to the metal disk, avoiding any variation of the double layer of charge. The electrode is filled with the gel and then attached to the skin by means of a double-sides adhesive-tape ring. These electrodes are found to be quite stable and are reusable after appropriate cleaning. The disposable version of these electrodes includes a disk of thin, open-cell foam saturated with electrolyte gel. Since the foam is fixed to the metal disk, the gel at the disk interface is mechanically stable. The other surface of the foam is able to move with the skin, reducing the motion artefact.

Flexible electrodes

Flexible electrodes can adapt to local curvature in body-surface. As shown in Fig. 3.6, their active element is made of a carbon-filled silicon rubber compound shaped as a thin strip or disk. The carbon particles make the silicon an electric conductor. Electrodes for monitoring

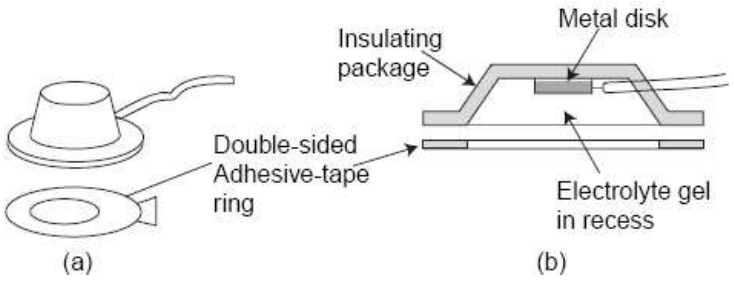

Figure 3.5: Floating electrodes structure, figure taken from [88]

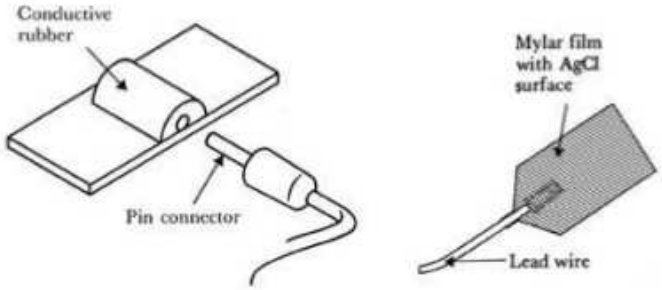

Figure 3.6: An example of carbon-filled silicon rubber flexible electrode and of a flexible thin-film electrode, figure taken from [88]

premature infants typically consist of a thin Mylar film on which Ag and AgCl film has been deposited. These electrodes are particularly flexible and are x-ray transparent. They need adhesive tape to be secured to the skin. New electrolytic hydrogel materials have been developed in the form of a thin flexible slab of gelatinous material, presenting a sticky surface and providing electrical conductivity thanks to the mobile ions. Nevertheless this material presents a relatively high electrical resistance with respect to that of the electrolyte gel and is less effective at hydrating the dry epidermial layer.

Electrode gel

The skin has a large impedance to current flow, mainly caused by the stratum corneum. An electrode gel or electrolyte is typically applied between the electrode and the skin to ensure the electrical contact and to prevent the reduction of the effective electrode area, caused by skin inhomogeneity or by hair. Some electrode gels contain abrasives to provide a better penetration on the skin, reducing the effect of the stratum corneum. Many commercial electrodes are pre-gelled, that means they include the electrode pastes in their structure. Mild abrasion of the skin with fine sandpaper can reduce the skin resistance with a factor 100 to 1000. Electrode gel must not cause too much skin irritation, especially in critical applications. Chloride concentration mainly determines the conductivity and the aggressiveness of the gel. Better electrolyte conductivity means less noise.

The composition of the electrolyte strongly influences the final impedance value. Different ions have different diffusion rates, some will move faster than others, creating a potential gradient. Potassium ions have mobility comparable to chloride ions. This is why potassium

chloride is used in preference to sodium chloride in better quality electrode gel.

3.1.3 Impedance evaluation of body-surface electrodes

As shown in the total equivalent circuit for a biopotential electrode in Fig. 3.2, there are two interfaces which contribute to the total impedance, one between the electrode and the electrolyte and one between the electrolyte and the skin. The first interface can be investigated by connecting two electrodes directly with an electrode paste. In skin impedance measurements, the electrode impedance is always included, but, when using low-impedance electrodes, the skin impedance is dominating. The layer of dead cells in the epidermis causes the largest impedance to current flow. The total impedance can be up to 5 MΩ.

The differences in impedance values between different electrodes are caused by various factors:

- electrode area: the impedance is inversely proportional to the area covered by electrode gel, but as the area is increased the information acquired becomes less selective;
- time of application: a trend of variation can be typically observed over time, that can be explained by initial contraction of pores due to cold gel that cause a high impedance value, the further penetration and spreading of electrolyte through the skin and the diffusion with sweat (decreasing trend), the recovery of the skin abrasion and of the stratum corneum together with the electrode gel drying (increasing trend);
- the condition of the skin: skin impedance is different for different subjects and between different parts of the body; skin abrasion reduce impedance value;
- the use and the composition of the electrode gel.

These characteristics make extremely difficult the prediction of the impedance values in real applications, highlighting the importance of using specific signal acquisition systems with high input impedance amplifiers, to prevent the recorded biopotentials being altered by impedance variations.

Since lowering the impedance results in less noise, skin abrasion and the use of an electrode paste is necessary in low-noise biopotential recording. For this reason a study of the distribution of impedance over the body, of the best skin treatment to reduce the skin impedance and of different commercial electrodes that can be used for non-invasive FECG application has been conducted.

Since disposable electrodes are more suitable for fetal ECG application with respect to the reusable ones because of their easier application and hypoallergenic condition, and taking into account the need of long-term monitoring application, we focused our attention on disposable electrodes.

Among the wide variety of available disposable commercial body-surface electrodes, the following have been selected:

- Kendall H135SG (Fig. 3.7a): this Ag/AgCl electrode can be used for short-term monitoring of EEG, ECG and EMG. It has a pre-gelled adhesive side with non-irritating gel, especially developed to prevent allergic reactions. The foam electrode is latex free and therefore suitable for every skin type. The snap-on connector can easily be pushed on or removed from the electrode lead. The diameter of the electrode is 35 mm.

- Kendall MediTrace MT133 (Fig. 3.7b): Ag/AgCl electrode for both short-term and long-term adult and pediatric ECG monitoring with a diameter of 30 mm. The conductive adhesive hydrogel maximizes adhesion and electrical contact and is designed to stay fresh up to 45 days out of the package.
- Kendall Care CA510 (Fig. 3.7c): Ag/AgCl tab electrode for resting ECG with large surface area (33x32mm) frequently used because of its easy application, high quality and comfort. This electrode is latex-free, x-ray transparent and with conductive adhesive hydrogel for strong adhesion and reliable tracings.
- Kendall Arbo H34SG (Fig. 3.7d): Ag/Ag electrode with solid hydrogel formula, foam backing and an extra-strong adhesive, particularly suitable for stress and Holter testing (tested for 72 hours of use, can remain in place during washing/showering). It is suitable for X-ray, CT and MRI and present a diameter of 45 mm with integrated abrader and stud adaptor.
- Kendall Arbo H34LG (Fig. 3.7e): Ag/Ag electrode with liquid hydrogel formula, foam backing and an extra-strong adhesive, particularly suitable for stress and Holter testing (tested for 72 hours of use, can remain in place during washing/showering). It presents a diameter of 45 mm and a stud adaptor.
- Kendall Arbo H83V (Fig. 3.7f): micropore Ag/AgCl electrode for neonatal monitoring with solid hydrogel, 30 mm round and with 50 cm white leadwires with 4 mm banana bush/socket connector. They are made of natural Karaya gel which guarantees the adhesiveness and are hypoallergenic and repositionable.
- Kendall H59P (Fig. 3.7g): cloth electrodes incorporates a full surface conductive adhesive hydrogel which provides strong adhesion, yet is gentle to delicate skin upon removal. The full surface gel allows the electrodes to be removed and reapplied without sacrificing adhesion. The spunlace cloth substrate is soft and allows moisture to evaporate. These electrodes are rectangular (35 x 22 mm).

Impedance values (magnitude and phase) have been measured using the *Agilent 4284a* precision LCR meter for precise component, semiconductor and material measurements in the frequency range between 20 Hz and 1 MHz. This meter is not a medical device, so it can not provide patient electrical safety and can not be used in a clinical setting. By setting the maximum potential according to the observed impedance, it is possible to control the maximum current amplitude injected for the measurement.

In order to identify the best skin treatment for removing the stratum corneum, 4 different approaches has been tested with the MT133 electrodes positioned in the abdomen.

1. positioning an adhesive tape on the skin and then removing to remove dead cells from the skin;
2. cleaning the skin using alcohol;
3. applying a conductive gel and then rubbing it in order to facilitate the penetration of the hydrogel into the skin;
4. using an abrasive paste based on pumice stone (*Everi cream from Spes Medica*) to remove the stratum corneum from the skin and then applying a conductive gel;

(a) Kendall H135SG

(b) MediTrace MT133

(c) Kendall Care CA510

(d) Kendall Arbo H34SG

(e) Kendall Arbo H34LG

(f) Kendall Arbo H83V

(g) Kendall H59P

Figure 3.7: Tested disposable commercial electrodes

As conductive gel, we used the *Spes Medica Neurgel 250F*, an elastic and conductive gel especially made to be used during the recording of EEG - EP - EMG. It is a clear viscous gel that contains water, potassium chloride, hydroxyethylcellulose, propylene glycol, Methylchloroisothiazolinone, Methylisothiazolinone, Benzyl alcohol.

Despite the frequency value on which the greatest part of the commercial electrodes are tested is 10 Hz, the minimum value at which the impedance can be measured with the LCR meter is 20 Hz. In order to evaluate the impedance trend over frequency a frequency sweep on 10 discrete values has been used between 20 Hz and 1 kHz, concentrating the measures in the typical bandwidth of the ECG (20, 25, 30, 40, 60, 80, 100, 200, 500, 1000 Hz). The obtained results on a single subject in steady conditions for the MT133 disposable electrode is reported in Fig.3.8 and shows that for low frequency values (which are the frequency compontents of greatest interest in FECG application) the last treatment, based on the use of both an abrasive paste and a conductive gel, allows obtaining the best performance.

All the selected disposable electrodes have been then evaluated adopting the fourth skin treatment (Every cream and Neurgel) on the abdomen of the same subject, in order to test their performance with the best skin treatment. The results are reported in Fig.3.9 and highlight that the best performance in terms of impedance values can be obtained using the H34LG, the H135SG and the H34SG electrodes. These electrodes present a strong adhesiveness. Despite this characteristic can be useful for long term monitoring (they are also tested for washing/showering), irritating effects can arise. For this reason, the research is directed towards the development of new electrodes technologies which can reduce the side effects of long term application, also improving the application procedure for home monitoring. This research is presented in Section 3.2.

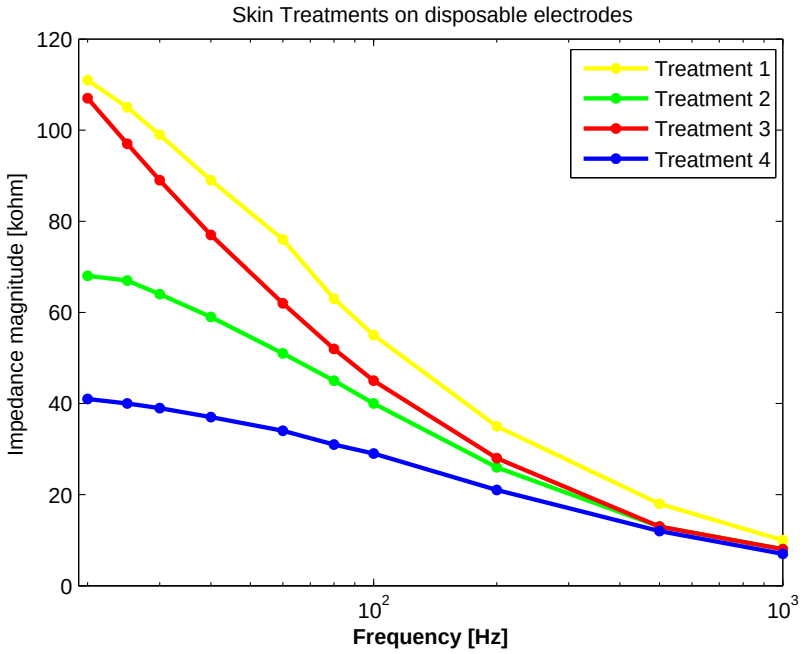

Figure 3.8: Effect of different skin treatments on impedance values of the disposable electrode (model MT133) on the same subjects

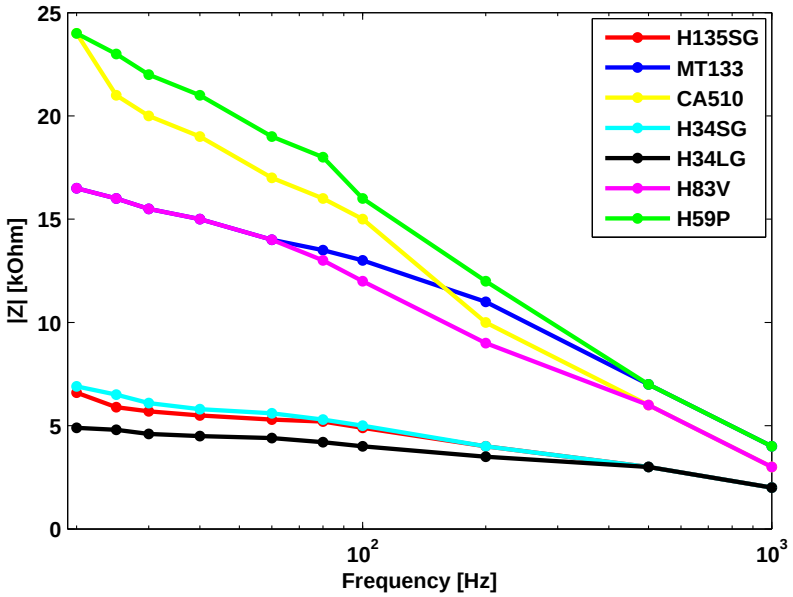

Figure 3.9: Impedance values of the disposable electrodes on the abdomen with the skin treatment 4

Figure 3.10: Reusable bridge electrode for EEG

Area of the body	20 Hz	25 Hz	30 Hz	40 Hz	60 Hz	80 Hz	100 Hz	200 Hz	500 Hz	1000 Hz
wrist	48	40	38	36	31	28	26	19	11	7
collarbone	51	40	39	36	32	29	26	18	11	8
breastbone	37	33	31	29	25	23	22	16	10	7
abdomen	57	53	51	48	43	38	35	25	15	10
side	63	55	53	48	43	37	34	23	13	8
iliac crest bone	106	80	79	70	59	50	44	28	15	8
ankle	251	219	197	158	128	101	86	50	23	13
head	37	31	30	28	26	24	23	18	12	7
back	34	30	29	27	24	21	20	15	9	6

Table 3.1: Impedance magnitude values in kOhm over frequency of the bridge electrode on different body areas of a test subject

3.1.4 Impedance evaluation on different part of the body

Reusable electrodes have been used to measure the impedance values of the skin in different areas of the body, to evaluate the impedance imbalance when the electrodes are placed for critical acquisition such as for fetal ECG. EEG bridge electrods, shown in Fig. 3.10, have been chosen because of their high performance and selectivity (due to the reduced sensing area). Their sensors are made of Ag/AgCl, whereas the bridge support is in hypo-allergenic plastic material. The perfect regulation of the distance of the electrode from the skin is provided by a screw which is also a universal connector for plug, spring plug and alligator clip. For these electrodes it is possible to assume that the greatest part of the impedance value is due to the skin-electrolyte interface with respect to the electrode-electrolyte interface. The results are reported in Tab. 3.1.

As we can observe, the lowest impedance values on a single test subjects are observable for the back and the head, whereas the highest ones are in the ankle and in the iliac crest bone. This information should be taken into account when placing the electrodes, in order to avoid the creation of impedance imbalance. Nevertheless, a study on a greatest number of subjects should be conducted in order to verify this trend.

3.2 Textile Electrodes for ECG Signals Acquisition

A collaboration with the *DEALAB Innovative Devices and Materials laboratory* of the University of Cagliari has been set up to study the use of textile conductive electrodes in FECG acquisition. The use of these technology for the conception of a wearable elastic band that the patient can easily wear without any skin treatment and irritation would be decisive for improving the acquisition setup in both diagnostic settings and home telemonitoring applications. Textile electrodes are expected to overcome the main limits of the widely used Ag/AgCl disposable electrodes, which, as mentioned above, require a gel electrolyte to properly work. This gel (along with the electrode adhesive), when applied for a long time, stimulates the skin, causing rashes or reaction. Moreover, gel drying causes increased impedance, which in turn means more noise and artifacts.

Dry textile electrodes can overcome these problems with the drawback of a higher contact impedance, due to the material but also to the irregular electrode surface. Most dry textile electrodes reported in literature present a high impedance that either limits their use when very small signals must be recorded [90] or poses doubts about the achievable signal quality [91, 92]. These textile electrodes are usually based on fine metal wires or metal coated yarns woven or stitched with conventional textile fibers, and a large variety of materials and fabrication methods has been presented so far [93]. With the development of conductive polymers, it became possible to transform non-conductive textile fibers into flexible and reliable conductors.

Among the different available conducting polymers, poly-3,4-ethylenedioxythiophene doped with poly(styrene sulfonate) (PEDOT:PSS) is one of the most used and has attracted wide attention as electrode material in a variety of applications due to its excellent characteristics such as low band gap and superior electrochemical and thermal stabilities. Due to its biocompatibility, it has been used to create electrodes for recording extracellular potentials both in vitro and in vivo [94]. PEDOT:PSS treated fabrics employed for fabricating electrodes, have an invaluable advantage compared to other conductive textiles: they show a decreased electrochemical impedance mismatch between tissue and electrode, thus avoiding the need for conductive gels. This is due to its mixed electronic and ionic conductivity and high ionic mobility. However, so far, there have been a few attempts to use PEDOT:PSS for making textile electrodes relying either on a rigid support [95] or on a semi-rigid Ag/AgCl wire [96].

In the following sections, textile electrodes, based on the treatment of a standard textile fabric with a highly conductive PEDOT:PSS solution, are described and evaluated by comparing their performance with respect to that of disposable gelled Ag/AgCl electrodes in ECG recordings.

3.2.1 Textile electrodes fabrication

Textile electrodes have been made by treating conventional fabrics with a highly conductive solution of PEDOT:PSS. The conductivity of these electrodes can be enhanced the addition of a second dopant. In this work, polyester fabrics treated with glicerol have been selected for impedance and ECG recordings.

Dried fabrics were cut in 35 mm x 65 mm pieces and the surface resistance measured. In order to evaluate the properties of the conductive fabrics as surface bio-potentials electrodes, without any disturbance due to other materials getting in touch with the skin, the conductive fabric was sewed to a non-conductive 35 mm x 35 mm layered structure of foam

(a) Front (b) Back

Figure 3.11: The prototypical electrode

(4 mm) and polyester, using simple cotton yarn. After sewing, the sensible area of electrodes is reduced to 30 mm x 30 mm. The introduction of foam layers allows improving the contact between the electrode and the skin by ensuring a more uniform pressure, which is especially beneficial in case of dry electrodes. In fact, some authors associate the baseline drift, which is a typical artifact in signals acquired by textile electrodes, to a variation in the contact pressure, which can be reduced by a soft layer of foam [97]. The presence of the foam also allows keeping the electrode wet (physiologically or artificially) in order to reduce the contact impedance [90].

The exceeding 20 mm x 30 mm of conductive fabric on one side was used to attach a metallic snap fastener, as shown in Fig. 3.11, which has a termination similar to the commercial disposable electrodes, allowing a direct connection with standard patient cables. The snap fastener was fixed to the fabric with a silver conductive paste and then secured by sewing with a silver-coated yarn (Shieldex 117/12x2 ply, Statex - Germany). In such a way, the snap fastener remains in a tail of the fabric that can be flipped over the rear of the electrode not getting in touch with the skin.

The choice of woven cotton and polyester fabrics was motivated by the idea of having common textile materials instead of rare and expensive ones. Notably, the proposed approach can be applied to any kind of textile material able to absorb and retain the conductive polymer. Furthermore, flexible but unstretchable fabrics have been chosen in order to reduce the effect of the stretch over the skin-electrode contact impedance. In fact, flexibility and stretchability can confer to conductive textile the ability to act as strain gauges, changing their impedance as a function of the stretch level. Clearly, this feature is not desirable for an electrode, which on the opposite should maintain its impedance constant against any mechanical deformation.

3.2.2 Experimental analysis

Several experimental strategies were adopted in order to evaluate the different aspects of the textile electrodes.

Skin-electrode impedance

The skin-electrode impedance of 20 textile electrodes was measured on a single subject (hereafter called subject 1) in order to evaluate the variability of the electrodes characteristics. Two types of impedance measurements were made: one at 10 Hz using the FDA approved Prep-Check impedance meter (General Devices) and one at other 10 different frequencies ranging from 20 Hz to 500 Hz using a high precision impedance meter (LCR Meter Agilent 4282A).

To improve reproducibility, a light skin preparation (with Everi Cream by Spes Medica) has been carried out in the area where the test electrode had to be placed (i.e. in the right hemithorax, in the space between the anterior axillary and midaxillary lines). The electrodes have been applied under an elastic belt, 47 mm large, positioned just below the chest muscles. The presence of the chest belt, as well as the skin preparation, allows measuring the electrodes in the same conditions, producing a constant pressure over them and a more reproducible state of the skin so that the contact impedance stays stable. Noticeably, skin preparation has a low impact on the dry electrode-skin impedance.

Two commercial Ag/AgCl electrodes (FIAB F9079, foam with solid hydrogel) have been applied just below the belt, 10 mm spaced, in the same anatomical zone. For them, a deep skin preparation consisting of gentle scrub with Everi Cream followed by a harder mechanical scrub (with a thin plastic scraper and Neurgel by Spes Medica) has been performed. Neurgel has been left in place to improve the conductivity of the solid hydrogel of the commercial electrodes. For the impedance at 10 Hz, the measurement has been carried out between the textile electrode and a commercial one so that the measured value includes both the skin-textile electrode and the skin-Ag/AgCl electrode contributions, plus the negligible body impedance. Such an inhomogeneous setup has been chosen to avoid saturation of the Prep-Check impedance meter, which has a saturation value of 200 kΩ. Moreover, this instrument provides only the modulus of the impedance, avoiding any a posteriori correction. The skin-electrode impedance for the Ag/AgCl electrode undergoing this hard skin preparation was 9 kΩ.

For the impedance at the other frequencies, from 20 to 500 Hz, a similar setup was used, keeping the injected sinusoidal current below 1 μA. In this case, the two Ag/AgCl electrodes have been used to measure the skin-electrode impedance on the same points, obtaining a reference complex impedance to be subtracted from the measured one. In order to reduce the noise potentially affecting these impedance measurements, they have been performed in an anechoic chamber with filtered mains and an isolation transformer for improved subject's safety. The temperature of the room has been kept at 25 °C during all the experimental trials, in order to reduce the influence of external temperature on the skin conductivity. A delay of 5 minutes between electrodes positioning and impedance measurement has been provided to allow the electrode stabilization.

The results of the evaluation of all the dry textile electrodes on subject 1, with a sweep in frequency between 20 Hz and 500 Hz, are presented in Fig. 3.12. The median impedance at 20 Hz is about 40 kΩ, with a clear decreasing trend in frequency and a noticeable good repeatability. Such results are of the same order of magnitude of disposable gelled Ag/AgCl electrodes.

Ten healthy subjects (aged 29±4, BMI 22.3±2.0) of the research group were enrolled in the study to evaluate both skin-electrode impedance. All of them gave their informed consent to the measurements, which lasted from 20 to 30 minutes per subject. The acquisition protocol

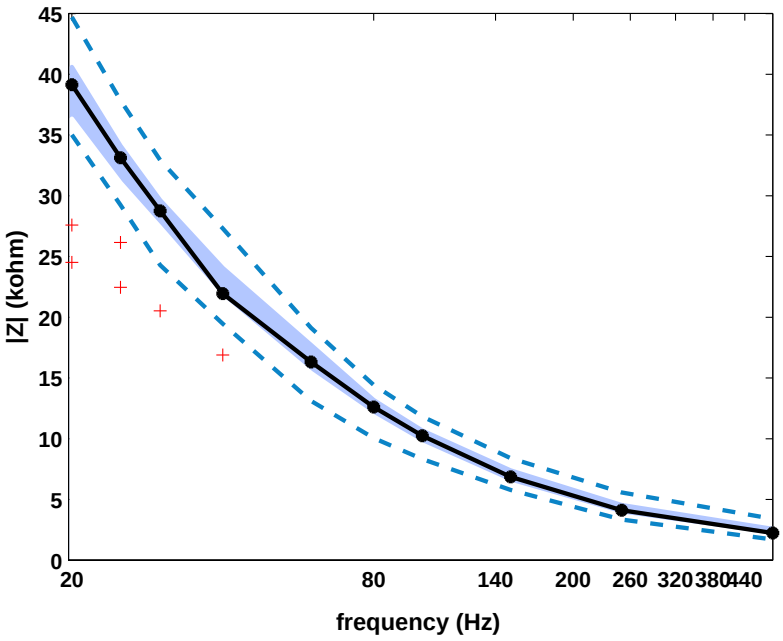

Figure 3.12: Impedance trend of dry textile electrodes (20 samples), evaluated on subject 1 at different frequency values. The median impedance is the solid line, the 25° percentile and the 75° percentile limit the shaded area, the dashed lines span between the minimum and maximum values, not considered as outliers (which are shown as red crosses).

for impedance measurement was the same described above, including the skin preparation procedure, but only the FDA cleared device at 10 Hz has been used to measure the total impedance between textile and Ag/AgCl electrodes. The results of the impedance module are reported in Fig. 3.13, without any correction, so including the contribution of the skin-Ag/AgCl electrode, which is around 9.0±2.6 kΩ (they underwent the hardest skin preparation and gel treatment to achieve the smallest impedance). Remarkably, the impedance distribution dispersion is quite high for the dry textile electrodes, and considerably reduced for the wet ones. However, for dry electrodes, this is mainly the consequence of the inter-subject skin differences (moisture, texture, composition, etc.) rather than a characteristic of the electrode. In fact, all the electrodes tested at 10 Hz on the first subject present a substantially lower dispersion with similar median values, as depicted in Fig. 3.13.

ECG signal quality analysis

The same 10 subjects were enrolled for ECG signal acquisition by using a dedicated battery-powered wearable bio-potentials recording system that allows the acquisition of two ECG channels simultaneously and independently, with minimal and known signal conditioning before A/D conversion in order to better evaluate quality differences among signals in various conditions. The developed recording unit is based on the ADS1292 monolithic analog front-end, specifically designed for ECG applications. The device has two independent inputs connected to as many programmable gain differential input/differential output amplifiers (PGA) with seven possible gain configurations and 1 GΩ input impedance. A sampling frequency of 512 Hz has been chosen. The analog front-end is controlled by a MSP430F5515

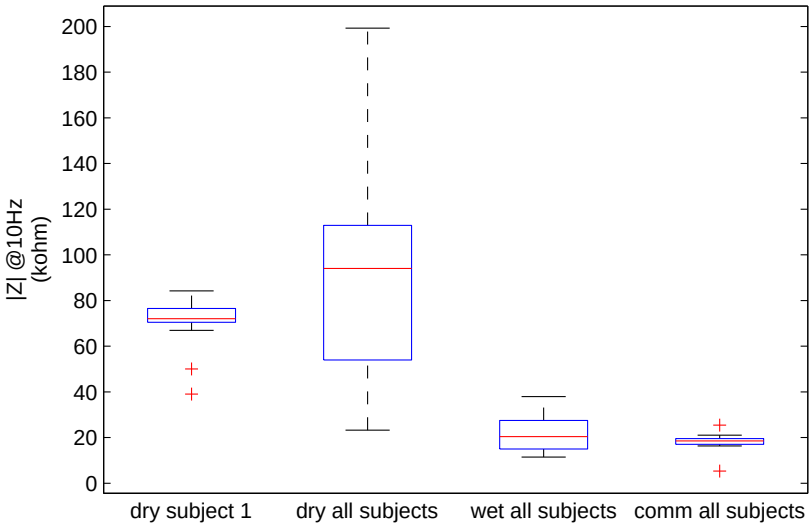

Figure 3.13: Boxplot of the skin-electrode impedances at 10 Hz of the dry electrodes on subject 1, of dry electrodes on all subjects, of wet electrodes on all subjects and commercial electrodes on all subjects.

microcontroller via an SPI port. This has been used to configure it, read the data whenever available and write them to a microSD card. The measurements have been carried out using unshielded cables (MLA0315, ADInstruments Inc.) connected to the safe-lead recessed connectors of the recording unit.

For ECG signal acquisition, rather than choosing convenient positions to reduce the artifacts, we opted for the single lead standard Holter placement (second lead for 7-electrode configuration). In this configuration, the negative electrode is placed close to the right clavicle (lateral to the mid-clavicle line) and the positive one is placed close to the 6th intercostal space on the anterior axillary line. Two couples of electrodes have been positioned, the textile ones below the line connecting said points, the Ag/AgCl ones above the same line, so that the homologous electrodes lay on the perpendicular to the lead direction. As ground electrode, the furthest Ag/AgCl electrode used for the impedance measurement was chosen. This configuration has the advantage of measuring almost along the cardiac axis direction, where the highest signals can be measured. The choice of a standard placement has the intrinsic advantage that, for clinical use, only the standard projection has meaningful information for a visual inspection by a cardiologist. The experimental protocol was designed to include both rest (subject sitting, no physical movements, normal breathing) and dynamic conditions:

- deep breathing (subject sitting, 6 deep respiratory acts)
- stairs climbing up and down, following a 1Hz pace (one stair-step per second)
- step exercise, following a 2Hz pace (every half second a movement up or down the step)

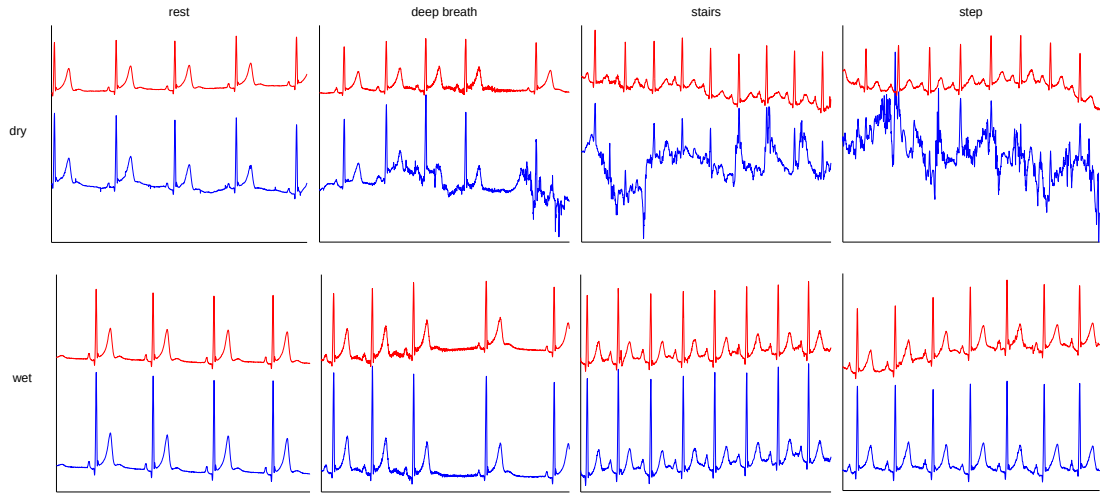

Figure 3.14: Five seconds excerpts of ECG signals acquired with dry and wet electrodes (in blue, lower signals) compared to those simultaneously acquired with gelled Ag/AgCl ones (in red, upper signals) during different activities.

Both dry and wet (two drops, about 0.10 ml, of saline solution, sodium chloride 0.9%) conditions were tested. Saline was chosen, as it is a liquid with a composition similar to the human sweat, normally acting as a weak electrolyte. An excerpts of the acquired ECG signals is shown in 3.14.

One of the main problems of dry electrodes in the literature is the presence of low-frequency artifacts in the signal. Different interpretations have been given to this phenomenon, partly attributed to the material characteristics and partly to contact stability (pressure), which in turn depends on the high skin contact impedance. To evaluate the amount of low-frequency artifacts, in our study we chose the basSQI index [98], which reflects the relative power in the baseline frequency (0-1Hz) with respect to the power in the ECG band (0-40Hz):

$$basSQI = 1 - \frac{\int_0^1 P(f), df}{\int_0^{40} P(f), df} \tag{3.4}$$

This index can assume values ranging from zero (all the power of the signal is in the low-frequency range) to one (no contribution of the low frequencies to the signal power), the higher the better. The signal power has been computed as the periodogram over 10 seconds of the signal. The advantage is to enable an objective evaluation of the baseline wandering contribution on the whole population over a large dataset of signals, including the different tests of the protocol. However, the basSQI index value during exercise (stairs and step) could be misleading. In fact, it could provide good results (close to one) either if the low-frequency components power is low (low baseline contribution) or if the one in the 0-40 Hz band is very high (artifacts). The former is more probable at rest, the latter during exercise. The obtained results are shown in Fig. 3.15. As can be seen, there is a bad performance of dry electrodes in terms of baseline wandering (first column of each boxplot) and a great improvement caused by wetting (second column). Wet textile electrodes show comparable or even better results with respect to the commercial ones.

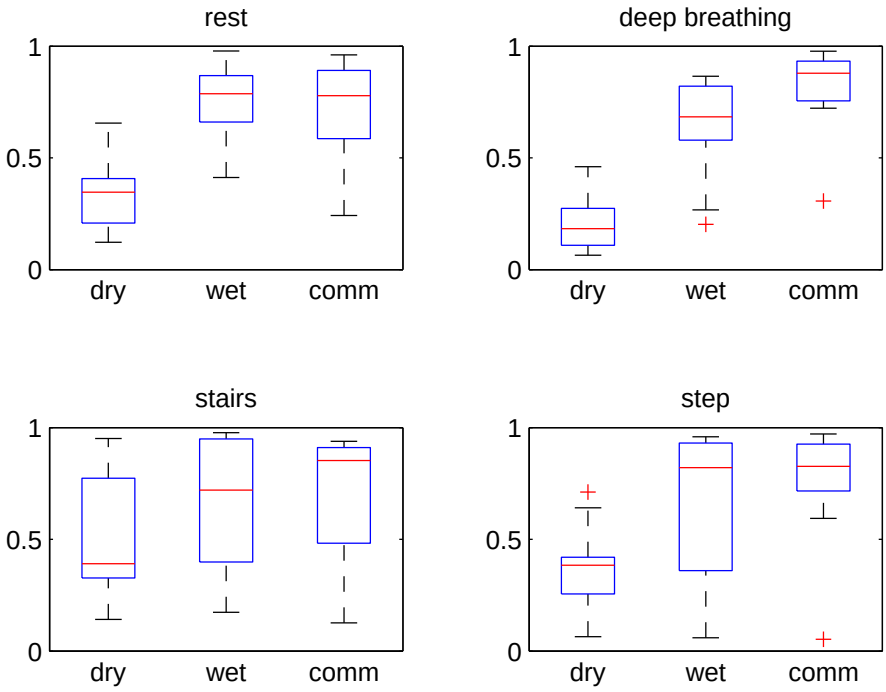

Figure 3.15: Boxplot of the basSQI indexes for rest ECG, deep breath, stairs and step. The first column represents dry textile electrodes, the second one the wet textile electrodes and the third Ag/AgCl electrodes.

In order to take into account the presence of EMG noise and movement artifacts that can compromise the signal quality even in term of QRS complexes detection, especially during physical exercises, other parameters have been also studied.

For rest ECG, the rms around the isoelectric line has been evaluated to quantify the noise level in absence of any physiological signal. To this aim, we first removed the baseline wandering interference by using a non-linear filter [99], without directly filtering the spectrum below 1 Hz. After baseline cancelling, a wavelet-based ECG delineator [70] has been used to segment the ECG signal extracting the portions between the end of a T wave and the onset of the next P wave. These pieces of signal have been concatenated to isolate the parts related to the isoelectric line only. This allows estimating the broadband signal noise without the interference of the main ECG waves, alternatively to residual signal analysis. Fig. 3.16 shows the rms distribution around the isoelectric line for dry, wet, and Ag/AgCl electrodes on the whole dataset of 10 subjects. It is clearly visible that wet and Ag/AgCl electrodes have a similar performance. Interestingly, the dispersion for the wet electrodes is even lower.

To check the distribution of the frequency components, on a single subject at rest, the PSD estimated with the Welch's method (1024 samples, 2 s, Hamming window of the same length, 256 samples overlap) has been exploited, reported in Fig. 3.17. The frequency bins from zero to 1 Hz have been cleared to zero in order to emphasize the spectral components otherwise towering over the other components producing an unreadable plot. This avoided any spectral modification that could derive from the application of filters, considering that our recording unit has no high-pass filtering stage. The spectral content for Ag/AgCl and tex-

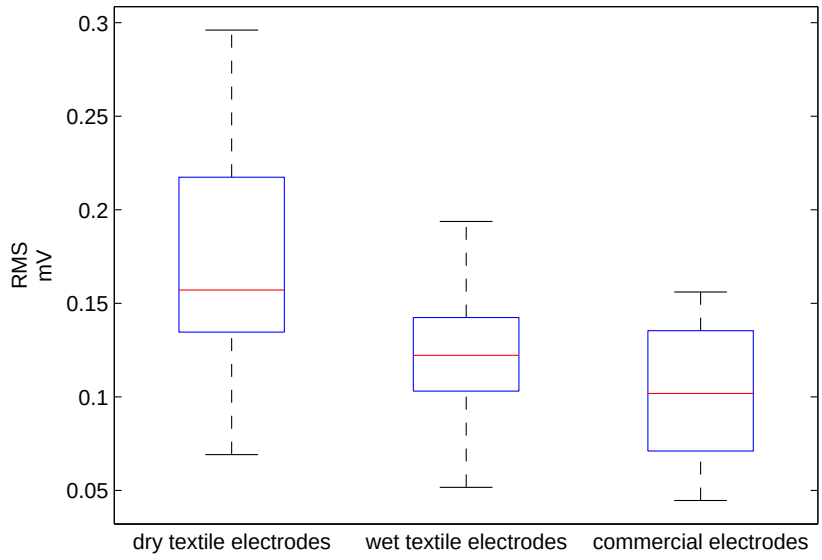

Figure 3.16: Boxplot of the RMS of the isoelectric line. The first column represents dry textile electrodes, the second one the wet textile electrodes and the third Ag/AgCl electrodes.

tile electrodes is quite similar, particularly for the peaks corresponding to the T wave, P wave and QRS complex. It is worth to note that no normalization has been computed, so the amplitude differences are due to the different signal amplitudes. Dry electrodes show strongest components at low frequencies than wet ones. The PSD trends of textile and commercial electrodes are reasonably close, similarly to other studies in the field. Remarkably, the result for dry electrodes is absolutely comparable to that of gelled Ag/AgCl electrodes, meaning that the proposed electrolyte-free approach is able to deal with ECG signal acquisition even in dry conditions.

The quality of the signals has also been evaluated in terms of QRS complexes detection by using the Pan-Tompkins algorithm [75] and through a visual inspection of the obtained results. Such an approach is useful to evaluate several signals, especially in dynamic condition, providing a numerical value over the whole population. The results reveal the detection of all the QRS complexes in the signals acquired at rest (with a percentage of false positive FP of 0.57%, 0% and 0.23% for dry, wet and Ag/AgCl electrodes respectively) or during deep breathing for wet and Ag/AgCl electrodes only (0% and 0.21% of FP) whereas dry electrodes presents also some undetected peaks (6.66% of FP, mainly due to a signal with sharp T waves, and 0.43% of false negative FN). For stairs climbing and step exercises, the results are reported in Table 3.2 in terms of Sensitivity (S defined as $TP/(TP+FN)$) and Positive predictivity ($P+ = TP/(TP+FP)$). These figures of merit have been computed only for the records in which the signal morphology was not compromised and the detected peaks could be recognized as QRS complexes by visual inspection. The results show the improvement due to wetting compared to dry condition, especially in terms of number of records (out of 10 subjects) in which it is possible to perform the QRS detection. Some subjects exhibit good quality signals even for dry textile electrodes. This is not always correlated to a low skin contact impedance, as could be deduced instead. Wet textile electrodes show comparable or

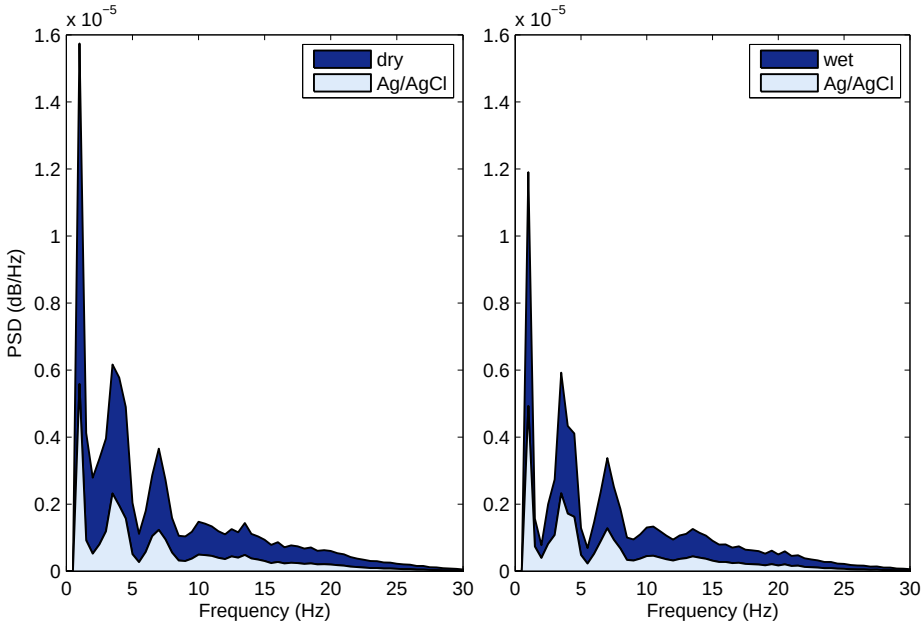

Figure 3.17: PSD for Ag/AgCl and dry/wet textile electrodes.

Type of electrode	Dry textile		Wet textile		Ag/AgCl	
Activity	stairs	step	stairs	step	stairs	step
# of usable records	4	3	10	10	8	10
Sensitivity	0.991	0.967	0.996	0.996	1	0.982
Positive Predictivity	0.915	0.958	1	0.984	1	0.983
Tot # of QRS	120	215	252	784	333	751

Table 3.2: QRS detection results in terms of sensitivity and positive predictivity over 10 subjects for wet/dry and Ag/AgCl electrodes

even better results than Ag/AgCl ones, especially during dynamic activities.

In dry conditions, the proposed electrodes are able to operate correctly at rest, whereas during physical exercise artifacts heavily affect their behaviour. This is due to the contact with the skin, which is not directly correlated to the active area of the electrode but rather to the skin deformation in that point leading to an unstable skin electrode contact. This problem can be mitigated by the adoption of a solid hydrogel membrane, which is said to be critical for a correct acquisition in dynamic conditions. Remarkably, wet electrodes do not suffer this problem, leading to results that are comparable or better than those of Ag/AgCl electrodes also during dynamical tests. Being the wetting solution analog in composition to human sweat, it is predictable that if the motion is intense enough to induce a small quantity of sweat, also dry electrodes can perform satisfactorily in dynamic conditions.

Taking into account the low-cost and simple fabrication process, and the fact that this is the first attempt to realize this kind of electrodes (to the best of our knowledge), these results are very encouraging. The research is currently directed toward the design of one ore more wearable elastic bands which can be easily positioned on the maternal abdomen for the acquisition of the non-invasive FECG. First experimental tests have been conducted by

stamping the electrodes directly on the elastic band, but the results show that the conductivity is strongly reduced with this fabrication technique and the absence of the foam layers causes a reduction of the skin-electrode contact surface. In the next future, a solution which allow the easy positioning of the electrodes with the foam support in an elastic band for the maternal abdomen will be designed.

3.3 The Evaluation of a Configurable ECG Acquisition Module

With the aim of developing a system for home telemonitoring of non-invasive FECG and driven by the need of investigating specific configurations for the signal acquisition, a low-cost configurable ECG acquisition module has been developed by our research group [100]. Signal acquisition setup, along with the number and position of the electrodes, strongly affect the extraction algorithm design and performance. Given the lack of a standard protocol for the signal acquisition it is important to have a flexible experimental platform to carry out experimental tests, even on animal models.

As mentioned above, for the time being, only two medical devices for non-invasive fECG have obtained FDA clearance and are commercially available: AN24 (MonICA Healthcare ltd) and Meridian (MindChild Medical Inc) [67], but their measurement setup is fixed and the acquisition unit details undisclosed. Other general-purpose biopotential acquisition system have been used so far for the same purpose such as the Porti by TMSi [52], or have been custom developed [101]. In both case, the measurement setup is quite marginal compared to the signal processing to be applied on the acquired signals.

In order to assess the device performance in terms of signal quality, this system has been compared to a commercial device (PORTI by TMSi) on a small dataset of abdominal ECG acquisitions from non-pregnant volunteers.

The acquisition system comprises a portable, battery-powered, digital module for the acquisition of biopotentials, and a custom PC software for managing data acquisition. It allows acquiring up to 8 channels simultaneously and can be interfaced to a PC or any host device for data visualization and recording. The acquisition module is based on the ADS1298 analog front-end by Texas Instruments, an 8-channel analog-to-digital converter (ADC) with an integrated ECG front-end. This monolithic chip can be easily interfaced to a master device via an SPI port to configure it and to stream the acquired data. The system architecture is shown in Fig. 3.18. It is composed of a controller unit, a power management section, the analog front-end and two communication interfaces.

The system operation is managed by the MSP430F5515, a 16-bit low-power microcontroller (uC) by Texas Instruments, which basically takes care of setting up and managing the peripherals in the system (e.g., the Bluetooth module and the ADS1298). Beyond this, it performs the data movement from the ADS1298 to the host processor through the USB port, without performing any signal processing operation on the acquired data. In fact, to pursue power efficiency, a platform with limited processing capabilities has been chosen as system controller, leaving all the software post-processing task to the host processor (a mainstream PC).

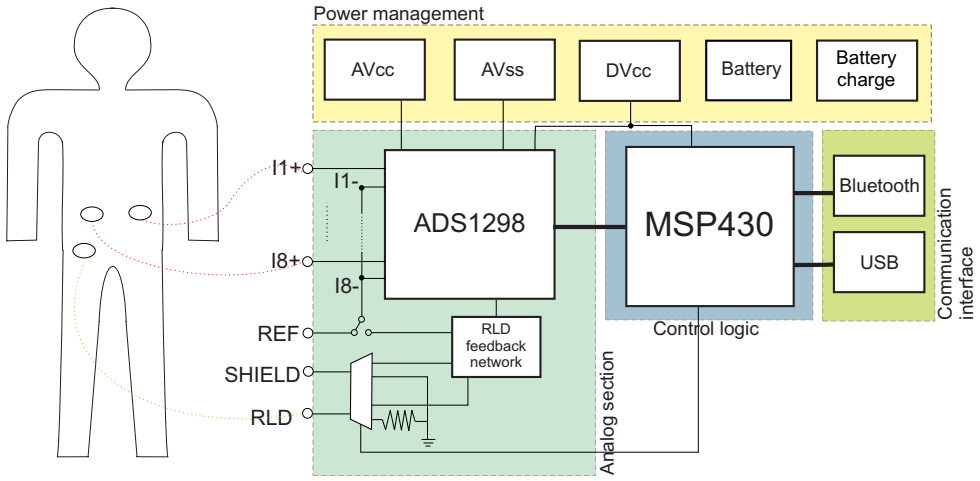

Figure 3.18: Biopotential acquisition module architecture.

Input stage design

As said above, the analog front-end is implemented exploiting the ADS1298 device. This integrated circuit (IC) embeds several features commonly used in ECG applications, thus reducing the requirements of external circuitry, allowing to save board area and to reduce power consumption. Chips of this family have been already adopted in previous works in the literature, such as the ADS1198 in [102], where a preprocessing stage is designed for the needs of the test with textile electrodes, and the acquisition is controlled directly by a LabView interface, and in [103] where an ADS1298-based preprocessing system for ECG acquisition is presented.

The ADS1298 features built-in programmable gain amplifiers (PGAs) at the inputs, which can be configured to provide a gain of up to $12V/V$. These stages have CMOS inputs which exhibits considerably high input impedance ($\sim 1G\Omega$). This makes the device less sensitive to high skin-electrode contact impedance. The IC also includes a voltage reference and an internal oscillator. Another interesting feature is the availability of a built-in right leg drive amplifier. In addition, it is easy to extract (at the RLDINV pin of the IC) the inputs common mode signal. The PGAs are followed by as many $\Sigma\Delta$ analog to digital converters which digitize the differential signal coming from each input channel at a configurable sampling frequency (up to 32ksps) with a 24bit resolution. The acquired data is made available through the embedded SPI port.

Exploiting the 24-bit resolution of the ADC, we chose to avoid adding any pre-amplifying or pre-conditioning stage before the IC inputs. This entails using a limited interval of the ADC dynamic range ($\pm 2.4V$), thus obtaining a signal with an actually reduced resolution. Nevertheless, by considering a dynamic range of the input signal of about $10mV_{pp}$, the corresponding resolution would be of about 15 bits, which is still satisfactory. Such an approach is common to the latest commercial biopotential acquisition systems (e.g. TMSi Porti, g.tec g.USBamp, etc.) because allows DC coupling and avoid introducing signal distortions due to the non-linear phase responses of the analog filters. Unfortunately, this could lead to saturation if strong baseline drift is present in the signal (typically because of high skin-electrode impedance and movements).

The alternatives to analog pre-processing of the signals are basically two: digital post-processing (where filtering with linear phase response can be applied, but also geometric

time-domain filtering, non-linear filtering, statistical signal processing, etc.) and/or definition of a measurement setup able to reduce from the first acquisition steps some artefacts.

To improve common mode rejection (CMR) the inputs are fed to the IC using a differential configuration. While the positive lead of each input channel is connected to one electrode, the negative one can be selected (by means of an analog switch) between:

- the signal coming from a reference electrode,
- the average reference signal extracted from the positive lead of each channel. The signal taken from the RLDINV pin of the IC is fed to the negative lead of the channel input via a voltage buffer implemented by means of a low-noise precision operational amplifier (OPA209).

Thanks to the ADS1298 features, the RLD stage can be generated by adding only few external components. The feedback network is composed of a single capacitor, whereas a protection resistor has been placed immediately after the RLD amplifier output. This allows having high gain of the RLD stage (improving CMR) still not losing stability. The system allows selecting whether to connect the RLD electrode to the actual RLD signal or to the system ground by means of a protection resistor. The latter option is useful when the common mode signal is so big that it would saturate the RLD amplifier, making the first solution ineffective [104].

To reduce the capacitive coupling between the environment and the electrodes lead, often it is desirable to use shielded cables. In this case, the system supports both a ground shield and a driven guard solution. While in the first configuration the shield is connected to the device ground, in the second one the common mode signal is applied via a voltage buffer (implemented by means of the OPA209 operational amplifier).

3.3.1 Performance evaluation

In order to evaluate the performance of the acquisition module developed in our Lab in terms of achievable signal quality, test measures have been performed with both the proposed device and a commercial biopotential acquisition system, namely the TMSi Porti. This device is a 32 channel ambulatory and stationary system for physiological research. It features very high input impedance ($10^{12}\Omega$ according to the device specifications) and, as already said, it does not exploit any filtering stage for signal conditioning before analog-to-digital conversion, but only a slight amplification is applied ($20V/V$). It uses a so called average reference amplifier configuration, where the average of all the connected electrodes is used as the reference signal for differential measurements. It also employs a proprietary architecture for shielding, called True Active Signal Shield, characterized by the fact that the signal coming from an electrode is re-injected in the shield of the same cable. The device sampling frequency is configurable up to 2048Hz and the output data resolution is 22 bits (input range $\pm 3V$). It supports both Bluetooth and USB connection (via optic fibre link).

The acquisitions of a series of abdominal ECG recordings were performed on a healthy volunteer (male, 36 years old) in a controlled environment. The same configuration in terms of electrodes placement has been used for the two systems and the measures were performed with at short time intervals in between. The signal was sampled at a 1024Hz, that is the typical setup used in fetal ECG applications [4]. A grid of 8 disposable electrodes was placed in the subject abdomen, covering the whole surface. The signals have been acquired

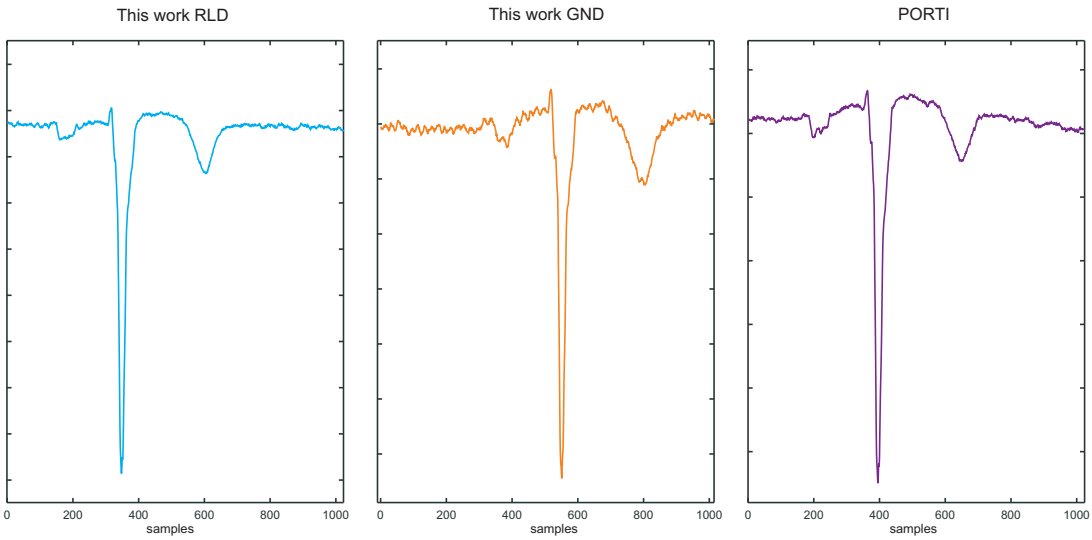

Figure 3.19: From left to right, a QRS complex taken from the signals acquired respectively with the tested device using the right-leg-drive setup, the same system with patient connection to the device GND, the commercial Porti TMSI acquisition system.

using both the commercial device and the proposed one, using for the latter two configurations: the first one was similar to that of the commercial device (i.e. average reference, patient connected to ground and driven shield), whereas in the second configuration the patient was grounded through RLD.

Since it is reasonable to suppose that the heart electrical activity remains constant for a healthy subject at rest, the measurements were not performed in parallel in order to reuse the same electrodes avoiding interferences between the two devices.

A PQRST waveform of the three acquisition setup in the same channel is shown in Fig. 3.19.

From the visual inspection of the depicted waveforms, it is noticeable that the performance are comparable. In order to give a more objective measure of the performance, the root mean square (RMS) of the isoelectric line of the acquired data and the crest factor (explained below) have been computed. To extract these quantities, since both the proposed device and the commercial one do not have any preprocessing filtering stage, a non-linear filter [99] has been used to estimate the baseline wander interference caused by patient breathing and movement, subtracting it geometrically and then preserving low frequency ECG components. The isoelectric line has been then identified by using a state-of-the-art ECG delineator [70] to segment the signal, and then making another signal composed of the T-P intervals of the original one.

The two configurations used with the proposed device have been compared by calculating the RMS value of the isoelectric line for all the 8 channels. The median value is $10.29\mu V$ (maximum $17.5\mu V$, minimum $6.4\mu V$) for the configuration using RLD and $12.7\mu V$ (maximum $20.41\mu V$, minimum $6.8\mu V$) for the configuration without RLD. The comparison with the TMSi device was carried out by computing the crest factor, getting rid of any difference in the amplification between the two devices. The crest factor is defined as the ratio between the peak amplitude of the waveform (the average amplitude of the R peaks in ECG application) and the RMS value. Since the amplitude of the acquired ECG strongly depends on the position of the electrodes with respect to the heart, we compare the signals channel by channel. The results are shown in Fig. 3.20.

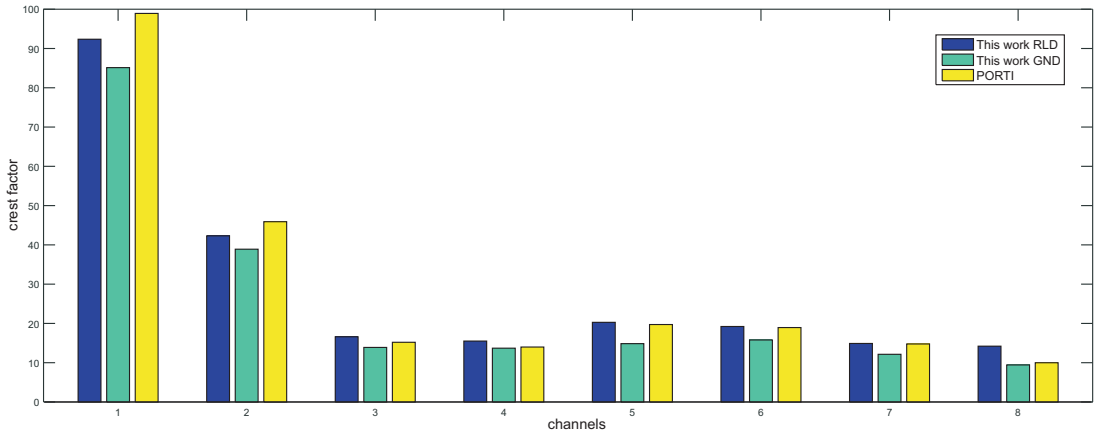

Figure 3.20: Crest factor values computed on the 8 channels individually for each of the configurations used.

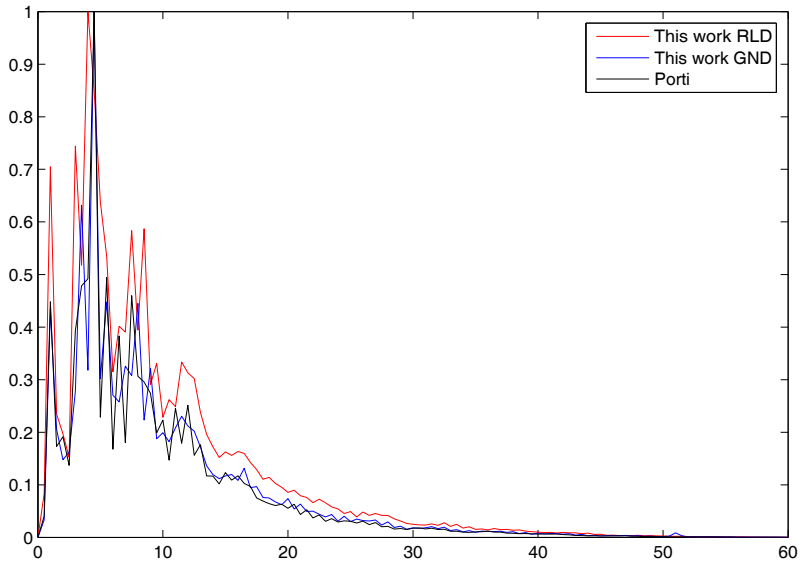

Figure 3.21: Power spectral densities computed on the channel with the best crest factor for the three configurations in exam.

From the histogram, it is noticeable that the performance are comparable for both the devices and both the configurations. In addition, we analysed the normalized power spectral density (PSD) of the acquired first channel to compare the frequency components. For this analysis, the low-frequency band (0-1) has been removed by linear phase non-causal bidirectional filtering to ease graphical comparison and the Welch's method with 2024 points and 512-point overlap was used. The results reported in Fig. 3.21 show overlapping peaks that correspond to the typical ECG components (T wave, P wave, and the QRS complex).

The fact that the proposed device performances levels are close to the commercial one discloses the possibility of employing it to perform experiments on the animal model. The flexibility in the measurement setup will allow studying the impact of the measurement setup over the signal processing algorithms for fetal ECG extraction.

Part II

HAND TELEREHABILITATION SYSTEM FOR RHEUMATIC PATIENTS

Chapter 4

Motivations and State of the Art

After an acute rehabilitation requiring in-person interactions, the adoption of alternative strategies passes through the exploitation of Information and Communication Technology (ICT). Telerehabilitation, dealing with delivering rehabilitation services over distance, can be used in a number of different scenarios, from post-stroke to invalidating chronic diseases. In such cases, it is important to step in with personalized kinesitherapies whose effectiveness strongly relies on the patient's rigour in following the medical protocol. With remote monitoring it becomes possible for therapists to assess the compliance to the rehabilitation protocol when it is performed at home and to adjust possible incorrect behaviours which could undermine the rehabilitation effectiveness.

It has been proven that the effective implementation of a telerehabilitation program can increase the access to the healthcare services and results in improved rehabilitation outcomes for non-hospitalized patients [105]. A comprehensive study reveals the actual benefits associated to rehabilitation even in post-stroke chronic patients exploiting rehabilitation services from their home [106]. Such results foster the development of new platforms for this purpose, with the main aims of cost reduction and equitable access to the rehabilitation services for the patients living in rural areas [107].

The introduction of any ICT tool in the clinical practice cannot neglect its overall acceptability from both the patient's and physician's viewpoints. The latter is usually overlooked compared to the former, with the result of drawing unrealistic conclusions about the possibility of exploiting such a tool in a real scenario. Physicians need intuitive and user-friendly software tools able to provide useful, informative data allowing to ease the assessment of the patient's performance, speeding up the evaluation process rather than complicating it. At the same time the system approach must be sustainable in terms of costs for both the patients and the Public Health System. The need of any burden such as having and managing additional external tools is also particularly important when dealing with elderly patients. In fact, it could leave out of a telerehabilitation program those patients who are not accustomed to such technologies, not equipped with the basic infrastructure, not able to pay for the connectivity costs.

4.1 Kinesiotherapy for Rheumatic Patients

Several diseases can affect the human hand, impairing its functionality and then leading to a reduction in self-sufficiency and a deterioration of quality of life. This condition can be caused by injuries, surgery and diseases. Its onset could be sudden or progressive, entailing different therapeutic approaches. Recovering the hand function requires pharmacological treatment together with a rehabilitation protocol including therapeutic exercises (kinesiotherapy)[108] adapted to the patient's specific needs.

According to the American Kinesiotherapy Association, kinesiotherapy is the application of scientifically based principles to design specific exercises aimed to enhance the strength, endurance, and mobility of individuals with functional limitations which require extended physical conditioning. A kinesiotherapic exercise program, prescribed by health professionals, is often a necessary step for individuals who have been inactive, have restricted joint motion or muscle strength, are experiencing join paint or are recovering from active disease [109][110]. Active kinesiotherapy involves both flexibility and strengthening exercises useful in recovering, maintaining and improving hand function. Such an approach has been demonstrated to be effective for the treatment of Rheumatoid Arthritis (RA) and Systemic Sclerosis (SSc) [111][112] together with a personalised pharmacological protocol.

SSc and RA are chronic rheumatic diseases with different pathogenetic mechanisms and outcomes that cause hand disability, which in turn strongly influences the activities of daily living [113]. SSc is an autoimmune disease that targets the vascular tissues ultimately leading to fibrosis in the skin, the musculoskeletal system and internal organs. Although SSc may affect various joints, the metacarpophalangeal (MCP) and the proximal interphalangeal (PIP) joints of the hands are primarily involved [114]. Thickening of the skin, tendon, and muscle can result in contractures of the fingers and hand impairment. RA is a systemic chronic inflammatory disease primarily affecting synovial joints, mostly the wrist, and the MCP and PIP joints of the hands. Patients with RA often experience joint and tendon restrictions and adhesions due to fibrosis. These patients are prone to muscle atrophy as well as erosion of cartilage and bone, which can led to substantial loss of function and, in the later stage, deformities [115]. RA has a worldwide distribution with an estimated prevalence of about 1% and mainly affects 30-50-year-old females [116]. When the lesions are localized on the hand, such invalidating diseases hamper the execution of normal daily life activities such as hair brushing, dressing or cooking. Both hand strength and fine movements are often compromised. In such diseases, kinesiotherapy aims to:

1. strengthen the muscles and provide greater joint support reducing load and stress through the affected joints;

2. maintain or improve the flexibility in affected joints and surrounding tissues;

3. help reduce bone loss related to inactivity, inflammation and the use of certain medications (e.g. corticosteroids)[117, 118].

Active kinesiotherapy would require constant monitoring by health professionals but often it is impossible to closely assist every patient, because of the reduced availability of specialized facilities and qualified staff. Therefore it is usual practice that active kinesiotherapy is performed at home using common objects (e.g. elastic bands) and self-managed by patients after an appropriate training. To this aim, during outpatient examination an expert

physician can evaluate the quality of the movements in order to effectively guide the patient through the training, avoiding the onset of inflammatory flares involving the hand. However, both a quantitative measurement and analysis of the patient's effort, and the definition of the best suited protocol for a specific patient, are hampered by the lack of instruments expressly designed and packaged to this aim. Beyond qualitative analyses including visual inspection and questionnaires administration, only for some exercises some digital devices are able to provide one-shot measurements. Unfortunately they are quite expensive and hardly integrable in a complete rehabilitation monitoring framework. Also, in order to achieve the best results, specifically designed physical exercises must be properly performed, with the right number of series and repetitions. By their very nature, when these exercises are performed at home with common-use objects they cannot be easily standardized in order to ensure the correct execution at home. Furthermore, relying on unsensorized objects, they cannot be quantitatively monitored in local or remote scenarios for the evaluation of the functional deficit. Such an unsupervised scenario leads to the impossibility of assessing whether the protocol is correctly followed or not, which has implications on the patients compliance and effectiveness of the therapeutic exercises.

4.1.1 Hand functional evaluation devices

The functional evaluation is performed in a clinical setting setting using biomechanical measurements such as the Range Of Movement (ROM), hand extension and strength. Also questionnaires gathering the subject's perception of his or her disability, e.g., the Dreiser test [119], are used for this purpose. For functional assessment only, the most common evaluation involves pinch and grip exercises. Both the *Jamar*®dynamometer (isometric) and the *Vigorimeter* (dynamic) represent well established commercial instruments for the clinical evaluation of the grip strength [120], whereas other systems also allows the evaluation of the single finger pinch force (e.g. *Jamar Pinch Gauge*). In principle, isometric wrist dynamometer can be also used to estimate the torque applied with the fingers when the wrist is in a fixed position, in order to evaluate the hand performance with respect to this task. Usually the digital versions of these devices are able to provide maximum, average and standard deviation of the force, but need additional electromyographic signals to provide temporal analysis within a series [121]. In [122], a grip measurement device is presented, able to perform also some time measurements but only on a single 4.4s grip exercise for the performance assessment in rheumatic patients. A similar work has been presented in [123] for the parkinsonian patients. In both cases the aim is a one-shot functional assessment rather than the monitoring of a series of exercises, since multiple repetitions are sometimes used only for statistical purposes. The commercial *Pablo* system by Tyromotion GmbH, designed for neurological rehabilitation, allows the measurements of grip strength, single finger pinch force and indirect ROM of the wrist for functional assessment of the hand.

The hand agility (severely affected by rheumatoid arthritis and scleroderma) can be in principle evaluated by means of finger tapping tests, originally conceived to assess both motor speed and control in neuropsychology. From the first mechanical devices, other approaches for the monitoring of this kind of exercise have arisen. Approaches including a passive marker-based motion analyzer [124] present a very complex setup not suited for a fast evaluation. Other approaches, based on sensorized gloves [125], are uncomfortable for patients with hand deformities caused by arthritis. In [126], a touch system based on a 4-finger active sensor (injecting on the hand a small sinusoidal current at 1.5 kHz) has been

presented along with its support software. An App (Digital Finger Tapping Test 1.0) with limited functionalities is also available for IPhone users.

4.1.2 Hand rehabilitation devices

Hand rehabilitation can be based on passive or active exercises. Passive exercises consist of repetitive movements of a part of the body as a result of an externally applied force, whereas in active exercise motion is imparted to a part by voluntary contraction and relaxation of its controlling muscles. Passive exercise can be used to prevent contractures and maintain joint mobility but does not promote muscle maintenance.

The largest part of studies in the field of the hand rehabilitation with biomedical devices deals with the post-stroke recovery, because of the high prevalence of this disease in the world and of the intensive, repetitive motion tasks required to recover the motor control. Some of them integrate the telerehabilitation features.

The commercial and prototypical rehabilitation systems for hand rehabilitation can be classified according to their technologies in:

- Robotic systems (for both passive or active-constrained rehabilitation);
- Active rehabilitation devices, with or without sensorized tools for monitoring purposes;
- Virtual Reality systems.

Actually, the dividing line between these systems is not so evident. For example, virtual reality is often integrated in many rehabilitation devices to guide and improve the patient involvement during the training.

Almost all of the commercial rehabilitation devices are specifically designed for recovering hand functionality after central or peripheral nervous system lesions (e.g. for post stroke rehabilitation). Among these systems we can find the *Gloreha* by Idrogenet SRL, a glove that passively mobilizes the metacarpophalangeal joints to execute many rehabilitation exercises, including sequential and simultaneous flexion-extension of all the fingers, functional movements, and other combinations of motions, also providing the possibility of cooperating with the movements following a 3D simulation on a video. It has mainly conceived for the use in a clinical setting, although a lighter version (*Gloreha Lite*) has been released for home rehabilitation exploiting patients' PC. Other commercial robotic rehabilitation systems are the *Amadeo*®(Finger-Rehabilitation) and *Pablo*®(Hand-Rehabilitation) by Tyromotion GmbH. *Amadeo*®allows both active and passive training, also providing the opportunity of an interactive theaphy in a virtual environment. It is based on finger taps to be fixed on the finger tips and thumbs to mobilize them. *Pablo* enables the most diverse gripping motions of the human hand and can be used as a measuring device of both strength and range of movement of the arm with its integrated position sensors and for the therapy. The *Amadeo* system has been mainly conceived for the use in a clinical setting and with the support of a therapist, whereas the *Pablo* system can be exploited at home but requires the use of the patient's PC. *Hand of Hope* by Rehab-Robotics®is an EMG-driven portable robotic device that helps paralysed patients to regain hand mobility through motor relearning. The system senses EMG signals from the patient that indicate intention to move and processes data to a motor on the brace to enable desired motion. The commercial systems *Kinetic Muscle* by Hand Mentor™and *ReoGo* by Motorika are based on the passive actuating of the

hand through a robotic device. The applications of these robotic systems are constrained to specific movements, often requiring the support of specialized nurses, representing a justified approach only for paralysed patients. The *HandTutor*™by MediTouch [127], the *YouGrabber*®by YouRehab and the *HumanGlove* by Humanware s.r.l. are commercial telerehabilitation systems based on sensorized gloves that allow the detection of fingers and wrist movements and are used for hand rehabilitation exploiting some simple video games on a PC which provides positive feedback to the patient. Also the *Curictus* system [128], based on virtual reality and haptic technology, has been proposed for home-based rehabilitation after stroke.

Also in the literature the greatest part of the studies deals with post-stroke recovery of the hand functionality. For example, in [6] cable-driven units connected to each finger by means of soft rings are exploited, being able to move the fingers with predefined patterns (passive movements) and/or to provide a tunable resistance to the hand movement. Other approaches make use of complex mechanical infrastructures [129] or exoskeletons in order to assist the movement [7] or help in restoring the motor function [130]. Many prototypical robotic systems have been presented, such as the *HandSOME* device [7] for the pinch-grasp movement, the *actuated thumb exoskeleton* (ATX) [131] or the *HANDEXOS* [132] wearable multiphalanges device. These systems are quite expensive and not usable for telerehabilitation purposes yet. Also, they are unsuited for rheumatic patients, who frequently present hands deformity caused by the illness progress.

Some systems in literature exploit sensorized tools to allow the monitoring of active rehabilitation exercises. These systems are usually low-cost and easy to transport, so they are suitable for a telemedicine approach. For example, both the devices presented in [133] and [134] exploit a tracking system for the upper limb monitoring and a graphical user interface on a PC to guide the post-stroke patient in the exercise execution and to send the monitored data to the physician. The system presented in [135] enables the evaluation of the follow-up of hand transplanted patients. It includes the above-mentioned commercial sensorized hand glove (*HumanGlove*) to perform kinematic assessment of the hand and the fingers, and two devices for the mechanical evaluation of the hand fingers force, and it is managed by an acquisition software on a PC with data storing onto a web server. These exercises are not specifically designed for the dysfunction of rheumatic patients and, as said, the use of these sensorized gloves is not suitable for patients with hand deformity. Another example of a rehabilitation system has been presented in the European project *HELLODOC* [136] for the recovery of the upper limb in neurological patients. It includes a portable unit based on a desk installed at the patient's home providing a computer and a set of sensorized daily life objects for the monitoring of some parameters during their use. An in-hospital server allows the clinicians to remotely monitor these parameters. Such a device is closer to the one developed and discussed in Chapter 5.

In the last decade virtual reality (VR) has been introduced in rehabilitation devices, improving the quality of the patient interaction with the rehabilitation system. For example, the telerehabilitation system described in [137], called *Java therapy*, exploits a force-feedback joystick capable of assisting or resisting in hand movements when interacting with therapy games that run on a PC, whereas the telemonitoring PlayStation 3 based system presented in [138] includes a five sensor glove to monitor the range of movement of the hand during the execution of games. The *TheraJoy system* [139] is based on a modified commercial joystick that allows arm to be monitored during the proposed therapeutic tasks using motivating gaming technology, supporting the application of light passive and actuated forces. The

study described in [140] exploits a VR activity station which includes a hand-held stylus for the active interaction with a set of games. It collects and analyses the data of hand movement and allows a video-conferencing approach. Another post-stroke telerehabilitation system has been developed in [141] using a shared virtual environment architecture with two sites, one for the therapist and the other for the patient, both including a telerehabilitation workstation with a webcam and the *Rutgers Master II* force feedback glove allowing the control of a virtual hand and the interaction with virtual objects, simulating physical interactions between therapist and patient with force feedback. Other systems exploit virtual reality to realize low-cost rehabilitation devices, such as the ones presented in [142] and [143]. These systems exploit a PC or a game console to manage the rehabilitation session and the communication from the patient's home to the physician's PC through a wired connection, thus requiring a physical installation in the patient's home. The majority of them require a great effort for both the physician in interpreting the acquired data and the patient in learning how to interact with the system .

As shown, the rehabilitation systems in literature are mainly focused on post-stroke rehabilitation and are not suitable for rheumatic patients. Also, they require the use of a PC or a game console which manages the rehabilitation session and the communication from the patient's home to the physician's PC through a wired connection, thus requiring an installation. The majority of these systems require a great effort for both the physician in interpreting the acquired data and the patient in learning how to interact with the system. Also VR systems needs patients' skill in interacting with therapy games, giving rise to results which are not easily interpretable by the physicians.

4.2 Telemedicine in Clinical Practice

Telemedicine is a field of medicine which deals with providing health services at distance, exploiting information and communication technologies (ICT) resources to diagnose, treat and prevent diseases and injuries [144]. The interest towards this practice is based on the possibilities disclosed in terms of efficacy, quality and cost-effectiveness of the health services delivered [145] to an increasing number of patients.

Telermedicine can be based either on store-and-forward or real-time approaches. Real-time remote interaction between patient and doctor/caregiver relies on the availability of the latter every time the former interacts with the system [146]. Several telehomecare systems have been developed including a videoconferencing support in order to interact with the patient, as for the *Twoway InterActive TeleVision* [146]. This kind of solution requires large bandwidth and it is expensive not only in terms of actual cost but also in terms of time dedicated by the physician to every patient, that is incompatible with the real workload of a clinician. This approach leads to a poor scalability and consequently is not sustainable when the number of patients is high (even though it could be useful in rural places). Store-and-forward approaches, allowing a deferred monitoring/interaction, could better meet the requirements of a real scenario involving more patients [147]. Such an approach can be used for long-term home rehabilitation when, after a training period, the patient is able to autonomously manage its rehabilitation. In this context, telemonitoring can occur less frequently over time, just to monitor the evolution of the patient' s state and the quality of the rehabilitation intervention. It is also used when monitoring of the parameters by a physician does not require a 24h frequency [148].

In the recent years, several scientific works in the field of telerehabilitation have been presented, and a few patents and off-the-shelf products appeared [149]. Despite the fact that these instruments represent valuable tools for rehabilitation, they rely on a (vertical) model of assistance based on a one-to-one interaction between the patient and the therapist, even when real-time interaction is not pursued. However, in case of chronic invalidating diseases or other severe conditions (e.g. neurorehabilitation), this model is inadequate to support a multidisciplinary teamwork for the follow-up of the patient, as required by the best clinical practice. Introducing such a feature adds an horizontal collaborative dimension, outlining a patient-centric scenario where all the medical actors involved in the treatment of the patient share telemonitoring data and contribute with their personal knowledge to the decisions about the progress of the rehabilitation.

Generally speaking both Patient to Doctor (P2D) and Doctor to Doctor (D2D) approaches to telerehabilitation help in crossing the boundaries of the hospitals and healthcare centers, promoting a fair access to good-level health services by everyone, even in rural places [150]. The first one is a vertical interaction scheme where the roles are clearly identified; the second one is an horizontal interaction scheme where hierarchical relationships between the actors can be hardly identified. For instance, remote consulting could be the expression of an asymmetrical collaboration where the expertise of the consultant is assumed to be superior to that of applicant when they have the same specialization [151]. Nevertheless, in case of different specializations, consultation aims at sharing opinions pertaining to the specific specialization field [152]. In this case, the telemedicine system should be able to combine communication with an efficient way of sharing the patient's data among the interested actors.

Teleconsultation and second opinion, such as the teleconsulting networks shown in [153] and [154], are based on the real-time transmission of ecocardiographic videos and images for consulting with a specialized cardiologist from a remote place, avoid moving the patients and trust an asymmetrical collaboration relationship. As discussed in [155], telehealth collaboration among primary and secondary health care providers would avoid the worsening of behavioral health problems in rural areas. Several systems have been presented so far for collaborative purposes. For instance, the *CoMed* system described in [156] represents a web-based real-time collaborative system that allows specialists to share patients' data and to communicate with each other exploiting a teleconferencing, whiteboard and chatting system. However, as for the teleconsulting, this system relies on real-time interactions between the specialists. This is a strong limiting factor that should be avoided whenever possible because often incompatible with the physicians' activity, especially when they belong to different hospitals. Messaging services, implemented in store-and-forward solutions, can avoid this critical synchronization need between the parts [157]. In some context, such as the one of remote rehabilitation, a hierarchical approach to the decision-making process could be also required, further unbalancing the collaborative relationship. This implies that some supplementary services aimed at defining different access rights to the available functionalities must be provided in order to build up an effectively usable collaborative system. For example, the system described in [158] allows the physicians to collaborate with their clinical assistants mediating the consultation with the patient in a teleconferencing system. The telemedicine system in [159] allows the assistants to collaborate with remote supervisors (physicians) exploiting a server able to share the patients' data among two or more authenticated remote healthcare providers.

Even though several studies report the main outcomes of clinical trials exploiting a given

telemedicine system in terms of the measured benefit for the patient, the evaluation of the systems from a medical perspective is usually overlooked. When addressed, the two main ways to obtain information are quantitative methods such as the number of patients which can benefit from the technology or the time spent by the physicians to follow the patients, and qualitative methods, such as interviewing, focus group or participants observation [160]. The latter are particularly helpful when developing new prototypical systems, in order to guide the improvements towards the real needs of the healthcare system. For example, in [161] a national survey among physicians has been used to evaluate the impact of electronic health records in ambulatory care. Not many works in the field of telerehabilitation focused on both these aspects, limiting their analysis to the developed technology and to patients physical improvements. The *TeleREHA* project [162] for the development of a cost-efficient platform for post-stroke neurorehabilitation recognizes the critical role of the therapist for successful introduction of telerehabilitation technologies, identifying critical points that need revision thanks to an open discussion with therapists involved in an experimental session, thus opening to a collaborative scenario.

Chapter 5

The Proposed Hand Telerehabilitation Device

Current clinical practice suggests that recovering the hand functionality lost or reduced by injuries, interventions and chronic diseases requires, beyond pharmacological treatments, a proper kinesiotherapy. Its effectiveness is strongly dependent on the patient's adhesion to such a program, as explained in the previous chapter.

In the following sections a solution mixing on a single device both a local and remote monitoring system for hand kinesiotherapy is presented [163]. The device has been designed thanks to a tight cooperation among bioengineers and specialists in rheumatology, starting from the current state of the art and introducing novel experimental protocols. The proposed system allows a simple and objective monitoring of the patients' rehabilitation sessions through a set of custom sensorized tools and is managed by a microcontroller unit (MCU). It can guide the patient by means of a simple user interface for home sessions, whereas for outpatient clinic evaluations the same device operates as a slave unit of a PC. The remote operating mode is supported by an embedded GSM/GPRS module able to transmit the main statistics about the rehabilitation session to a TCP/IP server for deferred analysis. From there, data can be retrieved as needed for local analysis; this functionality is supported by a custom software framework.

5.1 Design of the Kinesiotherapy Device

The first goal of this research has been the conception of a set of adapted physical exercises for the hands able to improve both the strength and the agility of the patient with RA and SSc and to provide an objective functional evaluation of the hand. Taking into account the common peculiarities of the two diseases, RA and SSc, the strength exercises were conceived and evaluated with the goal of avoiding joint stress and overload which can cause pain and the relapse of inflammation. To this aim, all of them require isometric muscle contraction, and should be tailored by the patients at a pain-free intensity. During isometric contraction the muscular contractile component shortens and stretches the elastic component, without changing the joint angles involved in muscle work, thus preventing relapse of inflammation in affected joints. Conversely, the agility and stretching exercises, which obviously are

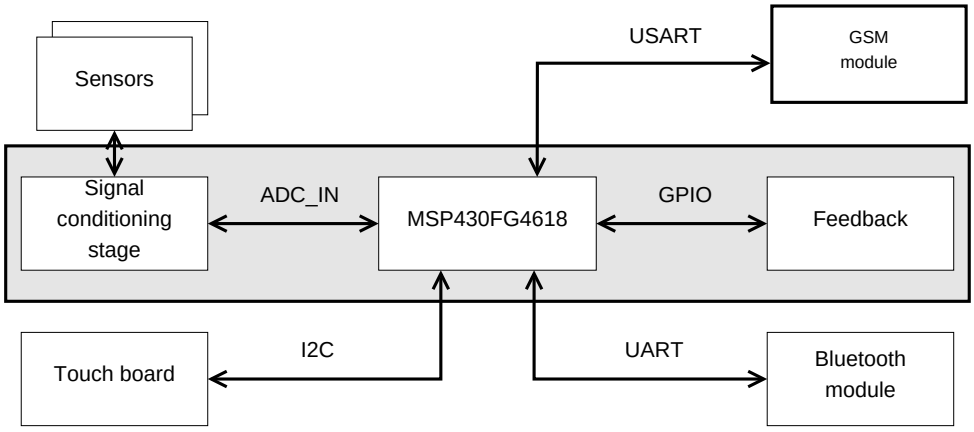

Figure 5.1: System block Diagram

dynamic, should present the minimum counter-resistance in order to emulate a tool-free exercise. Overall, the wrist should not be used as a lever but only as a support for the hand, leaving to the fingers the exercise effort, in every exercise. To this aim, seven different exercises have been conceived, all of them requiring multiple series, each one composed of multiple repetitions of the same gesture. Among them we have isometric exercises:

E1. hand pinch

E2. hand grip

E3. finger pinch (opposition to the thumb)

E4. rotation (screwing with the fingers)

and dynamic ones:

E5. hand extension

E6. rotation (fast manipulation)

E7. finger tapping (piano-like)

Despite the differences between the two rheumatic diseases, the proposed set of exercises is able to cope with the needs of both the populations of RA and SSc patients, producing significant improvements in their strength, agility and dexterity. At the same time, they probably could be successfully applied to other pathological conditions that require the same characteristics of the rehabilitation exercises, which may open the proposed device to a wider application scenario.

5.1.1 System architecture

Figure 5.1 shows the most important parts of the system and their interconnection. Beyond the MCU subsystem controlling the whole system, we can see:

- the analogue sensorized devices;
- the digital sensorized device (for finger tapping);

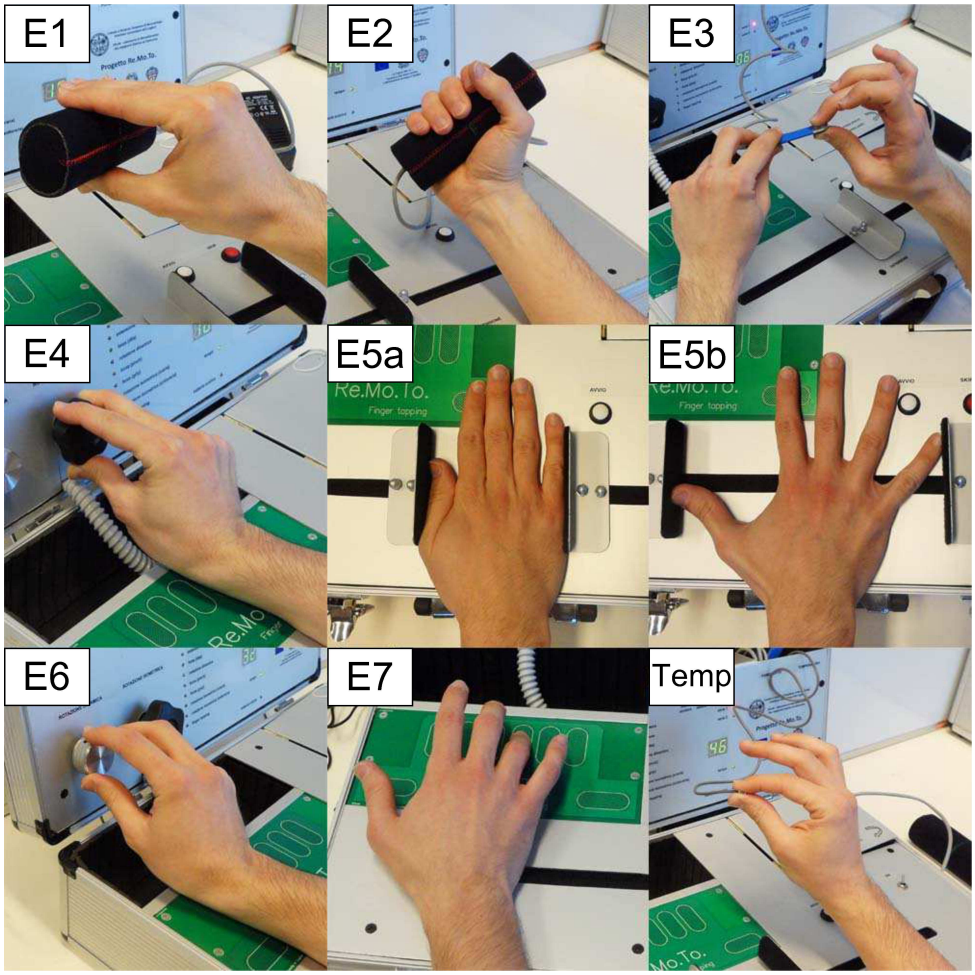

Figure 5.2: The different exercises and the related tools (plus the temperature sensor) supported by the proposed system.

- the analogue interface circuitry;
- a Bluetooth and a GSM modules, which provides a wireless link;
- additional components to provide a visible/audible feedback to the user.

The system can be easily supplied by a single-cell Li-Ion battery. For improved safety, the internal battery can be recharged only when the system is switched off. Along with the DC power supply adaptor to recharge the internal battery, the Bluetooth module (Bluegiga WT-11) is the only device that is not embedded in the metal briefcase.

5.1.2 Tools design

The exercises have been engineered with the sensorized tools depicted in Fig. 5.2 and embedded in a portable device :

- a tool for hand grasping exercises in pinch and grip (E1 and E2), which exploits a low-cost Flexiforce A201 force sensor by Tekscan (max force in linearity response: 440N), pressed between the two halves of a handle covered with neoprene;

- a tool made of an aluminum plate which sustains a Flexiforce A201 force sensor (110N). Its sensible area can be pressed against the plate through a silicon pad, with a finger acting in opposition to the thumb (E3);
- a tool with an exposed 5-lobe nylon handle which cannot spin but it is internally fixed to a bar which in turn presses one of two Flexiforce A201 force sensors (110N) as a torque is applied clockwise or counterclockwise respectively, using the fingers only (E4);
- a tool based on a moving metal structure, made of two rollers (CES30-88-ZZ by Rollon) on a rail for linear movement (TES30-1040 by Rollon), connected by an analog draw wire position sensor (LX-PA-15 by TME) which provides information on the relative distance between the rollers. The rollers are actuated by the patient, who inserts the hand between the two metallic profiles attached to them, by opening and closing the hand (E5). A small counter-resistance (about 4N) needed for the rope winding is opposed to the extension movement;
- a tool consisting of a multi-turn precision potentiometer (Vishay 534, 10 rounds) with an aluminium knob attached to its shaft. The resistant torque of the potentiometer is negligible (0.006Nm), providing a support for a low-resistance dynamic rotation exercise. The patient is asked to spin the knob using the fingers only, both clockwise and counterclockwise (E6);
- a capacitive touch board for a finger tapping test (piano-like). Compared to the one presented in [126], the capacitive approach is still able to provide a detection of the touch without any counter-resistance from the measuring device but also avoids any direct current injection in the patient's hand. The touch board is based on the MSP430F 2013 microcontroller unit (MCU), managing the reading of the capacitance associated to 8 key-shaped sensible areas on a PCB. The keys, which form a capacitor with the ground plane surrounding them, are sequentially charged by the MCU, which is able to measure the discharge time. Since the effect of touching a pad is the increase of the capacitance value, it is easy to detect whether a sensor is touched or not, comparing the measured discharge time with the base value obtained when the pad is untouched. The design of this device followed the guidelines given in [164] with some further consideration: the layout of the board must accommodate both left and right-handed exercises and the sensor shape should lead to an ergonomic device (it should accommodate different hand sizes and postures). Therefore the keys were made slightly larger than the suggested value, mesh-filled to keep the capacitance base value under an acceptable level. The device provides over an I2C bus, whenever required, the current status of the keys in a single byte: the interpretation of the data in the light of the exercise to execute is up to the main processor firmware. The patient is asked to orderly touch 5 of the 8 available sensible areas with the fingertips from the little finger to the thumb as fast (and precise) as possible (E7).

Additionally, a skin temperature probe (a NTC thermistor YSI 400 compatible from [165]) has been integrated to measure the temperature of the hand (between thumb and index) at the beginning and at the end of the session. This has been provided to evaluate the effect of the exercise session in patients with SSc, where one of the objective is to increase the blood

Exercise	Extracted Parameters and Related Statistics
E1 E2 E3 [*E*4*E*5]	Force [torque, extension]: max, min, avg, std Repetitions duration (only the active part): avg and std Number of repetitions
E6	Rotation angle and rotation speed: avg, std Exercise duration Number of repetitions
E7	Duration of correct/wrong sequences: avg, std Number of touches per second Number of correct/wrong sequences

Table 5.1: Relevant parameters for the statistical summary associated to the different exercises

inflow to the affected tissues. RA patients have been asked to measure the acral temperature only for comparative purposes.

The choice of the sensors and the consequent design of the tools has been driven by simplicity for the patients and a good trade-off cost/performance. Each tool, except the one for E7 corresponding to the touch board which provides a digital signal, is interfaced to the MSP430FG4618 microcontroller unit (MCU) in charge of controlling the device functionality, through a signal conditioning stage, before digitalization. The latter consist of low-pass active filters based on the TLV2375 operational amplifier. Since all the signals coming from the sensors are unipolar a single supply configuration can be employed, thus limiting the stage complexity and the number of resistive elements. A single pole RC cell sets the cut-off frequency at 48Hz, acting as anti-alias filter for the sampling, performed at 150Hz by the MCU through the internal A/D converter in order to guarantee an adequate time resolution for the signal processing algorithms.

5.1.3 Processing algorithms

The signals coming from the tools equipped with analogue sensors are low-passed filtered by an 8-tap moving average filter in order to further smooth the signal and then processed exploiting three different algorithms, whose use depends on the shape of the signal to be processed. Such a processing is useful to extract on-line the statistical parameters related to the execution quality, presented for the different exercises in Table 5.1. The extraction of these parameters from the raw signals is briefly described hereafter.

All the isometric exercises (E1-4) and the extension one (E5) yield a peak-shaped waveform (Fig. 5.3a), where each peak represents the patient's action on the device. In this case a threshold-based algorithm detects the peaks extracting also their magnitude, duration and distance. All the values are referred to a *zero* represented by the initial condition of the sensorized device when the user is ready to start. The peak event is validated only if at least 75 consecutive samples are above the threshold and only as soon as the samples go under the threshold again. The minimum detection threshold for E1-4 has been evaluated by the specialists for every different exercise whereas the latter (E5) has been imposed by the designers taking into account that the system performs a zero-calibration with the closed hand of the

(a) Peak waveform

(b) Terraced waveform

Figure 5.3: Shape of the processed signals

patient inserted into the tool so that the extension is measured in mm from that situation.

E6 yields a terraced waveform (Fig. 5.3b), where each plateau represents the phase when the patient releases the knob of the tool for repositioning the fingers in the correct way to spin it again and the edges represent the phase when the patients spins with the fingers the knob (thumb, first and second fingers holding it together). In this case the algorithm detects the edges (from the plateaus) and extracts their amplitude, leading to the rotation angle, and duration, leading to the rotation speed. Also the release time, i.e. the plateau duration, is computed. To detect both onset and end of an edge, a simple detection mechanism based on thresholds has been designed, exploiting the smoothness of the filtered signal. A FIFO buffer of 14 samples is linearly updated at every new sample. The mean value of the oldest 4 samples is computed and compared with the most recent sample. If the difference is greater than an empirically determined threshold, the algorithm detects an edge and marks the onset n samples before the most recent one. When the difference falls back under the threshold, the edge end is marked and the processing is repeated, until the potentiometer reaches the limit. By using absolute values, the processing is the same for both clockwise and counter-clockwise exercises. The number of rotations performed is also evaluated.

At last, for the temperature the algorithm detects when the signal becomes stable (i.e. its variations are under an empirically determined threshold but at least 60 seconds are passed from the measurement starting) and then extracts a stable voltage value proportional to the resistance by averaging a few samples in order to smooth the noise. The non-linear trend of the Resistance (Ω)– Temperature (K) relationship is well approximated by the $Steinhart-Hart$ equation [166]:

$$\frac{1}{T} = A + B\,(\ln R) + C\,(\ln R)^3 \tag{5.1}$$

The signal processing for the tapping exercise E7 differs from the others because there are no analogue signals involved. The MCU on the main board acts as the master of the I2C channel, requesting the 8-bit word (one bit for each key in the touchpad) provided by the sensorized aid whenever the sampling timer expires. For this exercise, the timer has been set differently for a sampling frequency of 50Hz, which is in line with the state of the art [124] and allows the complete scanning of the 8 keys in a sampling period, in the worst case (when all the keys are touched). As a new word is received, it is mirrored, if necessary, in order to have the least significant bit always referred to the thumb key. When the first not null data is received, the algorithm detects the less significant bit set to 1 and creates a mask used, at the next touch, to check if the next key tapped corresponds to a less significant bit or not. If this is true, the mask is updated and the processing goes on, otherwise an error flag is set. The

Figure 5.4: The appearance of the proposed telerehabilitation device.

sequence terminates when the thumb touch is detected (lsb = 1). If the number of touches is equal to five the valid sequence counter is incremented or, if either the error flag is set or the sequence length differs from five, the bad sequence counter is. This processing is performed in real-time and when the exercise is complete, an additional routine computes the relevant statistics.

The proposed device embeds all the aforementioned tools, providing all the electronics for the signal acquisition, processing, system control and data transmission.

5.1.4 The patient interface

The patient interface is minimal in order to be accessible by elderly people. It consists of an on/off switch and two push-buttons (for starting a series and for skipping a single repetition) for the input, a buzzer and several LEDS for the output (one LED for every exercise and for the temperature test, in order to pinpoint the exercise to perform, 2 LEDS to identify the right or the left hand, 2 LEDS for the first and second series, one LED blinking at 1Hz for a time reference in the sustained exercises) plus a multi-purpose 7-segment display. The latter is used alternately to show the number of correct repetitions performed within a series, the percentage of effort related to the full sensor range, the elapsed time for the temperature, and other exercise-specific feedbacks.

5.1.5 Device structure and control

In order to guarantee both robustness and portability, the device has been embedded into a metal briefcase. Its final appearance is shown in Fig. 5.4. An ultra low-power MCU, the MSP430FG4618 by Texas Instruments, is used for managing the whole system. The device handles only the integer values coming from the A/D converter, limiting the number of computations induced by the fixed-point numerical representation on the MCU. The conversion

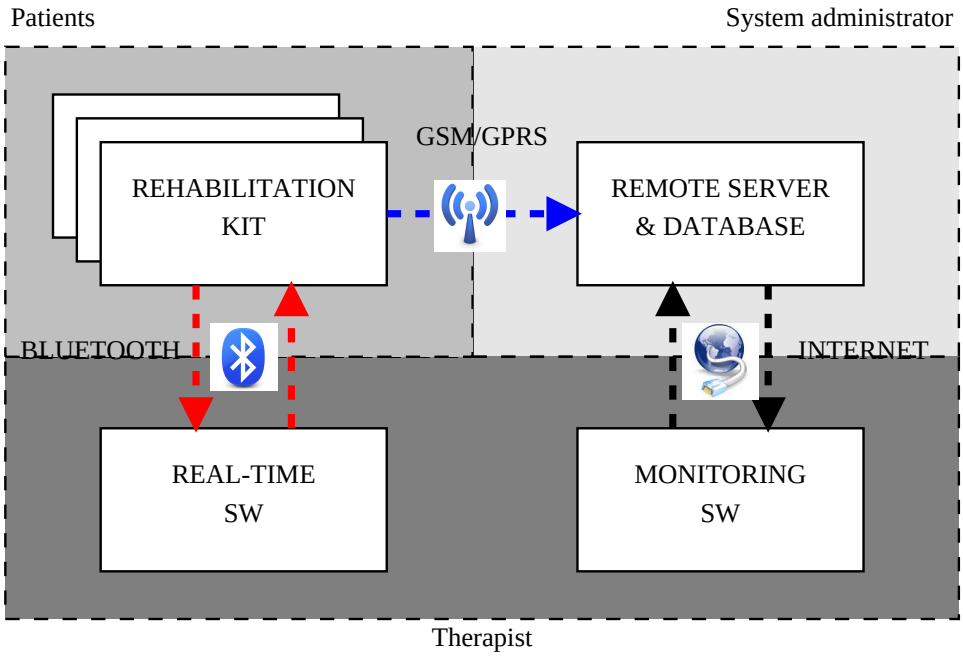

Figure 5.5: Main components of the telemonitoring system for hand kinesiotherapy.

into the corresponding physical quantities exploiting the calibration values embedded into the device software is performed either on the device (only on the statistical summary, at the end of the whole session, just before data transmission) or on the PC when locally controlling in real-time the device.

The underlining design idea is that the same computerized device should be able both to guide the patient in the execution of the exercises when he performs the kinesiotherapy session at home (*deferred telemonitoring mode*) and to execute the commands issued by a PC under the local supervision of a therapist (*real-time control mode*). The latter operating mode is useful either for rehabilitation sessions performed under the direct supervision of a therapist or for the functional evaluation of the hand in the context of a kinesitherapy exercise, as described in [167]. Figure 5.5 shows how the different elements of the proposed system mutually interact, highlighting the area of interest of each user in the different scenarios.

In case of a direct control, the raw signal and the running statistics are continuously sent to the PC whereas, in case of telemonitoring, the raw signal is discarded and the final statistics of every exercise are stored to be sent over the internet at the end of the session by a single GSM/GPRS communication. By reducing the amount of data sent over the internet is possible both to save connection costs and to save battery power, being the transaction completed in a very short amount of time.

The communication features are implemented by means of an internal GSM/GPRS module and an external Bluetooth one. The choice of an external Bluetooth module is dictated by the need of providing such a functionality only to the therapist.

Notably, the system is battery powered so also a power connector (for charging only), a charge led and low-battery led are included. In the light of the clinical trial, the device has been designed including several security mechanisms against macro-shocks (e.g. no operation when charging) and mechanical injuries (e.g. soft materials, rounded edges). Even

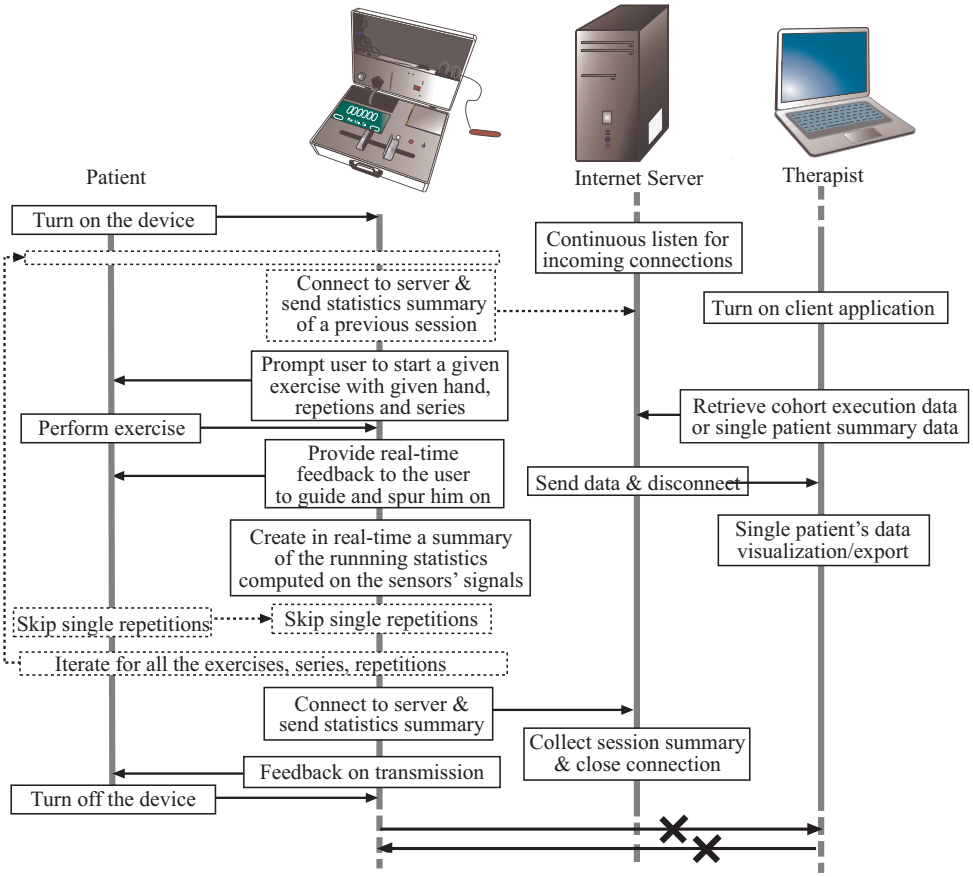

Figure 5.6: Deferred telemonitoring operating mode.

though it is always difficult to evaluate the final cost of a device, when it is in its prototypical form, from a simple estimation of the manufacturing costs including the materials, a value of about 700 Euros per device can be computed. This estimate does not include the researcher's and designer's wages.

Deferred telemonitoring mode

When the device operates in deferred telemonitoring mode (no Bluetooth module connected at boot), it launches a programmed sequence of rehabilitation exercises and collects, during the execution, the statistics representative of the patient's performances, storing them until the end of the session. The MCU firmware controls the patient interface on the device in order to assist him during the exercise execution, enabling a simple training experience.

In this operating mode, the raw signals are used to extract the performance parameters in real-time, but then they are discarded. At the end of the rehabilitation session, a local vector is filled with the related statistical summary and it is sent to the remote server via a TCP/IP connection established by the embedded GSM/GPRS module. The data is sent as a binary stream without encryption since no sensible data are sent and the patient is identified only by the unique International Mobile Subscriber Identity (IMSI) code of the SIM card hosted by the GSM/GPRS module. If the communication aborts, after a limited number of trials the data is stored into the MCU flash memory, informing the user through the 7-segment display, allowing him to safely turn off the device. At the next switch on, if data are present

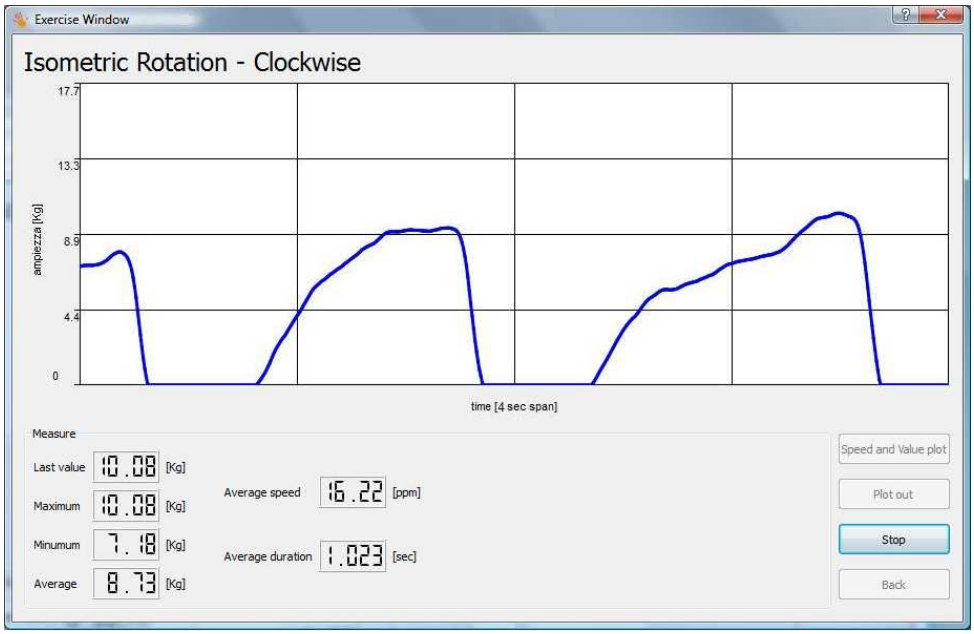

Figure 5.7: Therapist's real-time control interface.

in the flash memory a further forwarding attempt is performed, overcoming a temporary network or server malfunction. The role of the different actors involved in this scenario is depicted in Fig. 5.6. Details on the client application are given in section 5.2.

Real-time control mode

When the system is in real-time control mode (which happens when, at switch on, the MCU detects the Bluetooth module), after an handshake including the calibration constants transmission to the PC, the device puts itself in stand-by. On the PC, a standalone software application, gives to the therapist the possibility of controlling the device. In the main window it is possible to choose the exercise and the hand to use whereas the exercise progress can be analyzed in a different window, specific for the selected exercise, which pops up as soon as the exercise is started. An exemplary screenshot of the therapist interface is shown in Fig. 5.7. In every exercise-specific window there is the possibility both to stop the execution and to go back to the main window, where the physician can select a new exercise.

All the received samples are logged thus, at the end of the execution, the user can visualize a static plot of the whole signal including the relevant delineation markers extracted in real-time by the device (Fig. 5.8). The GUI receives the functional assessment relevant parameters (e.g. speed of execution, position and the amplitude of the last peak, the maximum, the minimum and the mean value of the executions), to be presented on the GUI, every 150 samples of the signal.

Beyond the whole plot of the acquired signal, the interface also enables the visualization of the "Speed and Value plot" (Fig. 5.8), which overprints to a bar graph showing the peak values, a line graph representing the frequency of the repetitions. This information can be useful to evaluate how much the performance is dependent by the execution speed, being important to know if smaller values achieved by the patient are caused by a higher execution speed or by fatigue. It should be noted that traditional assessment techniques do not

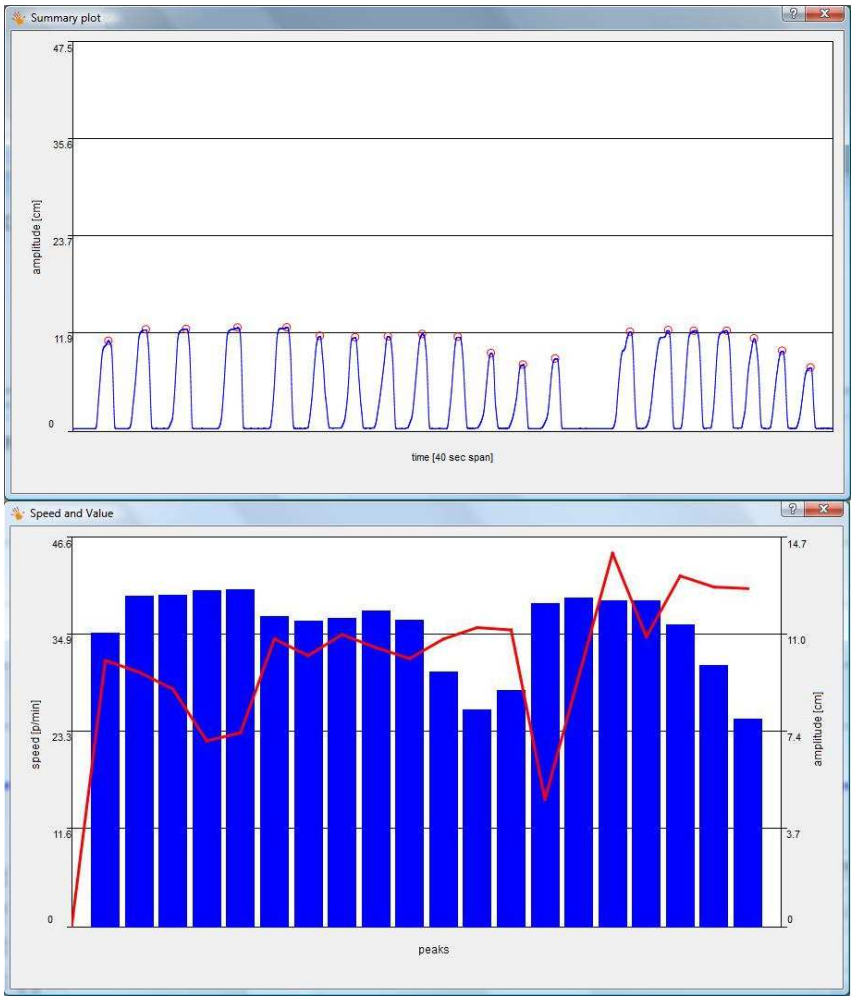

Figure 5.8: Marked whole signal plot (top) and “speed and value” plot (bottom) for the extension test.

consider time as discriminative factor, thus reducing the informative content of the measurements.

The real-time control mode is useful for outpatient clinic examination. During the experimental trial, it has been used for training the enrolled patients and for the periodic evaluations. The role of the different actors involved in this mode is depicted in Fig. 5.9.

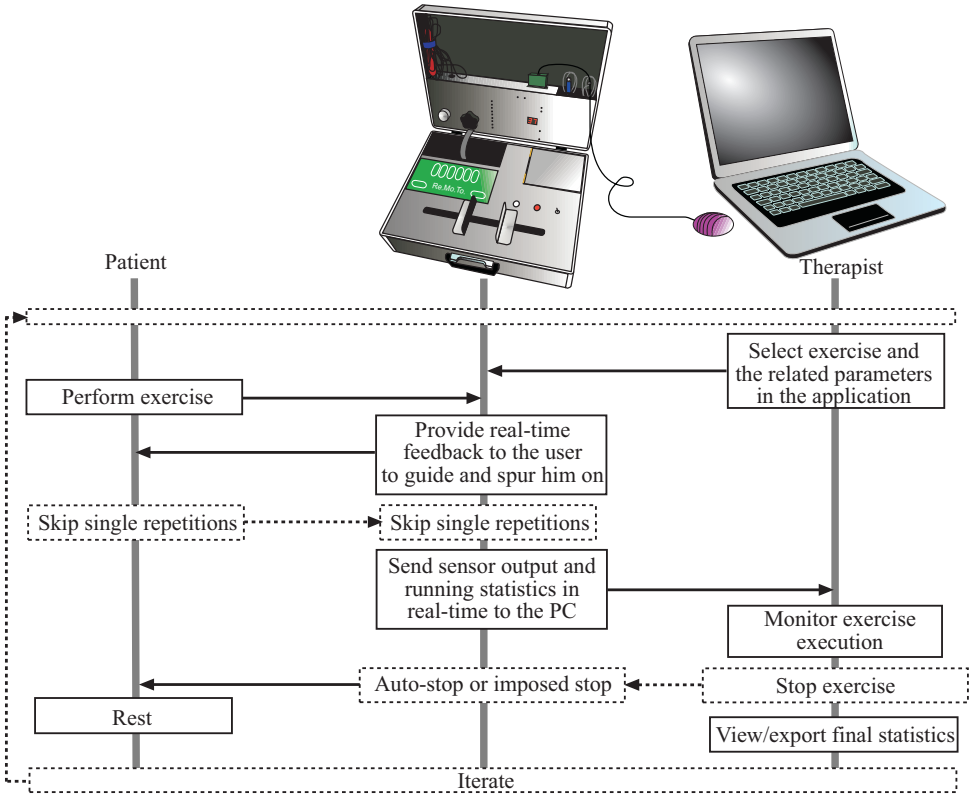

Figure 5.9: Real-time control of the device.

5.2 The External Telemonitoring Infrastructure

In order to enable the telemonitoring feature, the system has been completed with a server application and the therapist's client application for the patient's performance evaluation, described in [168].

The client monitoring application allows the data retrieval in order to check the patients' compliance to the rehabilitation protocol and to perform a basic performance analysis. The data downloaded from the server is stored in a portable file format (.csv) for further analysis in external programs. The monitoring application offers a bird's eye view of the patient's compliance by a table clearly showing when the patients have performed the rehabilitation session and when not. In a second window, the performances relative to each exercise for a given patient can be graphically visualized. An exemplary view of the two windows is shown in Fig. 5.10. These quantities can be used to gather clues on the quality of the rehabilitation session. For instance, in strength exercises the force values are connected to the execution speed, since the faster the action the lower the force. A poor patient's performance should be evaluated in the light of such considerations, in case getting in touch with the patient if needed.

5.3 The Introduction of a Collaborative Approach

The approach described in Section 5.2 has been tested in a clinical trial in Italy for rheumatic patients but its use could be easily extended to other diseases causing hand disability. It presents obvious limits when a larger number of patients are involved because it does not

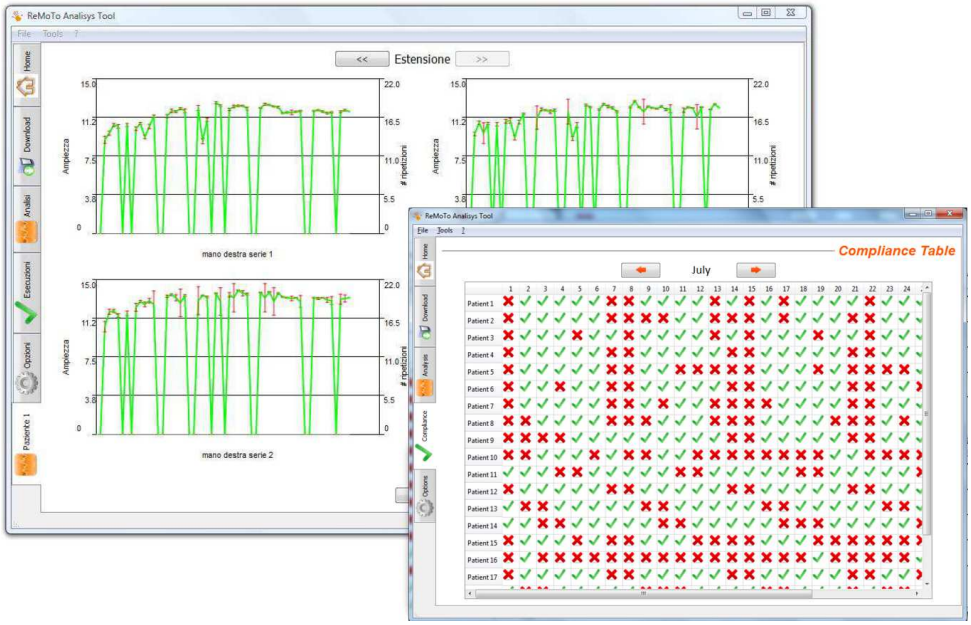

Figure 5.10: The monitoring software: a view of the main client monitoring software windows.

allow to tailor the therapy on the patient's need and adapt it at run-time to the recorded progress. However, for patients followed by more than one specialist, e.g. because of a neurological affection, the contribution in the decision phase of the different figures involved in their follow-up is of paramount importance.

The principal actors involved in the follow-up of a patient enrolled in a telerehabilitation program, and their roles, are sketched hereafter. The Rehabilitation Device (RD) would typically belong to a center where the patient is evaluated by a rehabilitation specialist (e.g. a physiatrist) to define the rehabilitation goals in terms of the concrete possibilities of recovering the functionality. This actor defines the protocol for both acute (in the center) and long term (at home) rehabilitation, assigning the patient to one or more therapists (e.g. a physiotherapist). Typically this second actor would be the one more directly involved in the analysis of the telemonitoring data. Such data can be useful to evaluate the progress and try to figure out the quality of the self-managed sessions from an objective perspective. The rehabilitation specialist will likely act at a higher level, periodically evaluating the patients to define a coarse/fine tuning of the rehabilitation protocol. During this decisional phase, the interaction with one or more specialists following the patient for systemic treatments is important. These new actors could be neurologists for stroke, orthopedists and the surgeons for hand surgery, rheumatologists for rheumatic diseases, etc. In fact, the functional evaluation performed by the rehabilitation specialist cannot include the aspects connected to the disease at a systemic level, if present, or the details on the specific condition (post-surgery, post-stroke, etc.) or modifications to the drug therapy the patient is assuming. A collaborative definition of the patient's protocol update should be pursued including all the identified professional figures.

A minimal support to the collaboration would include the possibility of: exchanging messages through the system, sharing data related to the patient's rehabilitation performance, and operating on the protocol definition. In order to preserve coherency, the division of

responsibility based on roles, expertise and competence or, in some contexts, on a hierarchical model, is required. A telerehabilitation system including support for this kind of interaction would promote the collaborative approach in the follow-up of the patient, in a patient-centric view of the teamwork.

5.3.1 Implementation of a collaboration model

In order to implement the collaborative model specifications, the new functionalities have been integrated in the pre-existing client-server framework described in Section 5.2. The developed software architecture, described in [169, 170], implements the envisioned collaborative scheme among the different actors at different levels. The first one is the sharing of the patients' performance data collected by the RDs, representing the basic information required for decision support in the rehabilitation program. The second one is the sharing and shared management of the rehabilitation protocol. In fact, each actor can access to information on the type of physical therapy the patient is undergoing, playing an active role in the decision making process when designing or adjusting the protocol. The last level consists of the direct interaction between doctors, implemented through a store-and-forward messaging system. One of the most important characteristics of the infrastructure is that it implements a hierarchical authorization level model which eases the patient management, avoiding losses of coherency. Each access level is characterized by different privileges:

1. administrator level: the administrators can insert patients and medical personnel in the system, managing their association, and they can modify/delete the inserted entries at any time. The administrators do not have access to any medical data, messages, etc.;

2. patient manager level: the managers have no restrictions in both viewing their patients' performance data and managing their protocols. They can exchange messages with other people in the medical team following the patient;

3. operative level: these users can view the performance of the assigned patients, can proactively apply minor changes to the protocol and issue major modification proposals to a manager. They can exchange messages with other people in the medical team following the patient;

4. consultant level: the consultants can only view the performance data and protocol of the associated patients and can exchange messages with the other actors to suggest possible protocol modifications in the light of their knowledge, which goes beyond the evaluation of the functional impairment.

Each user interacting with the system is assigned a specific access level, based on the role in the therapy and the relationship with the patient. The privileges associated with each level are predefined and cannot be changed, however the mapping between a role and an access level is somehow arbitrary, and can be adapted to the specific use-case.

Chapter 6

The Experimental Results

In the following sections the experimental results of the device described in Chapter 5 are presented. It has been first tested as a system for the hand functional evaluation in an outpatient clinic, comparing the obtained results with the traditional assessments of hand function. Then, with the telemonitoring featuers, the device underwent to a clinical trial in Italy as a telerehabilitation system. Finally, the proposed cooperative infrastructure has been evaluated by experts in the field using a semi-structured interview.

6.1 Hand Functional Evaluation in an Outpatient Clinic

The first test has been carried out in a rheumatological clinical setting in order to compare hand functional evaluation using the device described in the previous chapter with the traditional assessments of hand function. Six volunteers were enrolled from the outpatient clinic of the Chair of Rheumatology, Department of Medical Sciences, University of Cagliari, Italy. They were evaluated in order to participate to the clinical test if they fulfilled the following inclusion criteria: age $18-75$ years, ability to give informed consent, clinical remission of the inflammatory disease phase, no change in antirheumatic treatment in the three previous months, need to perform a rehabilitation program due to limitation in ability to perform usual self-care, vocational, and avocational activities because of an inactivity periods that preceded the clinical remission of inflammatory phase. All patients are female, underwent a clinical examination and were assessed according to international guidelines. Three of them present SSc and suffered from flexion contractures, caused by retraction of skin, subcutaneous tissues and tendon sheats. Three of them are affected by RA and suffered from muscular hypotrophy, capsular and tendon sheats fibrosis of the hands and wrists without deformities. They underwent a functional assessment through the traditional tools and the portable prototypical device to test its ergonomics and functionality.

Traditional assessments of hand function were performed using the Dreiser test [171], the Health Assessment Questionnaire (HAQ) [172], the Range Of Movement (ROM). For the latter, the movements leading to the hand positions presented in Fig. 6.1 have been considered, namely wrist flex-extension, wrist lateral-lateral and finger lateral-lateral. Hand extension ability was evaluated through the experimental device and by traditional tools. The patient dexterity (exercise of dynamic rotation and finger tapping exercise) and the rotation

Figure 6.1: ROM maximum excursions for angles measurements.

Table 6.1: Demographic characteristics and results of the traditional assessment. RA 1 to 3 are patients with RA whereas SSc 1 to 3 are patients with SSc. Normal values, if any, are presented in the *range* column.(R:right, L:left, F-E: flex-extension, L-L: lateral-lateral).

Parameter	Range	RA 1	RA 2	RA 3	SSc 1	SSc 2	SSc3
Age		47	53	58	45	43	47
Dreiser	0-30	15	16	20	18	21	21
HAQ	0-3	1.2	1.7	2.0	1.2	1.8	1.3
ROM wrist F-E R/L $[deg]$	65-90	90/42	70/60	50/40	80/90	75/65	90/75
ROM wrist L-L R/L $[deg]$	90	35/25	25/15	25/30	70/60	45/60	55/70
ROM fingers F-E R/L $[deg]$	90	65/85	60/60	70/65	88/88	65/80	90/95
Extension R/L $[cm]$		6.5/4.5	4.8/5.5	8.5/8	8/8.2	5.5/5.3	10.5/10.5

torque (isometric rotation exercise) were assessed only by the experimental device since no instruments are currently available for such evaluations. Demographic characteristics and results are shown in Tab. 6.1 and Tab. 6.2.

Although it is not possible to compare the results obtained with the traditional tools against those recorded using the experimental device, because of the low number of subjects, it is worth mentioning that the latter seems to fit with the former. As an example, the SSc2 patient, who showed the highest Dreiser's and HAQ scores and the poorest ROM and traditionally evaluated extension performances, due to high disability levels, had the poorest performances at the finger tapping, dynamic rotation and extension exercises evaluated through the experimental device. Since previous studies have reported that ROM was related to some kinds of hand function in patients with SSc [173, 174] and ROM seems related to the performances recorded by the experimental device, it is conceivable that in the future the latter might represent an instrument to quantify the hand function, or disability, in SSc patients. As another example, patient RA3, who showed the poorest wrists but the best fingers ROM performances, because of a prevalent anatomical damage at wrists level, had a good performances at the dynamic rotation exercise which do not involve wrist movement. Moreover, in the same patient, the low values recorded at the extension exercises evaluated using the experimental device as compared to those traditionally recorded might be ascribed to the counter resistance or to a difficulty in the execution of the exercise, as demonstrated by the low extension speed recorded. Therefore, the experimental device appeared able to differentiate the anatomic level of disability as well as ROM but differently from Dreiser or HAQ

Table 6.2: Results of the assessment through the experimental device. All the parameters are given for Right/Left hand. RA 1 to 3 are patients with RA whereas SSc 1 to 3 are patients with SSc. Data expressed in sec represent the mean time interval between consecutive repetitions. (FT: Finger Tapping, ICR: Isometric Clockwise Rotation, ICcR: Isometric Counterclockwise Rotation, DR: Dynamic Rotation).

Exercise	RA 1	RA 2	RA 3	SSc 1	SSc 2	SSc3
Extension $[cm]$	7.1/4.4	4.0/5.0	3.6/3.2	8.2/7.9	5.2/5.3	12.2/11.7
Extension $[s]$	1.8/1.3	2.2/5.0	2.9/2.2	1.5/1.4	2.9/2.3	1/0.8
Extension speed $[ppm]^{\dagger}$	22.1/24.2	40/40	8.7/10.9	28.7/27.6	10.9/16	38.4/50.2
FT correct $[\sharp]$	20/20	11/18	20/13	20/20	3/9	2/20
FT wrong $[\sharp]$	0/4	19/12	2/7	10/10	27/21	28/9
FT speed $[tps]^{\dagger\dagger}$	2.4/2.8	1.4/1.7	1.8/1.6	2.6/3.1	0.8/1.4	0.4/2.5
ICR $[Kg]$	2.0/2.5	3.8/3.3	2.4/3.3	2.6/5.0	3.9/3.6	1.2/3
ICR $[s]$	1.1/1.3	1.1/1.1	1.5/0.8	0.9/1.2	2.0/2.3	1.1/0.8
ICR speed $[ppm]^{\dagger}$	28.3/23.0	26/19.0	21.3/35.0	34.0/21.9	12.1/21.0	26.3/32.0
ICcR $[Kg]$	3.6/2.3	1.2/3.3	2.5/2.7	6.3/4.1	5.2/4.7	2.9/2.9
ICcR $[s]$	1.3/1.3	1.4/1.1	1.1/0.8	1.1/1.2	1.5/1.1	0.8/0.8
ICcR speed $[ppm]^{\dagger}$	27.8/24.8	25.0/26.0	24.6/28.2	30.0/31.3	22.0/30.0	39.0/41.0
DR $[deg]$	195/81	195/113	183/272	224.5/229	119/139	163/110
DR speed $[deg/s]$	340/472	257/189	381/388	334/387	544/869	646/297

† ppm = peaks per minute; †† tps = touches per second

which are general indicators. Moreover, allowing the registration of speed parameters, the experimental device might estimate the quality of the exercise or the difficulty in performing it.

6.2 The Clinical Trial with the Telemonitoring Infrastructure

The proposed non-CE marked medical device underwent a clinical trial, reviewed and approved by the Italian Public Health Department, with the aim of validating its use as a telerehabilitation system.

Fifty patients with RA and forty patients with SSc, diagnosed according to the American College of Rheumatology classification criteria, and referred to the rheumatology outpatient clinic of the Policlinico Universitario of Cagliari, were screened with the aim of identifying 20 patients per disease homogeneous for demographic, clinical, and functional characteristics. The presence of tender and swollen joints, deformities, functional deficit, or impairments in the hands and wrists was evaluated. Participants were eligible if they had a Dreiser's index score ≥ 6 and had been receiving stable medications for 3 months. Exclusion criteria were irreversible anatomical damage such as bony ankylosis, tendon rupture, joint dislocation and subluxation, active arthritis, and digital ulcers. A 28-joint Disease Activity Score (DAS28 [175]) higher than 2.6 was an exclusion criterion for patient with RA. Changes of therapy were not allowed during the trial and were a reason for withdrawal from the study.

Twenty patients per disease, matched for sex, age, disease duration, HAQ and Dreiser's Algo-Functional index (Functional Index of Hand OA, FIHOA) scores, were enrolled. In-

formed consent was obtained for all participants. The protocol of the clinical trial, with a medical device not assessed for compliance with European safety standard for commercial use, was reviewed by the Ethics Committee (Azienda Ospedaliera Universitaria of Cagliari, no. 245/2011), and the trial was authorized by the Italian Department of Health (approval no. 9751/2012).

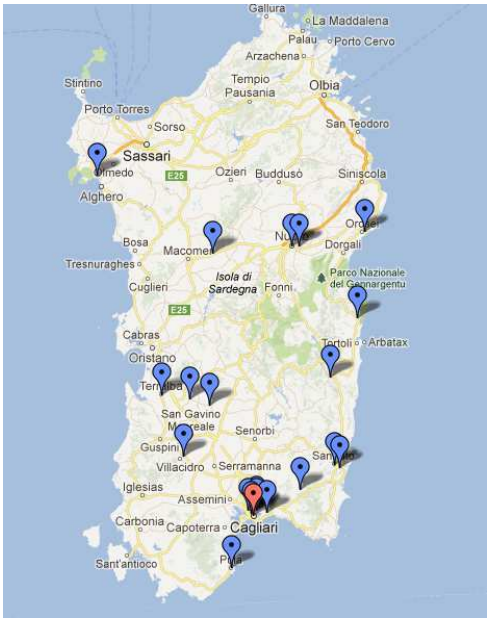

Figure 6.2: Patients distribution across the regional territory. In red is shown the position of the Rheumatology Unit in Cagliari

Once matched in pairs, patients were assigned to the experimental or the control arm by permutated block randomization. Ten patients with SSc and 10 with RA were trained on the autonomous use of the experimental device by investigators (experimental arm). Every patient received individual 1-h training on the proper and safe use of the device, along with a user manual comprehensively describing the functioning and maintenance of the device. Moreover, they received an illustrated booklet describing the exercises. The kinesiotherapy protocol of the experimental protocol was repeated 5 days per week for 12 weeks, each session lasting a maximum of 50 min. Every workout was conducted at home by patients and remotely monitored by physicians through the telemonitoring interface. Telemonitoring data were checked twice per week, allowing physicians to report the adherence to the protocol. To be aware of possible complications and minimize nonadherance and withdrawals, the investigator contacted patients by telephone if the following warning flags were detected: loss of one or more workout session or a worsening trend in exercise statistics during the week. The distribution pf the patients in the axperimental arm across the regional territory of Sardinia is shown in Fig. 6.2.

The remaining patients received individual training for 30 minutes to perform a kinesiotherapy protocol at home consisting of 3 strengthening and 3 mobility exercises using common objects, as similar as possible to the exercises proposed by the rehabilitation device, to be repeated 5 days per week for 12 weeks, each session lasting a maximum of 45 min. Patients receive a booklet with pictures describing the exercises. For patients enrolled in the control arm, no additional contact other than followup was scheduled, unless an ad-

verse event occurred. At each visit they were asked to report on their weekly adherence to protocol.

At the beginning (T0), at the half (T1) and the end (T2) of the clinical trial, every patient was assessed by a rheumatologist using HAQ, FIHOA, Medical Outcome Study Short Form-36 (SF-36), pain visual analog scale (VAS, unidimensional measure of pain intensity), and VAS Global Health (GH). Hand disability in patients with SSc was also bilaterally evaluated by the Hand Mobility in Scleroderma (HAMIS) test [176]. The DAS28 was calculated for patients with RA only to highlight any increase in inflammatory activity. Likewise, patients with SSc were evaluated for active joint inflammation, defined by the presence of synovitis and tendon friction rubs at clinical assessment. Afterwards, a kinesiotherapist quantitatively assessed the hand strength (grip and pinch) measured through a sphygmomanometer. The maximum hand abduction and the range of movement (ROM) of metacarpophalangeal (MCP) joints (ROM fingers) for both the hands was measured through a goniometer.

The trial was primarily designed to determine the effectiveness of the kinesiotherapy rehabilitation protocol in improving hand function, as mediated by increases in strength, dexterity, and range of motion (ROM) in patients with SSc and RA. The secondary goal of the trial was to compare the experimental protocol using the device versus a similar workout to highlight differences in hand function improvement and in patient compliance. Accordingly, the primary outcome of the trial was hand function measured by HAQ, FIHOA, and the HAMIS test for patients with SSc. Maximum hand abduction, joint ROM, grip strength, and pinch strength were secondary outcomes. The SF-36, VAS pain (0-100), and VAS-GH (0-100) were outcomes for quality of life (QoL) assessment. Compliance to protocol was defined by the number of patients who completed the three-month trial. If a major violation to protocol occurred, the patient was withdrawn from the study. Major violation were defined as a whole week without performing the workout sessions, or more than 2 missed workout sessions per week, every week. Compliance for patients in the experimental arm was derived from the telemedicine system, while for those in the control arm it could only be indirectly referred. These results are presented in 6.2.1.

The statistical analysis of functional improvement of the patients in the experimental arm at the end of the trial with respect to their baseline performance has been also carried out and described in 6.2.2 with the aim of evaluating the effect of the telerehabilitation sessions in these patients with respect to their initial conditions.

6.2.1 Results from the comparison of experimental and control arms

Data processing and statistical analysis were performed by the medical specialists directly involved in the clinical trial [177] using repeated measures ANOVA and pairwise comparison between each visit and the immediately preceding one to address within-subject effect and compare quantitative variables throughout followup. A mixed model ANOVA providing a grouping variable (experimental and control arm) was used to address the between-subjects and interaction effects. P values less than 0.05 were considered statistically significant. Only data from patients who completed the clinical trial were included in the statistical analysis. Patients with SSc showed improvement in primary outcomes in each arm, but no statistically significant difference between subjects was highlighted when findings from the two arms were compared.The FIHAO significantly improved in both arms (p=0.006), whereas the

HAQ (p=0.016) and the HAMIS (right hand p=0.016; left hand p=0.075) improved only in the experimental arm. Patients in both arms achieved statistically significant results over time in pinch strength and MCP (finger) ROM measures for the dominant (right) hand, but grip and pinch strength measures for non-dominant (left) hand significantly improved only in patients treated experimentally. Nevertheless, no statistically significant differences in secondary outcome measures between treatment methods were demonstrated. No QoL outcomes improved during followup in both arms. Two patients from the control arm reported discontinuing the protocol for more than one week for no specific reason and were withdrawn from the study. One patient from the experimental arm discontinued the exercise protocol because of major abdominal surgery and was withdrawn from the trial. Patients in the experimental arm performed 93.4% ± 8.7 % of the scheduled workout sessions (range from 71.4% to 98.8%). All of them were contacted by phone at least one during the study period following telemonitoring detection of a warning flag. No adverse event related to the use of the device was recorded.

About patients with RA, those in the experimental arm experienced a progressive improvement of the variables under study, pointing out that the positive effect of the telemedicine-assisted exercise protocol was sustained during followup. In particular, FIHAO (p=0.013) and HAQ (p=0.015) showed a statistically significant improvement over time but, although patients included in the control arm did not significantly improve, no statistically significant differences between subjects were highlighted when primary outcome findings from the 2 arms were compared. Patients in the experimental arm achieved statistically significant results in secondary outcomes over time on both grip and pinch strength, the latter showing a significant improvement when compared to results from patients enrolled in the control arm. According to DAS28, no disease relapse was recorded during the trial in either group. Three patients in the control arm reported major violations to the protocol and were withdrawn from the study. One patient from the experimental arm received intra-articular steroid for rhizarthrosis and was withdrawn from the trial. Patients in the experimental arm performed 89.1% ± 6.2% of the scheduled workout sessions (range from 77.9 % to 97.6%); all were contacted by phone at least once during the study period because of the telemonitoring detection of a warning flag. No adverse event related to the use of the device was recorded.

6.2.2 Evaluation of patients improvement with the proposed device

Although no statistically significant differences were found between the control and the experimental arms performing similar exercises, the previous results highlight a greater improvement for the latter. Therefore, we decided to investigate the improvement of the patients in the experimental arm comparing their performance at the end of the trial with respect to their baseline values. In fact, in the daily practice, patients neglect the rehabilitation, despite it is deeply recommended by physicians. Fig. 6.3 and Fig. 6.4 show the percentage variation (with respect to T0) of functional and performance indexes (measured using both traditional methods and the proposed device) at T2, using the dominant hand (the right for all the patients). The boxplot highlights the median value and the 25th and 75th percentiles, whereas the whiskers span the range of the outermost samples not taken as outliers (that in turn are identified as crosses in the graph). To highlight those parameters showing a significant within-subjects improvement throughout follow-up, the pre-test vs. post-test results

were compared using the paired sample Wilcoxon test. Statistically significant values were considered for a p value less than 0.05 and they have been marked in figures with an asterisk.

The increase in the four indexes ordinarily used in clinical practice (ROM fingers, ROM wrist, grip and extension), as depicted in Fig. 6.3, highlights the actual improvement of the patients' physical performance at the end of the clinical trial. The same increasing trend is shown by the other parameters in the two figures, measured with the proposed device, confirming the significance of the proposed method according to the standard evaluation methods, as discussed in Section 6.1. The discrepancies between the grip and extension results, with or without the device, can be ascribed to the different modalities that characterized the test execution. In fact, the device measures an isometric grip force whereas a non-isometric grip is performed during the traditional assessment. Similarly, hand extension measurement with the device imposes a counter-resistance, not present in the traditional assessment.

In order to use a typical clinical index for the evaluation of the patient's health perception, the Dreiser index was also analysed in the same time frame. The percentage reduction of this index for both RA and SSc patients is depicted in Fig. 6.3. It should be noted that since the reduction of this index in T2, with respect to T0, corresponds to a better perceived hand functionality, the result in Fig. 6.3 is expressed as a positive percentage variation even though actually such an index decreased over time.

The proposed device allows the evaluation of other strength/agility parameters not used in the clinical practice, whose percentage variations are shown in Fig. 6.4. The first three indexes highlight an increasing trend in clockwise/counterclockwise rotation torque (E4 according to the terminology adopted in Section 5.1 on page 80) and in the finger tapping (E7) speed. The improvement of the latter index is due both to the improvement of patients' agility and to their ability in learning how to execute the exercise, proved by the correlated increase of the right number of touches. The last four indexes, representing the trend of the finger pinch exercise (E3), show worse results. These are supported by the telemonitoring data which show that the time spent in the exercise and the performance tend to decrease after the very first days, becoming stable, despite the overall improvement in the hand functionality. Further investigations revealed that the exercise was perceived as being really difficult for almost every patient. Since the proposed threshold technique gives the patient a feedback (a chiming buzzer) as soon as the minimum required effort is reached, the patients were prone to execute this exercise with the smallest effort, avoiding applying the maximum force. In a future trial such a feedback will be modified in order to avoid this issue, providing a goal for the patient.

The values of dynamic rotation angles (E6), are not realistic, since the patients tend to cheat the exercise when rotating the knob, spinning it in order to exploit its inertia thus achieving very large angles, above physiological limits. This is completely perceivable from the remote monitoring and has been confirmed by the periodic evaluations of the patients. Such a result highlights the limits of an autonomous home rehabilitation system which can be cheated by non-conscientious patients. The introduction of a counter resistance in the rotation knob would avoid the free rotation, thus reducing this problem. It will be interesting to see whether such a hardware control is able or not to provide the same results that a doctor-patient interaction would in the light of the telemonitoring data.

Although a study on acral temperature regulation would require taking into account several influencing factors, exploiting the embedded temperature sensor we observed an increasing trend of the mean temperature difference $\Delta T = Tend - Tstart$, where Tend is the temperature after the rehabilitation session and Tstart that before it. The results of our anal-

Group	Hand	pre-exercise [°C]	post-exercise [°C]	P value
SSc	**Dx**	30.6(±1.3)	32.3(±1.6)	< 0.0007
SSc	**Sx**	30.9(±1.6)	33.0(±1.3)	< 0.0001
AR	**Dx**	32.5(±2.3)	34.1(±1.6)	< 0.0005
AR	**Sx**	33.6(±2.1)	34.9(±1.3)	< 0.0057

Average (± standard deviation)

Table 6.3: Acral temperature analysis

ysis are presented in Table 6.3. As can be seen, the results suggest the efficacy of the kinesiotherapy approach implemented in the proposed device in increasing blood inflow to the hand, which was one of the goals of the therapeutic exercises for the SSc patients. They, starting from lower values of the temperature, achieve a larger improvement compared to the RA patients, who do not present such a microcirculation problem.

From a clinical perspective, the effectiveness of the kinesiotherapic sessions was demonstrated by the findings of a statistically significant improvement in both subjective (Dreiser's index) and objective (e.g. ROM, strength) parameters. At the end of the follow-up both RA and SSc patients showed an increased average amplitude of the movements (in E5, E6), a higher speed of execution (E5, E6, E7) and a better ability to perform fast and precise movements (E7).

Moreover, an increased endurance was developed, as demonstrated by the increased average duration of the strength exercises (E1, E2, E4) despite a stable average of the amplitude. These satisfactory results might also be ascribed to a very high compliance of the patients to the exercise protocol. The exception represented by E3 may be in part related to the medical need to keep the exercise intensity at a pain-free level. It can be noticed that the patients enrolled in the RA and in the SSc group achieved different results. Furthermore, there is a difference in the between-subject results achieved by patients from the same group. This should not be surprising and must be attributed to the biological variability of the subjects and to the fact that the best results can only be achieved through a personalized rehabilitation program. However, for the purpose of this pilot uncontrolled clinical trial, aimed at evaluating the feasibility and effectiveness of the proposed approach, we chose to define the working parameters at the beginning and not change them over the duration of the trial in order to effect a more rigorous evaluation of the method. As a consequence, not enabling any protocol personalization, we could not ensure an equal level of improvement. Starting from the achieved results, further studies, based on adjustable working parameters, will address the effectiveness of telemonitored personalized rehabilitation programs.

In terms of adherence to the protocol, Figure 6.5 reveals that more than one half of the trial participants of the experimental arm performed more than 95% of the prescribed rehabilitation sessions. The patients with the worst adherence to the protocol still executed more than 70% of the prescribed sessions. A second interesting data concerns the distribution throughout the day hours of the registered training sessions. As shown in Figure 6.6, although a considerable concentration of execution in the early evening is noticeable (37% within three hours from 16:00 to 19:00), more than a one half are distributed among the rest of the day. This means that the patients took advantage of the flexibility this kind of approach

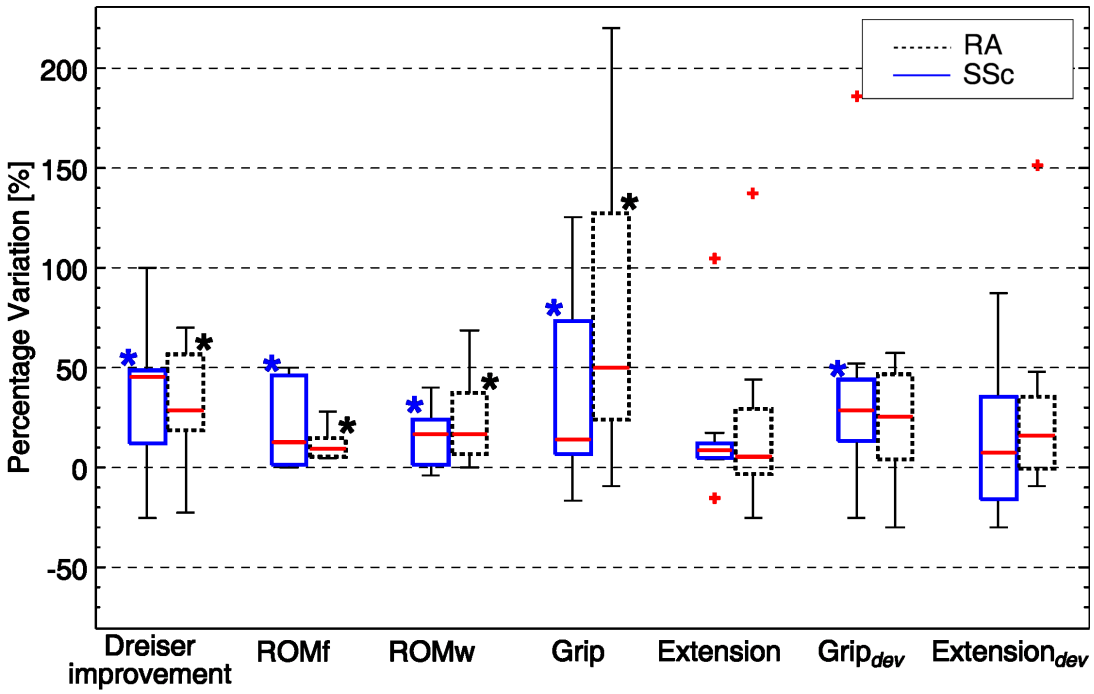

Figure 6.3: From left to right the mean percentage variations of respectively the Dreiser index, the ROM finger measurements, the ROM flexo-extension measurement, the grip strength, the extension amplitude, the grip strength measured by the device, the extension amplitude measured by the device, at the end (T2) of the trial with respect to the beginning (T0).

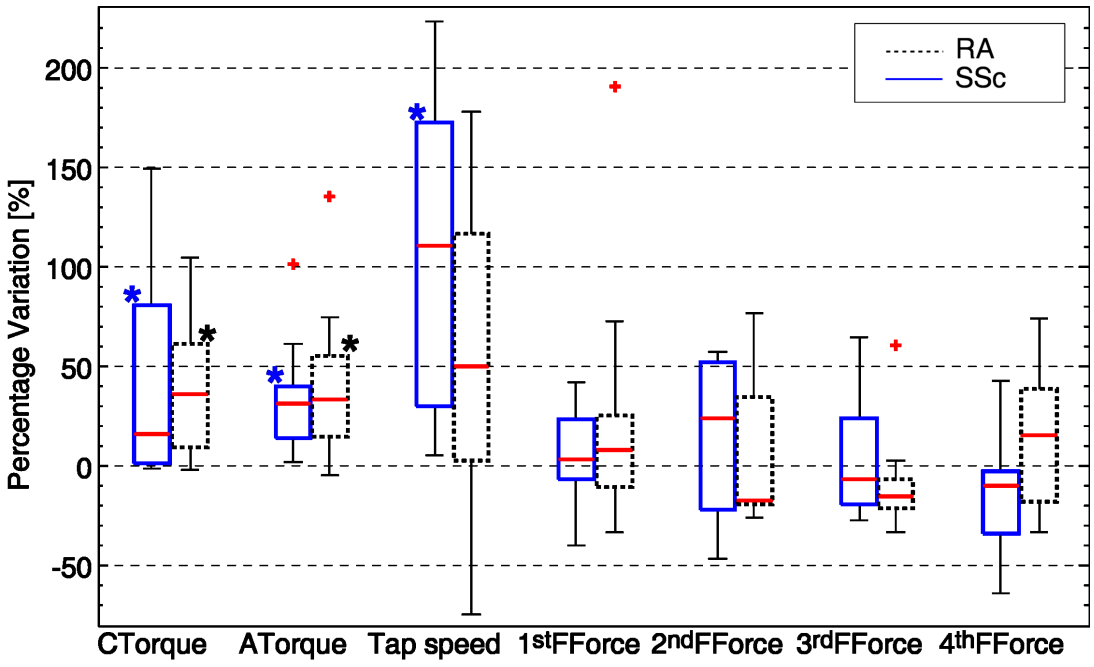

Figure 6.4: From left to right the mean percentage variations of respectively the clockwise rotation torque, the anticlockwise rotation torque, the finger tapping speed, the index finger pinch force, the middle finger pinch force, the ring finger pinch force and the little finger pinch force measured by the device at the end (T2) of the trial with respect to the beginning (T0).

allows and they appreciated this aspect, in opposition to the strict schedule a therapy performed in a care center would impose. At last it is worth to note that the dropout rate during the trial was of 10%, since only two participant left, because of problems not related with the rehabilitation program.

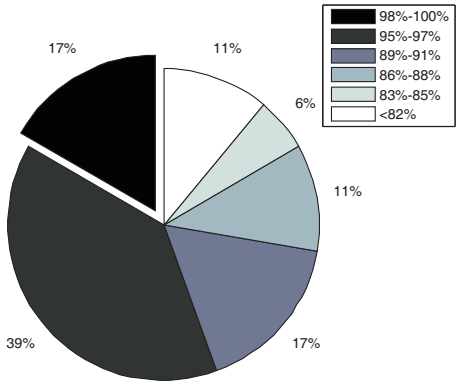

Figure 6.5: Pie chart of the adherence to the protocol (in terms of percentage of performed rehabilitation sessions with respect to the prescribed number) for the whole group of patients in the experimental arm.

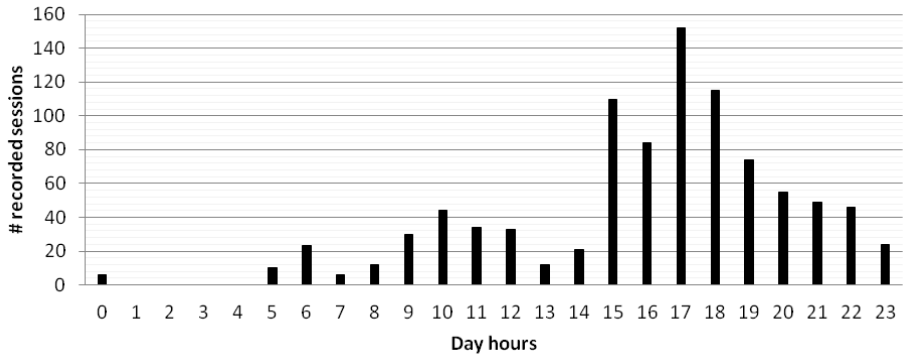

Figure 6.6: Distribution of executed training session during the day hours

6.2.3 User evaluation of the device

At the end of the clinical trial, patients were given the opportunity to evaluate the device according to the Quebec User Evaluation of Satisfaction with Assistive Technology (QUEST 2.0 [178]). It consists of 12 items rated on a 5-point scale to assess the patient's satisfaction where 1 stands for "completely unsatisfied" and 5 for "completely satisfied", presented in Figure 6.7, where the error bars represent the standard deviation. It also allows the patients to identify the three most important items for the device evaluation. The total QUEST score was 4.47 ± 0.30 (min 3.83: max 4.83), while the services subscale scored 4.79 ± 0.32 (min 4.00; max 5.00), and the device subscale scored 4.31 ± 0.38 (min 3.50; max 4.87). The results show that 75% of patients considered the effectiveness and the simplicity of use as two of the three most important items when evaluating the device. These items obtained an average evaluation

score of 4.22 and 4.88 respectively. On the contrary nobody considered important neither the dimensions nor the weight of the device, which obtained an average evaluation score of 4.05 and 3.11 respectively, in which the latter fits the definition “more or less satisfied”. Such a negative evaluation is probably due to the prototypical version of the device, which weighs about 6.5kg. Despite the patients did not consider important these items for the evaluation of the device, it would be advisable a reduction of both the weight and the size of the device in order to improve its portability.

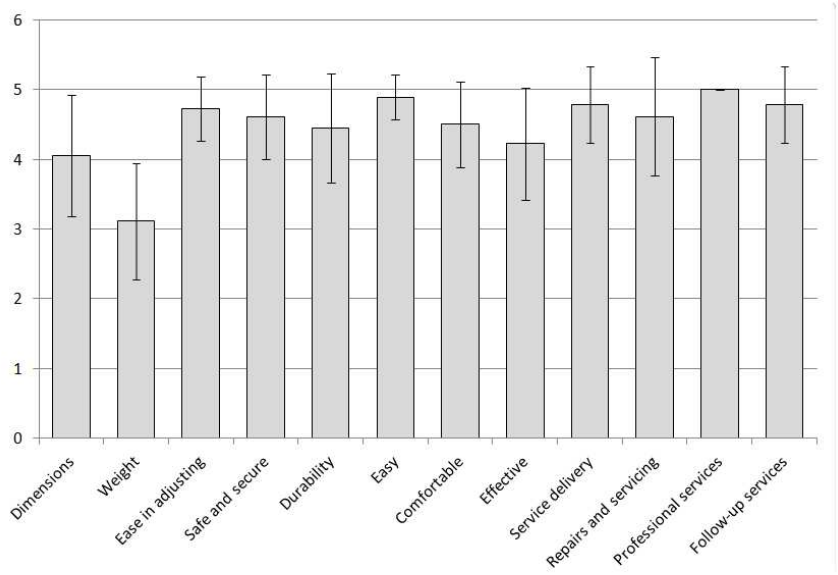

Figure 6.7: Average and standard deviation of the answers to the individual QUEST questions.

The Individually Prioritised Problem Assessment test (IPPA, [179]) evaluates the improvement in the daily life activities of the patients, thanks to a double administration of the same questionnaire: at the beginning of the trial every patient was asked to define up to 7 tasks he had difficulties with, scoring both the importance and the difficulty level from 1 to 5, obtaining a global baseline score. At the end of the trial, every patient was asked to score again the same tasks after the rehabilitation (only difficulty level), not viewing the baseline scores. The resulting global follow-up score is computed and, if it is lower than the baseline one, an improvement has been perceived. This can be measured as the difference between the baseline and the follow-up scores. In our test we achieved 3.7 (with a standard deviation of 3.4), ranging from 0 to 11.6. Detailed results are shown in Figure 6.8.

The PIADS [180] is a 26 items questionnaire that measures the impact in the quality of life of using assistive technologies from the patient’ s point of view. The items can be grouped in three subscales, pertaining to competence (perceived functional capability, independence and performance), adaptability (motivation, inclination) and self-esteem. For each item the respondent must assess in what measure the device has affected that specific aspect of his life, by rating with a score ranging from -3 (negative impact) to $+3$ (positive impact). The mean PIADS score can be obtained by adding the rates obtained for each item and dividing it by the number of total items. The result obtained in our case was a mean score of 0.84

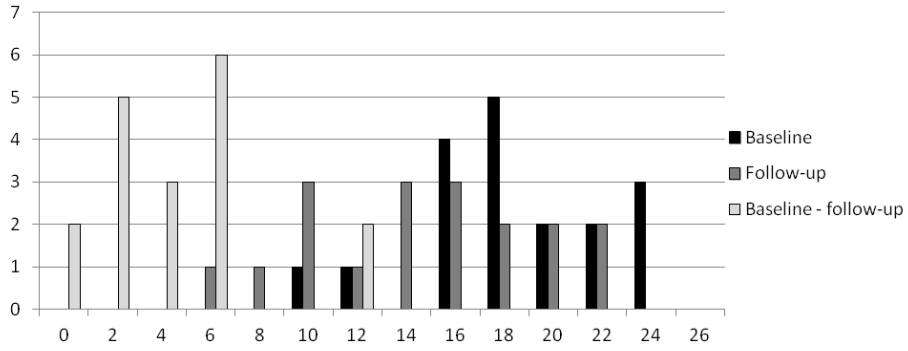

Figure 6.8: IPPA questionnaire results (baseline - follow-up)

± 0.8 points overall. The individual results in the three subscales (Figure 6.9) show that the patients felt the use of the device beneficial for their ability in performing common tasks (competence scale), whereas the aspects related to the self-esteem were the least affected.

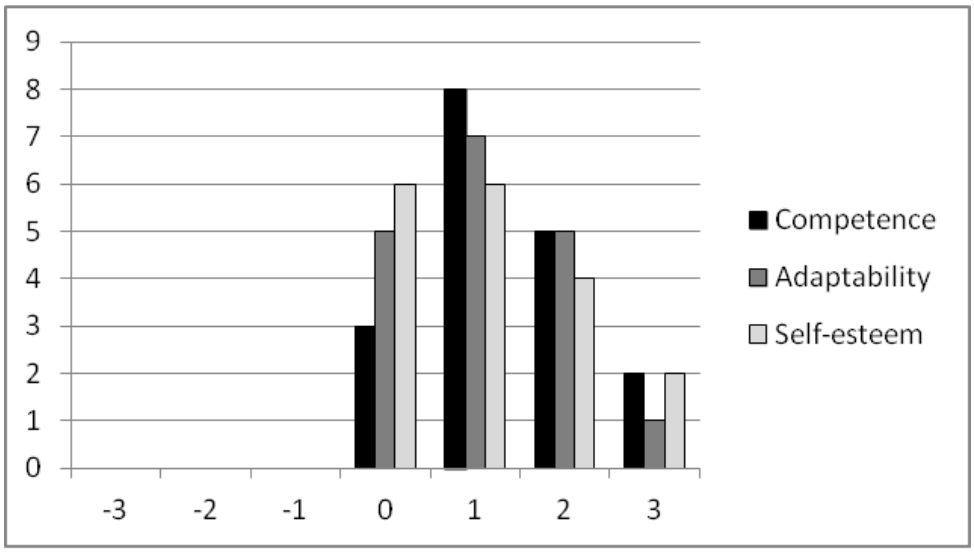

Figure 6.9: PIADS scores for the 3 categories separately

6.3 Physician's Evaluation of the Proposed Telerehabilitation System

In order to assess the usability of the telerehabilitation system, a panel of 9 rheumatologists not directly involved in the trial has been asked to undergo a simple test. The choice of asking to experts in the field descends from the need to ensure the user has an idea of the usefulness of the system and all the more so he is able to understand what he is analysing in terms of patient's data.

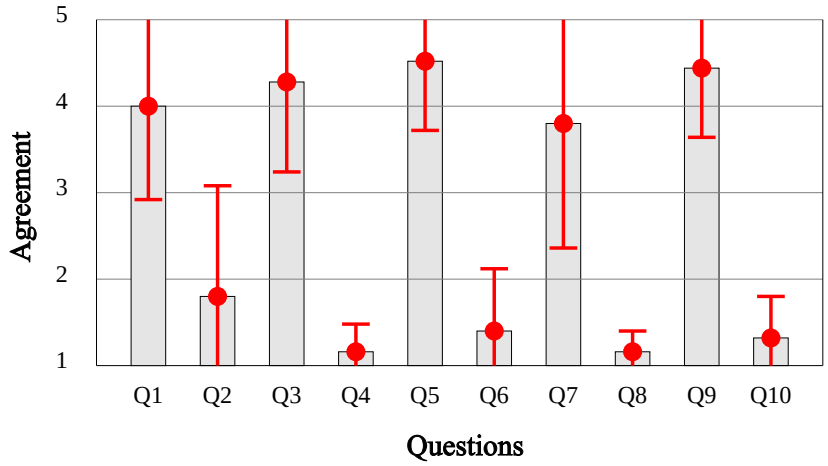

Figure 6.10: Mean and standard deviation of the answers to the individual SUS questions (the vertical scale represents the level of agreement, with 1 for "strongly disagree" and 5 for "strongly agree").

After attending an half-an-hour presentation on the whole telemedicine infrastructure with details on the physician's monitoring application, the rehumatologists had the possibility of using the system for the time required to carry out 3 simple tasks, without any possibility of interacting with the designers, reporting if they were able to perform a given task and their difficulty in performing it (on a scale from 1 to 5). The tasks were a synthesis of common operations included in a normal use case and consisted of: data download, execution data and statistics visualization, and raw data comparison through the graphic interface.

Then, a questionnaire for the evaluation of the system usability has been administered. To this aim, we chose the System Usability Scale (SUS) questionnaire [181]. Such a scale tries to measure the perceived usability of the system (from the physician's perspective) within the reference context. In fact, usability can be intended as the perceived appropriateness to a context of a given artefact, and cannot be fairly evaluated outside it (for instance with physicians with a different background and specialization). The 10-item scale yields a single number from 0 to 100 representing a composite measure of the overall usability of the system being studied. The questions concern the system ease of use, complexity and usefulness (the complete questionnaire con be found at www.usabilitynet.org/trump/documents/Suschapt.doc).

In the proposed test all the tasks have been performed correctly by the physicians, and the average difficulty level marked was 1.4. In Fig. 6.10 the results of the SUS assessment are shown. It is possible to see the distribution of the answers to the 10 questions proposed by the questionnaire in terms of mean and standard deviation (the scale is from 1 to 5, where 1 is for "strongly disagree" and 5 for "strongly agree" with the questionnaire statements). The final score is a mean SUS of 85.3 (minimum value 55, maximum value 97.5) with a standard deviation of 13.8. Taking into account that the system has been used for the first time by the panel of physicians in that occasion, it is overall a very good result.

From a physician perspective the system presents several advantages under different viewpoints. At first, the whole infrastructure is completely standalone, i.e. it can be used as it is, without the need of any additional support device at both ends (patient's and physician's), limiting possible additional costs for both the patient and the Public Health System.

All the low level aspects of the whole telemedicine infrastructure are completely transparent. In this way the physician can better focus on the monitoring aspect and the interac-

tion with the patient. The execution table on the monitoring application allows a birdview of the patients population in terms of execution without entering the details. Further analyses on the single patient are also allowed.

6.4 Collaboration Framework Evaluation

The aim of the improved telerehabilitation infrastructure, presented at end of the previous chapter, is to facilitate the collaboration among the different actors involved in the rehabilitation of patients affected by any diseases requiring a specific kinesiotherapy for recovery. In order to investigate this aspect and the potential use of the system in the daily professional activity, a semi-structured interview to a panel of experts has been carried out. Such an approach has been chosen because there are no validated instruments to measure the potential efficacy of the proposed collaborative framework in the clinical practice.

The panel was chosen using a convenient sampling method and it is composed of 7 physiatrists and 9 rheumatologists. The panel member's age is between 24 to 58 (mean 36.3 ± 9.0), with a seniority from 1 to 29 years (mean 8.9 ± 7.8), and 62.5% are females. The experts were contacted by e-mail and were asked to participate to the survey. Upon acceptance, they received a link to a video concerning the Rehabilitation Device (RD) and the collaborative infrastructure. The video presented:

- a scenario showing how patients work with the RD, both in the medical center and at home;
- a description about how the medical staff and the patients interact with the system (respectively the telemonitoring application and database interface, and the RD minimal interface and real-time feedback);
- the main results of the clinical trial;
- a use-case underlining the added features promoting the collaboration among the medical staff.

The use-case was intentionally simple and linear in order to allow participants to figure out new scenarios, add further details, provide feedback and compare the use-case scenario with their daily working experience. The following five roles have been identified for the actors in this system:

(i) the patient,

(ii) the physiotherapist (operative level),

(iii) the physiatrist (rehabilitation specialist level, patient manager),

(iv) the rheumatologist (consultant level),

(v) the administrator.

The rehabilitation protocol is defined by the physiatrist and uploaded on the RD at its first connection to the server. Slight modifications to the protocol can be defined for individual patients and applied directly by the physiotherapist. More significant modifications could be required by the health status of the patient (e.g. pain in one hand, so the exercises must be performed only with the other one; removing/adding some exercises to the protocol) or the performance trend (e.g. changing the number of series). However the new protocol has to be validated by the physiatrist after a medical examination or after the analysis of the patient's time series.

The physiatrist could require a second opinion to the specialist (in this case the rheumatologist and seldom the orthopaedist) that is treating that patient for his primary disease. In turn, the specialist could be proactive, signalling to the physiatrist the occurrence of changes in the patient's therapy or in the progress/activity of the disease. This is a form of collaboration between peers which imposes the exchange of messages and alerts and requires that all the actors have access, with different privileges, to the patient's data and rehabilitation protocol details. However, the direct modification of the protocol is reserved to one specialist only, in this use-case the physiatrist, who is responsible of the rehabilitation. The use-case can be schematically described as in Fig. 6.11 in terms of the relationships between the different actors.

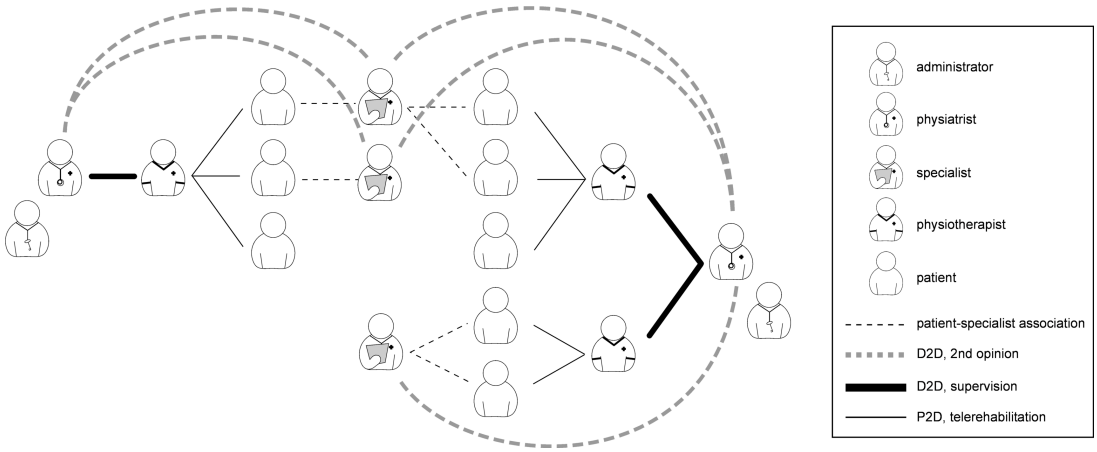

Figure 6.11: Exemplifying schematic representation of the actors of the system and their interaction.

6.4.1 Semi-structured interviews

The interview is divided in two sections. The first one tries to gather information about the experts' daily routine and inclination. The second one assesses the experts' perception of the proposed system in case of a real use of the system in their clinic/hospital. The experts were asked to figure out how their work could be influenced by the proposed system and to propose some improvements.

In particular, the first section investigates:

1. the expertise in the field of rheumatic diseases,

2. the habit of collaborating with colleagues with different specializations,

3. the role of the experts in the rehabilitation process,
4. the frequency of analysis of the patient's performance data.

The second section investigates:

1. the perceived applicability of the proposed collaboration scheme in the light of the roles assigned to each specialist,
2. the need of assigning different rights/privileges to the different specialists,
3. strengths and weaknesses of the proposed scenario.

The interview lasted about 20 minutes on average.

Data analysis

From the analysis of the interviews it is possible to summarize the following information.

All but one physiatrist work with patients affected by rheumatic diseases suffering from hands disability, even though they are not the majority of the patients. Experts highlighted their experience in the field providing examples about other diseases which could benefit from using the rehabilitation device, mainly in the field of neurorehabilitation and hand surgery. All but one of the experts (94%) state they usually collaborate with other specialists (e.g., orthopedists, speech therapists, neurosurgeons, neurologists) in an informal and unstructured way. They admit that sometimes the communications are patient-mediated and that they would prefer a more structured collaboration infrastructure, easily adaptable to different patients needs, including formalized protocols fostering the collaboration, which is often overlooked. Only 25% of the experts are favourable to the introduction of collaborative softwares where roles and tasks are pre-assigned. This data is justified by the habit of the experts to interact with their colleagues by phone (76%).

All the experts but one physiatrist were able to remember successful patients cases, showing empathy with their patients. Only 56% of them were able to recall a patient case with a negative outcome, usually associated to a poor compliance or a wrong/missing timely diagnosis.

About the opportunity to follow patients' rehabilitation in real time, 31% of the experts consider this practice useless, even though they all agree that it is necessary at the beginning of the rehabilitation to correct the patients during the execution of the exercises, whereas 25% of them think it is infeasible in a real scenario. All of them believe it should be important to change the rehabilitation protocol, monitoring patients performance at fixed time intervals (but there is no agreement on such intervals) and providing them some feedback in a timely manner. The experts believe that it is important to provide feedback to patients about the rehabilitation progress for various reasons: i) it is challenging, ii) patients can better understand their progresses, iii) the feedback could help them in recalibrating the exercise execution, iv) it improves their motivation. All the experts but one believe the automatic analysis of the rehabilitation performance data would be useful (both to assist them and and to provide automatic feedback to the patients) only if coupled to traditional physiatric indexes evaluated periodically through in-person examinations. If available, they would like to use it in the clinical practice.

About the basic use-case presented in the video, all the experts assert that it could be quite useful in the real world to share information within the medical staff. Some of them think that this approach requires to modify some procedures already adopted and bad habits. They would like to use the proposed cooperative infrastructure, provided that different authorizations are guaranteed according to the role. In fact, they believe that it is necessary to assign different rights to the various actors but not all of them agree on the proposed assignment of the rights even though they agree on the roles assigned to the different specialists.

All the experts think this system would be beneficial for the improvement of the quality in the follow-up, considering that the adoption of a telerehabilitation approach would provide a more enjoying rehabilitation therapy, motivating them and allowing a quick supervision by the specialists and therapists.

Concluding remarks

Telemonitoring allows Public Health costs reduction, while preserving patients' conditions and improving their comfort, reducing the need of long term hospitalizations. Nevertheless extracting clinical data from signals acquired with an unsupervised setup and in variable environments, can imply many difficulties, which need to be deeply investigated.

In this thesis, two telemonitoring applications have been presented, highlighting the main limitations, caused by the absence of an in-person interaction, and the proposed solutions.

The first telemonitoring application is fetal electrocardiography, a non-invasive and safe procedure that allows to record the fetal electrical signals from the maternal abdomen for the identification of the beat-to-beat heart rate variability, whose analysis has been proved to be beneficial for the fetal health assessment during all the pregnancy. Fetal electrocardiography presents many difficulties that are exacerbated in telemonitoring applications because of the variability of the measurement setup. In this field, two processing algorithms have been developed for the extraction of the fetal heart rate. The first one can be used as a post-processing stage of on-line ICA algorithms when high density recordings setup are used, allowing the real-time identification of both instantaneous fetal heart rate and of an average fetal PQRST complex. The latter is an independent algorithm, based on a subtractive approach of the maternal main source of interference, that allows the extraction of the fetal heart rate from a reduced number of electrodes, that is a configuration more suitable for long-term monitoring. This algorithm took part to the international "Physionet/Computing in Cardiology Challenge" in 2013 entering into the top ten best-performing open-source algorithms. The improved version, released under the GNU GPL-2.0 open-source license, obtained the median values for sensitivity and positive predictivity of 0.982 and 0.976 in fetal QRS complexes detection when tested on the Physiobank database. This version would mark the 5th and 4th position in the final ranking related to the fetal heart rate and fetal RR interval measurements performance, reserved to the open-source challenge entries, taking into account both official and unofficial entrants.Since the quality of the extracted signals is strongly affected by the SNR of the recordings, surface electrodes and acquisition systems have been investigated with the aim of reducing noise levels in the acquired signals. In particular both commercial disposable and textile electrodes have been tested to evaluate the best solution for telemonitoring acquisition, which typically requires the patient to autonomously position the electrodes. The results highlighted the potential of the textile electrodes in this critical application. The definition of the whole telemonitoring system requires further studies to prove the efficacy of the proposed methods, with the assessment of both the processing algorithms and acquisition setup on more extended database, which is currently in progress.

The second telemonitoring application deals with hand telerehabilitation of rheumatic patients. Rheumatic diseases are chronic invalidating illnesses which slowly compromise physical functionalities, being particularly critical when affecting the hands. Beyond a pharmacological therapy, their treatment requires a rehabilitation program to recover the lost functionalities. Due to the high costs and to the chronic nature of these disease, patients are asked to perform the rehabilitation exercises at home using common objects, causing the physicians to be unable to evaluate their performance and demotivating the patients. In this application, a telerehabilitation device for the execution of active exercises at patients' home, also providing objective performance parameters, has been presented. The telemedicine infrastructure is based on a store and forward approach, allowing the physicians to telemonitoring many patients with a reduced effort. The system underwent a clinical trial in the University Hospital of Cagliari involving 10 patients with Rheumatoid Arthritis and 10 with Systemic Sclerosis in the experimental arm, enrolled for 12 weeks in a home rehabilitation program with the proposed device, plus other 20 patients for the control arm, which perform similar exercises using common objects. Patients showed a sustained improvement during the rehabilitation trial, highlighting the potentials of the introduction of such a system in the clinical practive. Both the patients and the physicians positively evaluated the system through validated questionnaires, recognizing the feasibility of this telemonitoring system introduction, even for different diseases affecting the hand functionalities. However, further clinical trials are needed to confirm this hypothesis.

The presented telemonitoring applications reveal deep differences which required the investigation of several aspects. In particular the first one is a diagnostic application which presents particularly heavy obstacles in terms of signal acquisition and processing, hampering the conception of the final telemonitoring system. The latter, dealing with the telemonitoring of physical parameters which are not particularly critical to be processed, has allowed the conception of the whole system, requiring more effort in the clinical evaluation of the obtained results.

Bibliography

[1] S. Inglis, R. Clark, F. McAlister, J. Ball, C. Lewinter, D. Cullington, S. Stewart, and J. Cleland, "Structured telephone support or telemonitoring programmes for patients with chronic heart failure." *Cochrane Database Syst Rev.*, vol. 8, Aug. 2010. [cited at p. 1]

[2] I. Amer-Wahlin, C. Hellsten, H. Noren, H. Hagberg, A. Herbst, I. Kjellmer, H. Lilja, C. Lindoff, M. Mansson, L. Martensson, P. Olofsson, A. Sundstrom, and K. Marsal, "Cardiotocography only versus cardiotocography plus ST analysis of fetal electrocardiogram for intrapartum fetal monitoring: a swedish randomised controlled trial," *The Lancet*, vol. 358, no. 9281, pp. 534–538, 2001. [cited at p. 1, 9]

[3] R. Sameni and G. D. Clifford, "A review of fetal ECG signal processing, issues and promising directions," *The Open Pacing, Electrophysiology and Therapy Journal (TOPETJ)*, vol. 3, Jan. 2010. [cited at p. 1, 8, 11, 12, 20]

[4] M. J. Taylor, M. J. Smith, M. Thomas, A. Green, F. Cheng, S. Oseku-Afful, L. Y. Wee, N. M. Fisk, and H. M. Gardiner, "Non-invasive fetal electrocardiography in singleton and multiple pregnancies," *BJOG International Journal of Obstetrics and Gynaecology*, vol. 110, no. 7, pp. 668–678, 2003. [cited at p. 2, 12, 13, 16, 20, 66]

[5] L. C. Li, "What else can i do but take drugs? the future of research in nonpharmacological treatment in early inflammatory arthritis," *The Journal of Rheumatology*, vol. 72, pp. 21–24, 2005. [cited at p. 2]

[6] L. Dovat, O. Lambercy, R. Gassert, T. Maeder, T. Milner, T. C. Leong, and E. Burdet, "HandCARE: A cable- actuated rehabilitation system to train hand function after stroke," *IEEE Trans. on Neural Systems and Rehabilitation Engineering*, vol. 16, no. 6, pp. 582–591, Dec. 2008. [cited at p. 2, 75]

[7] E. B. Brokaw, I. Black, R. J. Holley, and P. S. Lum, "Hand spring operated movement enhancer (HandSOME): a portable, passive hand exoskeleton for stroke rehabilitation," *IEEE Tran. on Neural Systems and Rehabilitation Engineering*, vol. 19, no. 4, pp. 391–399, 2011. [cited at p. 2, 75]

[8] M. Hasan, M. Reaz, M. Ibrahimy, M. Hussain, and J. Uddin, "Detection and processing techniques of fecg signal for fetal monitoring," *Biological Procedures Online*, vol. 11, pp. 263–295, 2009. [cited at p. 7]

[9] S. Stern, "Electrocardiogram: Still the cardiologist's best friend," *Circulation*, vol. 113, pp. e753–e756, 2006. [cited at p. 7]

[10] D. F. Dickinson, "The normal ECG in childhood and adolescence," *Heart*, vol. 91, pp. 1626–1630, 2005. [cited at p. 7]

[11] G. Q. Sharieff and S. O. Rao, "The pediatric ECG," *Emergency Medicine Clinics of North America*, vol. 24, no. 1, pp. 195–208, 2006. [cited at p. 7]

[12] B. Chester and J. Martin, "Electronic fetal monitoring: a brief summary of its development, problems and prospects," *European Journal of Obstretics and Gynecology and Reproductive Biology*, vol. 78, pp. 133–140, 1998. [cited at p. 9]

[13] P. Groves and N. Oriol, "How useful is intrapartum electronic fetal heart rate monitoring?" *International Journal of Obstretic Anesthesia*, vol. 4, pp. 161–167, 1995. [cited at p. 9]

[14] Z. Alfirevic, D. Devane, and G. Gyte, "Continuous cardiotocography (CTG) as a form of electronic fetal monitoring (EFM) for fetal assessment during labour (review)," *The Cochrane Library*, vol. 5, 2013. [cited at p. 9]

[15] E. B. C. Ang, V. Gluncic, A. Duque, M. E. Schafer, and P. Rakic, "Prenatal exposure to ultrasound waves impacts neuronal migration in mice," *Proceedings of the National Academy of Sciences of the United States of America*, vol. 103, no. 34, pp. 12 903–12 910, Aug. 2006. [cited at p. 9]

[16] J. Newnham, S. Evans, C. Michael, F. Stanley, and L. Landau, "Effects of frequent ultrasound during pregnancy: a randomised controlled trial." *Lancet*, vol. 342, pp. 887–891, Oct. 1993. [cited at p. 9]

[17] J. Neilson, "Fetal electrocardiogram (ecg) for fetal monitoring during labour," *Cochrane Database Syst. Rev.*, vol. 2, p. CD000116, 2003. [cited at p. 9]

[18] L. Devoe, "Fetal ECG analysis for intrapartum electronic fetal monitoring: A review," *Clinical Obstetrics and Gynecology*, vol. 54, no. 1, pp. 56?–65, Mar. 2011. [cited at p. 9]

[19] H. Noren, I. Amer-Wahlin, H. Hagberg, A. Herbst, I. Kjellmer, K. Marsal, P. Olofsson, and K. G. Rosen, "Fetal electrocardiography in labor and neonatal outcome. data from the swedish randomized controlled trial on intrapartum fetal monitoring," *American Journal of Obstetrics and Gynecology*, vol. 188, no. 1, pp. 183–192, Jan. 2003. [cited at p. 10]

[20] M. Peters, J. Crowe, J. Pieri, H. Quartero, B. Hayes-Gill, D. James, J. Stinstra, and S. Shakespeare, "Monitoring the fetal heart noninvasively:a review of methods," *J.Perinat. Med.*, vol. 29, pp. 408–416, 2001. [cited at p. 10, 11]

[21] T. Perri, B. Cohen-Sacher, M. Hod, M. Berant, I. Meizner, and J. Bar, "Risk factors for cardiac malformations detected by fetal echocardiography in a tertiary center," *Journal of Maternal-Fetal & Neonatal Medicine*, vol. 17, no. 2, pp. 123–128, Feb. 2005. [cited at p. 11]

[22] M. Cremer, "Uber die direkte ableitung der aktionsstrome des menschlichen herzens vom oesophagus und uber das elektrokardiogramm des fotus," *Munchn Wschr*, vol. 53, pp. 811–813, March 1906. [cited at p. 11]

[23] E. M. Symonds, D. Sahota, and A. Chang, *Fetal Electrocardiography*. London: Imperial College Press, 2001. [cited at p. 11]

[24] M. Sato, Y. Kimura, S. Chida, T. Ito, N. Katayama, K. Okamura, and M. Nakao, "A novel extraction method of fetal electrocardiogram from the composite abdominal signal," *IEEE Transactions on Biomedical Engineering*, vol. 54, no. 1, pp. 49–58, Jan. 2007. [cited at p. 11]

[25] B. Hayes-Gill, S. Hassan, F. G. Mirza, S. Ommani, J. Himsworth, M. Solomon, R. Brown, B. S. Schifrin, and W. R. Cohen, "Accuracy and reliability of uterine contraction identification using abdominal surface electrodes," *Clinical Medicine Insights: Women's Health*, vol. 5, pp. 65–75, 2012. [cited at p. 11]

[26] M. Rooijakkers, H. de Lau, C. Rabotti, S. Oei, J. Bergmans, and M. Mischi, "Fetal movement detection based on qrs amplitude variations in abdominal ecg recordings," in *Engineering in Medicine and Biology Society. EMBS 36th Annual International Conference of the IEEE*, 2014, pp. 1452–1455. [cited at p. 11]

[27] D. Paladini, M. Russo, M. Felicetti, and R. Calabro, *Cuore fetale normale e patologico*. North Holland, Springer Milan, pp. 133–170. [cited at p. 11]

[28] J. M. P. J. Breur, G. H. A. Visser, A. A. Kruize, P. Stoutenbeek, and E. J. Meijboom, "Treatment of fetal heart block with maternal steroid therapy: case report and review of the literature," *Ultrasound in Obstetrics and Gynecology*, vol. 24, no. 4, pp. 467–472, 2004. [cited at p. 11]

[29] Y. O. C. V. Ananth, "Placental abruption," *Obstetrics & Gynecology*, vol. 108, no. 4, pp. 1005–1016, 2006. [cited at p. 11]

[30] V. Vigneron, A. Paraschiv-Ionescu, A. Azancot, O. Sibony, and C. Jutten, "Fetal electrocardiogram extraction based on non-stationary ICA and wavelet denoising," in *Proc. 7th International Symposium on Signal Processing and its Applications*, vol. 2, Jul. 2003, pp. 69–72. [cited at p. 12]

[31] M. Peters, J. Crowe, J. Piéri, H. Quartero, B. Hayes-Gill, D. James, J. Stinstra, and S. Shakespeare, "Monitoring the fetal heart non-invasively: a review of methods," *Journal of Perinatal Medicine*, vol. 29, no. 15, pp. 408–?416, Jun. 2005. [cited at p. 12]

[32] R. T. Wakai, J. M. Lengle, and A. C. Leuthold, "Transmission of electric and magnetic foetal cardiac signals in a case of ectopia cordis: the dominant role of the vernix caseosa," *Physics in Medicine and Biology*, vol. 45, no. 7, pp. 1989–1995, 2000. [cited at p. 12]

[33] G. Clifford, F. Azuaje, and P. E. McSharry, *Advanced Methods and Tools for ECG Data Analysis*. Artech House, 2006. [cited at p. 12]

[34] T. F. Oostendorp, A. van Oosterom, and H. W. Jongsma, "The effect of changes in the conductive medium on the fetal ECG throughout gestation," *Clinical Physics and Physiological Measurement*, vol. 10, no. 4B, pp. 11–20, 1989. [cited at p. 13]

[35] G. Clifford, R. Sameni, J. Ward, J. Robinson, and A. Wolfberg, "Clinically accurate fetal ECG parameters acquired from maternal abdominal sensors," *American Journal of Obstetrics and Gynecology*, vol. 205, no. 1, 2011. [cited at p. 13, 15]

[36] L. De Lathauwer, B. D. Moor, and J. Vandewalle, "Fetal electrocardiogram extraction by blind source subspace separation," *IEEE Trans. on Biomedical Engineering*, vol. 47, no. 5, pp. 567–572, May 2000. [cited at p. 13, 16, 20]

[37] M. Sabry-Rizk, W. Zgallai, A. McLean, E. Carson, and K. Grattan, "Virtues and vices of source separation using linear independent component analysis for blind source separation of non-linearly coupled and synchronised fetal and mother ECGs," in *Engineering in Medicine and Biology Society, 2001. Proceedings of the 23rd Annual International Conference of the IEEE*, vol. 2, 2001, pp. 1985–1989. [cited at p. 13]

[38] D. M. B., "Database for the identification of systems (DaISy)," 1997. [Online]. Available: http://homes.esat.kuleuven.be/ [cited at p. 14, 21]

[39] A. Goldberger, L. Amaral, L. Glass, J. Hausdorff, P. Ivanov, R. Mark, J. Mietus, G. Moody, C. Peng, and H. Stanley, "Physiobank, physiotoolkit, and physionet: Components of a new research resource for complex physiologic signals," *Circulation*, vol. 101, no. 23, pp. e215–e220, Jun. 2000. [cited at p. 14]

[40] "The Open Source Electrophysiological Toolbox." [Online]. Available: http://spc.shirazu.ac.ir/products/Featured-Products/oset/ [cited at p. 14, 19, 26]

[41] Hayes-Gill et al., "Apparatus and method for detecting the fetal heart rate," U.S. Patent No. 7,532,923, May 2009. [cited at p. 15]

[42] W. R. COHEN, S. OMMANI, S. HASSAN, F. G. MIRZA, M. SOLOMON, R. BROWN, B. S. SCHIFRIN, J. M. HIMSWORTH, and B. R. HAYES-GILL, "Accuracy and reliability of fetal heart rate monitoring using maternal abdominal surface electrodes," *Acta Obstetricia et Gynecologica Scandinavica*, vol. 91, no. 11, pp. 1306–1313, 2012. [Online]. Available: http://dx.doi.org/10.1111/j.1600-0412.2012.01533.x [cited at p. 15]

[43] J. Reinhard, B. Hayes-Gill, J. Yuan, S. Schiermeier, and F. Louwen, "Intrapartum st segment analyses (stan) using simultaneous invasive and non-invasive fetal electrocardiography: A report of 6 cases," *Z Geburtshilfe Neonatol*, vol. 218, no. 03, pp. 122–127, 2014. [cited at p. 15]

[44] A. Nandi and V. Zarzoso, "Foetal ECG separation," in *IEE Colloquium on the Use of Model Based Digital Signal Processing Techniques in the Analysis of Biomedical Signals (Digest No. 1997/009)*, Apr. 1997, pp. 1–6. [cited at p. 16]

[45] L. De Lathauwer, "Fetal Electrocardiogram Extraction by Source Subspace Separation," in *Proc. IEEE Workshop on HOS*, Girona (Spain), 1995, pp. 134–138. [cited at p. 16]

[46] R. Sameni, F. Vrins, F. Parmentier, C. Herail, V. Vigneron, M. Verleysen, C. Jutten, and M. Shamsollahi, "Electrode selection for noninvasive fetal electrocardiogram extraction using mutual information criteria," in *MaxEnt2006 - 26th International Workshop on Bayesian Inference and Maximum Entropy Methods in Science and Engineering*, Jul. 2006, pp. 97–104. [cited at p. 16]

[47] F. Vrins, C. Jutten, and M. Verleysen, "Sensor array and electrode selection for non-invasive fetal electrocardiogram extraction by independent component analysis," in *Proc. of ICA04*, 2004, pp. 1017–1024. [cited at p. 16]

[48] V. Zarzoso and A. K. Nandi, "Noninvasive fetal electrocardiogram extraction: Blind separation versus adaptive noise cancellation," *IEEE Trans on Biomed Eng*, vol. 48, no. 1, Jan. 2001. [cited at p. 16]

[49] T. Blumensath and M. E. Davies, "Blind separation of maternal and fetal ECG recordings using adaptive sparse representations," in *Proc. ICA Research Network International Workshop 2006*, 2006, pp. 23–26. [cited at p. 16]

[50] R. Sameni, C. Jutten, and M. B. Shamsollahi, "What ica provides for ecg processing: Application to noninvasive fetal ecg extraction," in *Signal Processing and Information Technology, 2006 IEEE International Symposium on*, 2006, pp. 656–661. [cited at p. 16]

[51] B. Widrow, J. R. Glover, J. M. Mccool, J. Kaunitz, C. S. Williams, R. H. Hean, J. R. Zeidler, E. Dong, and R. C.Goodlin, "Adaptive noise cancelling: Principles and applications," in *Proc. of the IEEE*, vol. 63, no. 12, Dec. 1975, pp. 1692–1716. [cited at p. 17]

[52] S. M. M. Martens, C. Rabotti, M. Mischi, and R. J. Sluijter, "A robust fetal ECG detection method for abdominal recordings," *Physiol. Meas.*, vol. 28, pp. 373ï¿½–388, 2007. [cited at p. 17, 32, 34, 64]

[53] L. Tong, R. wen Liu, V. C. Soon, and Y.-F. Huang, "Indeterminacy and identifiability of blind identification," *IEEE Transactions on Circuits and Systems*, vol. 38, no. 5, pp. 499–509, May 1991. [cited at p. 20]

[54] G. Spence, I. Clarke, and M. Smith, "Blind signal separation and its application to long-term bio-medical monitoring," in *Medical Applications of Signal Processing*, Nov. 2005, pp. 93–98. [cited at p. 20]

[55] S. Muceli, D. Pani, and L. Raffo, "Real-time fetal ECG extraction with JADE on a floating point DSP," *Electronics Letters*, vol. 43, no. 18, pp. 963–965, Aug. 2007. [cited at p. 20, 21, 25, 35, 39]

[56] D. Pani, A. Dessí, B. Cabras, and L. Raffo, "A real-time algorithm for tracking of foetal ecg sources obtained by block-on-line bss techniques," in *Computing in Cardiology*, 2012, pp. 65–68. [cited at p. 20]

[57] D. Pani, S. Argiolas, and L. Raffo, "Real-time back-projection of fetal ECG sources in OL-JADE for the optimization of blind electrodes positioning," in *37th Int. Conf. on Computing in Cardiology*, 2010, pp. 289–292. [cited at p. 20]

[58] Kolluri et al., "Extrapolating ICA knowledge from one epoch to another for improved fetal ECG separation," U.S. Patent No. US 7,831,300, Nov 2010. [cited at p. 20]

[59] Marossero et al., "Maternal-fetal monitoring system," U.S. Patent Application No. US2005/0267377, Dec 2005. [cited at p. 20]

[60] N. A. Mensah-Brown, W. J. Lutter, S. Comani, J. F. Strasburger, and R. T. Wakai, "Independent component analysis of normal and abnormal rhythm in twin pregnancies," *Physiological Measurement*, vol. 32, pp. 51–64, 2011. [cited at p. 20]

[61] D. Pani, S. Argiolas, and L. Raffo, "Impact of the approximated on-line centering and whitening in OL-JADE on the quality of the estimated fetal ecg," in *37th Int. Conf. on Computing in Cardiology*, 2010, pp. 549–552. [cited at p. 21]

[62] S.Suppappola and Y. Sun, "Nonlinear transforms of ECG signals for digital QRS detection: a quantitative analysis," *IEEE Transactions on Biomedical Engineering*, vol. 41, no. 4, pp. 397–400, Apr. 1994. [cited at p. 23]

[63] R. A. Balda, G. Diller, E. Deardorff, J. Doue, and P. Hsieh, *The HP ECG analysis program*. North Holland, 1977, pp. 197–205. [cited at p. 23, 30, 40]

[64] R. Sameni, G. D. Clifford, C. Jutten, and M. B. Shamsollahi, "Multichannel ECG and Noise Modeling: Application to Maternal and Fetal ECG Signals," *EURASIP Journal on Advances in Signal Processing*, vol. 2007, pp. Article ID 43 407, 14 pages, 2007, ISSN 1687-6172, doi:10.1155/2007/43407. [cited at p. 26]

[65] D. Pani, G. Barabino, and L. Raffo, "NInFEA: an embedded framework for the real-time evaluation of fetal ecg extraction algorithms," *Biomedizinische Technik/Biomedical Engineering*, vol. 58, no. 1, pp. 13–26, Dec. 2012. [cited at p. 28]

[66] "PhysioNet research resource for complex physiologic signals." [Online]. Available: http://www.physionet.org [cited at p. 28]

[67] G. Clifford, I. Silva, J. Behar, and G. Moody, "Non-invasive fetal ecg analysis," *Physiological Measurement*, vol. 35, no. 8, Aug. 2014. [cited at p. 28, 64]

[68] A. Dessi, D. Pani, and L. Raffo, "An advanced algorithm for fetal heart rate estimation from non-invasive low electrode density recordings," *Physiological Measurement*, vol. 35, no. 8, pp. 1621–1636, Jul. 2014. [cited at p. 29]

[69] "Physiological measurement 2014 special issue (volume 35, number 8) source code." [Online]. Available: http://physionet.org/challenge/2013/sources/ [cited at p. 29]

[70] J. Martínez, R. Almeida, S. Olmos, A. Rocha, and P. Laguna, "A wavelet-based ECG delineator: Evaluation on standard databases," *IEEE Trans. on Biomedical Engineering*, vol. 51, no. 4, pp. 570–581, Apr. 2004. [cited at p. 30, 61, 67]

[71] S. Suppappola and Y. Sun, "Nonlinear transforms of ecg signals for digital qrs detection: A quantitative analysis," *IEEE Trans. Biomed. Eng.*, vol. 41, no. 4, 1994. [cited at p. 30]

[72] V. Chouhan and S. Mehta, "Detection of qrs complexes in 12-lead ecg using adaptive quantized threshold," *IJCSNS International Journal of Computer Science and Network Security*, vol. 8, no. 1, 1979. [cited at p. 30]

[73] M. Okada, "A digital filter for the qrs complex detection," *IEEE Trans. Biomed. Eng.*, vol. 26, no. 7, pp. 700–703, 1979. [cited at p. 30]

[74] I. S. N. Murthy and M. R. Rangaraj, "New concepts for pvc detection," *IEEE Trans. Biomed. Eng.*, vol. BME-26, no. 7, pp. 409–416, jan 1979. [cited at p. 30]

[75] J. Pan and W. Tompkins, "A real-time QRS detection algorithm," *IEEE Transactions on Biomedical Engineering*, vol. 32, pp. 230–236, 1985. [cited at p. 30, 31, 62]

[76] B. U. Kohler, C. Hennig, and R. Orglmeister, "The principles of software qrs detection," *Engineering in Medicine and Biology Magazine, IEEE*, vol. 21, no. 1, pp. 42–57, Jan. 2002. [cited at p. 31]

[77] U. Rutishauser, E. M. Schumand, and A. N. Mamelakb, "Online detection and sorting of extracellularly recorded action potentials in human medial temporal lobe recordings, in vivo," *Journal of Neuroscience Methods*, vol. 154, pp. 204–224, 2006. [cited at p. 32]

[78] P. Bloomfield, *Fourier Analysis of Time Series: An Introduction*. WILEY, 2000. [cited at p. 34]

[79] J. Cardoso and A. Souloumiac, "Blind beamforming for non-Gaussian signals," in *IEEE Proc-F*, vol. 140, no. 6, 1993, pp. 362–370. [cited at p. 35]

[80] I. Silva, J. Behar, R. Sameni, T. Zhu, J. Oster, G. D. Clifford, and G. B. Moody, "Noninvasive fetal ecg: the physionet/computing in cardiology challenge 2013," in *Computing in Cardiology*, 2013, pp. 149–152. [cited at p. 35]

[81] G. Cliffor, I. Silva, J. Behar, and G. Moody, "Editorial: Noninvasive fetal ECG analysis," *Physiological Measurement*, vol. 35, no. 8, 2014. [cited at p. 35]

[82] A. L. Goldberger, L. Amaral, L. Glass, J. M. Hausdorff, P. C. Ivanov, R. G. Mark, J. E. Mietus, G. B. Moody, C. Peng, and H. E. Stanley, "Physiobank, physiotoolkit, and physionet: Components of a new research resource for complex physiologic signals," *Circulation*, vol. 101, no. 23, 2000 (June 13). [cited at p. 35]

[83] "Wfdb applications guide. heart rate tachometer." [Online]. Available: http://www.physionet.org/physiotools/wag/tach-1.htm [cited at p. 38]

[84] "Wfdb applications guide. ansi/aami-standard measurement-by-measurement annotation comparator." [Online]. Available: http://www.physionet.org/physiotools/wag/mxm-1.htm [cited at p. 38]

[85] "Recomendations for measurement standards in quantitative electrocardiography," *European Heart Journal*, 1985, the CSE Working Party. [cited at p. 39]

[86] A. Dessí, D. Pani, and L. Raffo, "Identification of fetal qrs complexes in low density non-invasive biopotential recordings," in *Computing in Cardiology*, 2013, pp. 321–324. [cited at p. 40]

[87] "Noninvasive fetal ecg: the physionet/computing in cardiology challenge 2013." [Online]. Available: http://physionet.org/challenge/2013 [cited at p. 41]

[88] J. Webster, *Medical Instrumentation: Application and Design*. WILEY, 2009. [cited at p. 44, 47, 48, 49]

[89] J. D. Bronzino, *The Biomedical Engineering Handbook, third edition*. Taylor and Francis, 2006. [cited at p. 44, 46]

[90] J. Lofhede, F. Seoane, and M. Thordstein, "Textile electrodes for eeg recording-a pilot study," *Sensors*, vol. 12, no. 12, pp. 16 907–16 919, Dec. 2012. [cited at p. 55, 56]

[91] K. Hoffmann and R. Ruff, "Flexible dry surface-electrodes for ecg long-term monitoring," in *Engineering in Medicine and Biology Society. EMBS 29th Annual International Conference of the IEEE*, 2007, pp. 5739–5742. [cited at p. 55]

[92] M. Puurtinen, S. Komulainen, P. Kauppinen, J. Malmivuo, and J. Hyttinen, "Measurement of noise and impedance of dry and wet textile electrodes, and textile electrodes with hydrogel," in *Engineering in Medicine and Biology Society. EMBS 28th Annual International Conference of the IEEE*, 2006, pp. 5739–5742. [cited at p. 55]

[93] M. Stoppa and A. Chiolerio, "Wearable electronics and smart textiles: A critical review," *Sensors*, vol. 14, no. 7, pp. 11 957–11 992, 2014. [cited at p. 55]

[94] D. Khodagholy, J. N. Gelinas, T. Thesen, W. Doyle, O. Devinsky, G. G. Malliaras, and G. Buzsaki, "Neurogrid: recording action potentials from the surface of the brain," *Nature Neuroscience*, vol. 18, pp. 310–315, Dec. 2014. [cited at p. 55]

[95] T. InOh, S. Yoon, T. E. Kim, H. Wi, K. J. Kim, E. J. Woo, and R. J. Sadleir, "Nanofiber web textile dry electrodes for long-term biopotential recording," *IEEE Transactions on Biomedical Circuits and Systems*, vol. 7, pp. 204–211, Apr. 2013. [cited at p. 55]

[96] S. Tsukada, H. Nakashima, and K. Torimitsu, "Conductive polymer combined silk fiber bundle for bioelectrical signal recording," *PLoS ONE*, vol. 7, Apr. 2012. [cited at p. 55]

[97] G. Paul, R. Torah, S. Beeby, and J. Tudor, "The development of screen printed conductive networks on textiles for biopotential monitoring applications," *Sensors and Actuators A: Physical*, vol. 206, pp. 35–41, Feb. 2014. [cited at p. 56]

[98] G. Clifford, J. Behar, Q. Li, and I. Rezek, "Signal quality indices and data fusion for determining clinical acceptability of electrocardiograms," *Physiological Meaurement*, vol. 33, no. 9, pp. 1419–1433, 2012. [cited at p. 60]

[99] J. Leskia and N. Henzel, "Ecg baseline wander and powerline interference reduction using nonlinear filter bank," *Signal Processing*, vol. 85, pp. 781–793, 2005. [cited at p. 61, 67]

[100] G. Barabino, D. Pani, A. Dessì, and L. Raffo, "A configurable biopotentials acquisition module suitable for fetal electrocardiography studies," in *Accepted for the MeMeA 2015 IEEE International Symposium on Medical Measurements and Application*, 2015. [cited at p. 64]

[101] A. Fanelli, M. Signorini, M. Ferrario, P. Perego, L. Piccini, G. Andreoni, and G. Magenes, "Telefetalcare: A first prototype of a wearable fetal electrocardiograph," in *Engineering in Medicine and Biology Society, EMBC, 2011 Annual International Conference of the IEEE*, Aug. 2011, pp. 6899–6902. [cited at p. 64]

[102] T. Pereira, H. Carvalho, A. Catarino, M. Dias, O. Postolache, and P. Girao, "Wearable biopotential measurement using the ti ads1198 analog front-end and textile electrodes," in *Medical Measurements and Applications Proceedings (MeMeA), 2013 IEEE International Symposium on*, May 2013, pp. 325–330. [cited at p. 65]

[103] D. Campillo, R. Guardarrama, R. Gonzalez, J. Rodriguez, and D. Jimenez, "A real time ecg preprocessing system based on ads1298," 2013, pp. 947–950. [cited at p. 65]

[104] J. Coosemans, B. Hermans, and R. Puers, "Integrating wireless ecg monitoring in textiles," *Sensors and Actuators A: Physical*, vol. 130, pp. 48–53, Aug. 2006. [cited at p. 66]

[105] N. Chumbler, P. Quigley, J. Sanford, P. Griffiths, D. Rose, M. Morey, E. Ely, and H. Hoenig, "Implementing telerehabilitation research for stroke rehabilitation with community dwelling veterans: Lessons learned," *International Journal of Telerehabilitation, North America*, vol. 2, Jul. 2010. [cited at p. 71]

[106] Outpatient Service Trialists, "Rehabilitation therapy services for stroke patients living at home: systematic review of randomised trials," *The Lancet*, vol. 363, no. 9406, pp. 352–356, 2004. [cited at p. 71]

[107] J. A. Sanford, P. C. Griffiths, P. Richardson, K. Hargraves, T. Butterfield, and H. Hoenig, "The effects of in-home rehabilitation on task self-efficacy in mobility-impaired adults: A randomized clinical trial," *Journal of the American Geriatrics Society*, vol. 54, no. 11, pp. 1641–1648, 2006. [cited at p. 71]

[108] L. Li, "What else can i do but take drugs? the future of research in nonpharmacological treatment in early inflammatory arthritis." *J Rheumatol Suppl.*, vol. 72, pp. 21–24, Jan. 2005. [cited at p. 72]

[109] S. Brorsson, M. Hilliges, C. Sollerman, and A. Nilsdotter, "A six-week hand exercise programme improves strength and hand function in patients with rheumatoid arthritis," *J Rehabil Med.*, vol. 41, pp. 338–342, Apr. 2009. [cited at p. 72]

[110] P. Heine, M. Williams, E. Williamson, C. Bridle, J. Adams, A. O'Brien, D. Evans, and S. Lamb, "Development and delivery of an exercise intervention for rheumatoid arthritis: strengthening and stretching for rheumatoid arthritis of the hand (sarah) trial." *Physiotherapy*, vol. 98, pp. 121–130, Jun. 2012. [cited at p. 72]

[111] H. Flint-Wagner, J. Lisse, T. Lohman, S. G. abd T Guido abd E Cussler, D. Gates, and D. Yocum, "Assessment of a sixteen-week training program on strength, pain, and function in rheumatoid arthritis patients," *J Clin Rheumatol.*, vol. 15, pp. 165–171, Jun. 2009. [cited at p. 72]

[112] N. Mugii, M. Hasegawa, T. Matsushita, M. Kondo, H. Orito, K. Yanaba, K. Komura, I. Hayakawa, Y. Hamaguchi, M. Ikuta, K. Tachino, M. Fujimoto, K. Takehara, and S. Sato, "The efficacy of self-administered stretching for finger joint motion in japanese patients with systemic sclerosis." *J Rheumatol.*, vol. 33, pp. 1586–1592, Aug. 2006. [cited at p. 72]

[113] J. Poole, D. D. Santhanam, and A. L. Latham, "Hand impairment and activity limitations in four chronic diseases," *Journal of Hand Therapy*, vol. 26, no. 3, Sep. 2013. [cited at p. 72]

[114] J.AVOUAC, U. WALKER, A. TYNDALL, A. KAHAN, M. MATUCCI-CERINIC, Y. ALLANORE, and EUSTAR, "Characteristics of joint involvement and relationships with systemic inflammation in systemic sclerosis: Results from the EULAR scleroderma

trial and research group (EUSTAR) database," *The Journal of Rheumatology*, vol. 37, no. 7, pp. 1488–1501, 2010. [cited at p. 72]

[115] E. Hallert, M. Bjork, O. Dahlstrom, T. Skogh, and I. Thyberg, "Disease activity and disability in women and men with early rheumatoid arthritis (ra): An 8-year followup of a swedish early RA project," *Arthritis Care and Research*, vol. 64, no. 8, pp. 1101–1107, 2012. [cited at p. 72]

[116] Y. Shapira, N. Agmon-Levin, and Y. Shoenfeld, "Geoepidemiology of autoimmune rheumatic diseases," *Nature Reviews, Rheumatology*, vol. 6, pp. 468–476, 2010. [cited at p. 72]

[117] G. Neuberger, L. Aaronson, B. Gajewski, S. Embretson, P. Cagle, J. Loudon, and P. Miller, "Predictors of exercise and effects of exercise on symptoms, function, aerobic fitness, and disease outcomes of rheumatoid arthritis," *Arthritis Rheum.*, vol. 15, pp. 943–952, Aug. 2007. [cited at p. 72]

[118] J. Poole, "Musculoskeletal rehabilitation in the person with scleroderma," *Current Opinion in Rheumatology*, vol. 22, pp. 205–212, 2010. [cited at p. 72]

[119] R. Dreiser, E. Maheu, G. Guillou, H. Caspard, and J. Grouin, "Validation of an algofunctional index for osteoarthritis of the hand," *Rev Rhum Engl*, vol. 62, no. 1, pp. 43s–53s, Jun. 1995. [cited at p. 73]

[120] M. J. H. Peters, S. I. van Nes, E. K. Vanhoutte1, M. Bakkers, P. A. van Doorn, I. S. J. Merkies, and C. G. Faber, "Revised normative values for grip strength with the jamar dynamometer," *Journal of the Peripheral Nervous System*, vol. 16, pp. 47–50, 2011. [cited at p. 73]

[121] N. J. Seo, W. Z. Rymer, and D. G. Kamper, "Delays in grip initiation and termination in persons with stroke: Effects of arm support and active muscle stretch exercise," *J Neurophysiol*, vol. 101, no. 6, pp. 3108–3115, Jun. 2009. [cited at p. 73]

[122] P. Helliwell, A. Howe, and V. Wright, "Functional assessment of the hand: reproducibility, acceptability, and utility of a new system for measuring strength," *Ann Rheum Dis*, vol. 46, pp. 203–208, 1987. [cited at p. 73]

[123] G. Andria, F. Attivissimo, N. Giaquinto, A. Lanzolla, L. Quagliarella, and N. Sasanelli, "Functional evaluation of handgrip signals for parkinsonian patients," *IEEE Transactions on Instrumentation and Measurement*, vol. 55, no. 5, pp. 1467–1473, Oct. 2006. [cited at p. 73]

[124] A. Jobbágy, P. Harcos, R. Karoly, and G. Fazekas, "Analysis of finger-tapping movement," *Journal of Neuroscience Methods*, vol. 141, pp. 29–39, 2005. [cited at p. 73, 84]

[125] P. Bustamante, K. Grandez, G. Solas, and S. Arrizabalaga, "A low-cost platform for testing activities in parkinson and ALS patients," in *12th IEEE International Conference on e-Health Networking Applications and Services (Healthcom)*, Jul. 2010, pp. 302–307. [cited at p. 73]

[126] S. R. Muir, R. D. Jones, J. H. Andreae, and I. M. Donaldson, "Measurement and analysis of single and multiple finger tapping in normal and parkinsonian subjects," *Parkinsonism related disorders*, vol. 1, no. 2, pp. 89–96, 1995. [cited at p. 73, 82]

[127] "Meditouch handtutor," last accessed march 29th 2015. [Online]. Available: http://www.meditouch.co.il/en/HandTutor [cited at p. 75]

[128] "Curictus," last accessed march 29th 2015. [Online]. Available: https://code.google.com/p/curictus-vrs/ [cited at p. 75]

[129] Y. Huang and K. Low, "Initial analysis and design of an assistive rehabilitation hand device with free loading and fingers motion visible to subjects," in *IEEE International Conference on Systems, Man and Cybernetics, SMC 2008*, Oct. 2008, pp. 2584–2590. [cited at p. 75]

[130] J. Iqbal, N. Tsagarakis, A. Fiorilla, and D. Caldwell, "A portable rehabilitation device for the hand," in *2010 Annual International Conference of the IEEE Engineering in Medicine and Biology Society (EMBC)*, 2010, pp. 3694–3697. [cited at p. 75]

[131] F. Wang, M. Shastri, C. L. Jones, V. Gupta, C. Osswald, X. Kang, D. G. Kampe, and N. Sarkar, "Design and control of an actuated thumb exoskeleton for hand rehabilitation following stroke," in *2011 IEEE International Conference on Robotics and Automation*, 2011, pp. 3688 – 3693. [cited at p. 75]

[132] A. Chiri, N. Vitiello, F. Giovacchini, S. Roccella, F. Vecchi, and M. C. Carrozza, "Mechatronic design and characterization of the index finger module of a hand exoskeleton for post-stroke rehabilitation," *IEEE/ASME transactions on mechatronics*, vol. 17, no. 5, pp. 1106–1111, 2012. [cited at p. 75]

[133] W. K. Durfee, S. A. Weinstein, E. Bhatt, A. Nagpal, and J. R. Carey, "Design and usability of a home telerehabilitation system to train hand recovery following stroke," *Journal of Medical Devices*, vol. 3, no. 4, Dec. 2009. [cited at p. 75]

[134] H. Zheng, R. Davies, T. Stone, S. Wilson, J. Hammerton, S. Mawson, P. Ware, N. Black, N. Harris, C. Eccleston, H. Hu, H. Zhou, and G. Mountain, "SMART rehabilitation: Implementation of ICT platform to support home-based stroke rehabilitation," in *Proc. of the 4th International Conference on Universal Access in Human-Computer Interaction*, Beijing,China, Jul. 2007, pp. 831–840. [cited at p. 75]

[135] D. Giansanti, S. Morelli, G. Maccioni, and V. Macellari, "Validation of a tele-homecare for hand-telerehabilitation," in *Proceedings of the 29th Annual International Conference of the IEEE EMBS CitÃ© Internationale*, Lyon, France, 2007, pp. 3830 –3832. [cited at p. 75]

[136] S. S. Marchese, S. Baratta, P. Cingolani, A. Fadda, C. Giacomozzi, and V. Macellari, "Technical assessment of the hellodoc service," *Ann. Inst. Super Sanita*, vol. 44, no. 2, pp. 135–144, 2008. [cited at p. 75]

[137] D. J. Reinkensmeyer, C. T. Pang, J. A. Nessler, and C. C. Painter, "Web-based telerehabilitation for the upper extremity after stroke," *IEEE Transactions on Neural Systems and Rehabilitation Engineering*, vol. 10, no. 2, pp. 102–108, Jun. 2002. [cited at p. 75]

[138] M. Huber, B. Rabin, C. Docan, G. Burdea, M. E. Nwosu, M. Abdelbaky, and M. R. Golomb, "Playstation based telerehabilitation for children with hemiplegia," in *Virtual Rehabilitation*, 2008, pp. 105–112. [cited at p. 75]

[139] L. M. Johnson and J. M. Winters, "Enhanced therajoy technology for use in upper-extremity stroke rehabilitation," in *Proceedings of the 26th Annual International Conference of the IEEE EMBS San Francisco, CA, USA*, Sep. 2004, pp. 4932–4935. [cited at p. 75]

[140] J. Broeren, A. Bjorkdahl, L. Claesson, D. Goude, A. Lundgren-Nilsson, H. Samuelsson, C. Blomstrand, K. S. Sunnerhagen, and M. Rydmark, "Virtual rehabilitation after stroke," in *Studies in Health Technology and Informatics*, vol. 136, 2008, pp. 77–82. [cited at p. 76]

[141] G. V. Popescu, G. Burdea, and R. Boian, "Shared virtual environments for telerehabilitation," in *Proceedings of Medicine Meets Virtual Reality 2002 Conference*, Cambridge, UK, 2002, pp. 362–368. [cited at p. 76]

[142] K. Morrow, C. Docan, G. Burdea, and A. Merians, "Low-cost virtual rehabilitation of the hand for patients post-stroke," in *Virtual Rehabilitation, 2006 International Workshop on*, New York, NY, USA, 2006, pp. 6–10. [cited at p. 76]

[143] M. K. Holden, T. A. Dyar, and L. Dayan-Cimadoro, "Telerehabilitation using a virtual environment improves upper extremity function in patients with stroke," *IEEE TRANSACTIONS ON NEURAL SYSTEMS AND REHABILITATION ENGINEERING*, vol. 15, no. 1, pp. 36–42, 2007. [cited at p. 76]

[144] World Health Organization, "A health telematics policy: in support of the who's health-for-all strategy for global health development, report of the who group consultation on health telematics," WHO, Tech. Rep., Dec. 1997, WHO/DGO/98.01. [cited at p. 76]

[145] J. Craig and V. Patterson, "Introduction to the practice of telemedicine," *Journal of Telemedicine and Telecare*, vol. 11, no. 1, pp. 3–9, 2005. [cited at p. 76]

[146] S. Guillen, M. Arredondo, V. Traver, J. Garcia, and C. Fernandez, "Multimedia telehomecare system using standard TV set," *Biomedical Engineering, IEEE Transactions on*, vol. 49, no. 12, pp. 1431–1437, Dec. 2002. [cited at p. 76]

[147] H. A. Brandling-Bennett, I. Kedar, D. J. Pallin, G. Jacques, G. J. Gumley, and J. C. Kvedar, "Delivering health care in rural cambodia via store-and-forward telemedicine: A pilot study," in *Telemedicine and e-health*, vol. 11, no. 1, 2005, pp. 56–62. [cited at p. 76]

[148] G. Angius, D. Pani, L. Raffo, P. Randaccio, and S. Seruis, "A tele-home care system exploiting the dvb-t technology and mhp," *Methods of Information in Medicine*, vol. 47, no. 3, pp. 223–228, 2008. [cited at p. 76]

[149] S. Devaraj and K. Ezra, "Current trends and future challenges in wireless telemedicine system," in *Proceedings of the 3rd International Conference on Electronics Computer Technology (ICECT)*, vol. 4, Kanyakumari, India, Apr. 2011, pp. 417–421. [cited at p. 77]

[150] A. Martinez, V. Villarroel, J. Seoane, and F. D. Pozo, "Rural telemedicine for primary healthcare in developing countries," *Technology and Society Magazine, IEEE*, vol. 23, no. 2, pp. 13–22, 2004. [cited at p. 77]

[151] H. Audebert, "Telestroke: effective networking," *The Lancet Neurology*, vol. 5, no. 3, pp. 279–282, 2006. [cited at p. 77]

[152] R. Harrison, W. Clayton, and P. Wallace, "Can telemedicine be used to improve communication between primary and secondary care?" *British Medical Journal*, vol. 313, no. 7069, pp. 1377–1380, 11 1996. [cited at p. 77]

[153] A. Taddei, A. Gori, E. Rocca, T. Carducci, G. Piccini, N. Assanta, B. Murzi, and G. Ricci, "Tele-consulting for collaborative diagnosis and care of heart malformations," in *38th International Conference on Computing in Cardiology*, Hangzhou, China, 2011, pp. 253–256. [cited at p. 77]

[154] R. Triunfo, R. Tumbarello, A. Sulis, G. Zanetti, L. Lianas, V. Meloni, and F. Frexia, "COTS technologies for telemedicine applications," *nternational Journal of Computer Assisted Radiology and Surgery*, vol. 5, pp. 11–18, January 2010. [cited at p. 77]

[155] R. E. Gantenbein, "Telehealth-based collaboration among primary and behavioral health care providers in rural areas," in *International Conference on Collaboration Technologies and Systems*, Denver, Colorado, USA, 2012, pp. 485–489. [cited at p. 77]

[156] M. Y. Sung, M. S. Kim, M.-W. Sung, E. J. Kim, and J. H. Yoo, "CoMed: a real-time collaborative medicine system," in *13th IEEE Symposium on Computer-Based Medical Systems*, Houston, Texas, USA, 2000, pp. 215–220. [cited at p. 77]

[157] G. Angius, D. Pani, L. Raffo, and P. Randaccio, "KeepInTouch: A telehealth system to improve the follow-up of chronic patients," in *Collaboration Technologies and Systems (CTS), 2011 International Conference on*, Philadelphia, Pennsylvania, USA, May 2011, pp. 311–318. [cited at p. 77]

[158] D. Stevenson, "Training and process change: a collaborative telehealth case study," in *Proceedings of the 20th Australasian Conference on Computer-Human Interaction: Designing for Habitus and Habitat*, Cairns, Australia, 2008, pp. 65–72. [cited at p. 77]

[159] C. Sima, R. Raman, R. Reddy, W. Hunt, and S. Reddy, "Vital signs services for secure telemedicine applications," in *Proceedings of the AMIA Annual Symposium*, Orlando, Florida, USA, 1998, pp. 361–365. [cited at p. 77]

[160] J. C. Wyatt and S. M. Wyatt, "When and how to evaluate health information systems," *International Journal of Medical Informatics*, vol. 69, pp. 251–259, 2003. [cited at p. 78]

[161] C. M. DesRoches, E. G. Campbell, S. R. Rao, K. Donelan, T. G. Ferris, A. Jha, R. Kaushal, D. E. Levy, S. Rosenbaum, A. E. Shields, and D. Blumenthal, "Electronic health records in ambulatory care. a national survey of physicians," *The New England Journal of Medicine*, vol. 359, pp. 50–60, 2008. [cited at p. 78]

[162] J. C. Perry, J. A. Ruiz-Ruano, and T. Keller1, "Telerehabilitation: toward a cost-efficient platform for post-stroke neurorehabilitation," in *2011 IEEE International Conference on Rehabilitation Robotics*. [cited at p. 78]

[163] D. Pani, G. Barabino, A. Dessi, I. Tradori, M. Piga, A. Mathieu, and L. Raffo, "A device for local or remote monitoring of hand rehabilitation sessions for rheumatic patients," *IEEE Journal of Translational Engineering in Health and Medicine*, vol. 2, 2014. [cited at p. 79]

[164] Z. Albus, *PCB-Based Capacitive Touch Sensing With MSP430*, Texas Instruments Inc., Oct. 2007, SLAA363A Application report. [cited at p. 82]

[165] "Advanced Industrial Systems, Inc." [Online]. Available: http://www.advindsys.com/ApNotes/YSI400SeriesProbesRvsT.htm [cited at p. 82]

[166] I. Steinhart and S. Hart, "Calibration curves for thermistors," *Deep Sea Research*, vol. 15, no. 3, pp. 497–503, 1968. [cited at p. 84]

[167] D. Pani, G. Barabino, A. Dessi, M. Piga, I. Tradori, A. Mathieu, and L. Raffo, *An Integrated Portable Device for the Hand Functional Assessment in the Clinical Practice*. Springer Link, 2013, vol. 357, pp. 97–110. [cited at p. 86]

[168] D. Pani, G. Barabino, A. Dessì, M. Piga, A. Mathieu, and L. Raffo, "An optimized infrastructure for deferred telemonitoring of home rehabilitation in chronic rheumatic patients," in *Proc. 5th International Conference on eHealth, Telemedicine, and Social Medicine, eTELEMED*, 2013, pp. 301–306. [cited at p. 90]

[169] D. Pani, G. Barabino, A. Dessi, and L. Raffo, "A collaborative approach to the telerehabilitation of patients with hand impairments," in *2013 International Conference on Collaboration Technologies and Systems (CTS)*, San Diego, CA, USA, 2013, pp. 481–486. [cited at p. 92]

[170] D. Pani, G. Barabino, A. Dessi, S. Uras, and L. Raffo, "The challenge of collaborative telerehabilitation: conception and evaluation of a telehealth system enhancement for home-therapy follow-up," *Concurrency and Computation: Practice and Experience*, 2014. [cited at p. 92]

[171] R. Dreiser, E. Maheu, G. Guillou, H. Caspard, and J. Grouin, "Validation of an algofunctional index for osteoarthritis of the hand," *Rev Rheum Engl*, vol. 62, no. 6 suppl 1, pp. 43S–53S, Jun. 1995. [cited at p. 93]

[172] J. Poole and V. Steen, "The use of the health assessment questionnaire to determine physical disability in systemic sclerosis," *Arthritis Care Res*, no. 4, pp. 27–31, 1991. [cited at p. 93]

[173] J. Poole, "Grasp pattern variations seen in the scleroderma hand," *Am J Occup Ther*, no. 48, pp. 46–54, 1994. [cited at p. 94]

[174] E. Badley, S. Wagstaff, and P. Wood, "of functional ability (disability) in arthritis in relation to impairment of range of joint movement," *Ann Rheum Dis*, no. 43, pp. 563–569, 1984. [cited at p. 94]

[175] "Das(28): an instrument to measure the disease activity in people with rheumatoid arthritis," http://www.das-score.nl/das28/en/. [Online]. Available: http://www.das-score.nl/das28/en/ [cited at p. 95]

[176] G. Sandqvist and M. Eklund, "Hand mobility in scleroderma (hamis) test: the reliability of a novel hand function test," *Arthritis Care and Research*, vol. 13, no. 6, pp. 369–374, 2000. [cited at p. 97]

[177] M. Piga, I. Tradori, D. Pani, G. Barabino, A. Dessi, L. Raffo, and A. Mathieu, "Telemedicine applied to kinesiotherapy for hand dysfunction in patients with systemic sclerosis and rheumatoid arthritis: Recovery of movement and telemonitoring technology," *The Journal of Rheumatology*, vol. 41, no. 7, pp. 1324–1333, 2014. [cited at p. 97]

[178] L. Demers, R. Weiss-Lambrou, and B. Ska, "The quebec user evaluation of satisfaction with assistive technology (QUEST 2.0): An overview and recent progress," *Technology and Disability*, vol. 14, pp. 101–105, 2002. [cited at p. 102]

[179] R. Wessels, L. de Witte, R. Andrich, M. Ferrario, J. Persson, and B. Oberg, "Ippa, a user centred approach to assess effectiveness of assistive technology provision," *Technology and Disability*, vol. 14, no. 3, pp. 141–145, 2002. [cited at p. 103]

[180] J. Jutai and H. Day, "Psychosocial impact of assistive devices scale (piads)," *Technology and Disability*, vol. 14, no. 3, pp. 107–111, 2002. [cited at p. 103]

[181] J. Brooke, "Sus: a "quick and dirty" usability scale," in *P. W. Jordan, B. Thomas, B. A. Weerdmeester, and A. L. McClelland. Usability Evaluation in Industry*. Taylor and Francis, 1996. [cited at p. 105]

List of Published Publications Related to the Thesis

Journal papers

- Alessia Dessì, Danilo Pani, Luigi Raffo, *An advanced algorithm for fetal heart rate estimation from non-invasive low electrode density recordings*, Physiological Measurement Vol. 35 Num. 8, doi:10.1088/0967-3334/35/8/1621, 28 July 2014
- Danilo Pani, Gianluca Barabino, Alessia Dessì, Selene Uras, Luigi Raffo, *The challenge of collaborative telerehabilitation: conception and evaluation of a telehealth system enhancement for home-therapy follow-up*, Concurrency and Computation: practice and experience, 27 Nov 2014
- Danilo Pani, Gianluca Barabino, Alessia Dessì, Iosto Tradori, Matteo Piga, Luigi Raffo, Alessandro Mathieu, *A Device for Local or Remote Monitoring of Hand Rehabilitation Sessions for Rheu-matic Patients*, IEEE Journal of Translational Engineering in Health and Medicine, 9 Jan 2014
- Matteo Piga, Iosto Tradori, Danilo Pani, Gianluca Barabino, Alessia Dessì, Luigi Raffo, Alessandro Mathieu, *Telemedicine Applied to Kinesiotherapy for Hand Dysfunction in Patients with Systemic Sclerosis and Rheumatoid Arthritis: Recovery of Movement and Telemonitoring Technology*, The Journal of rheumatology, 1 June 2014

Book chapters

- Danilo Pani, Gianluca Barabino, Alessia Dessì, Matteo Piga, Iosto Tradori, Alessandro Mathieu, Luigi Raffo, *An Integrated Portable Device for the Hand Functional Assessment in the Clinical Practice*, Biomedical Engineering Systems and Technologies, Springer Berlin Heidelberg, 1 Jan 2013
- Sylvain Cremoux, Jaime Ibanez Pereda, Serdar Ates, Alessia Dessì: *Neuromodulation on Cerebral Activities*, Emerging Therapies in Neurorehabilitation, Springer Berlin Heidelberg, 1 Jan 2013

Patents

- Danilo Pani, Gianluca Barabino, Alessia Dessì, Alessandro Mathieu, Luigi Raffo, *Apparatus, a system and a relating method for local or remote rehabilitation and functional evaluation of the hands*, US20130143718 A1, 30 Jan 2013

Conference papers

- Alessia Dessì, Danilo Pani, Luigi Raffo, *Identification of fetal QRS complexes in low density non-invasive biopotential recordings*, Computing in Cardiology Conference (CinC) 2013, 22 Sept 2013
- Gianluca Barabino, Danilo Pani, Alessia Dessì, Luigi Raffo, *A configurable biopotentials acquisition module suitable for fetal electrocardiography studies*, MeMeA 2015 IEEE International Symposium on Medical Measurements and Application, May 07-09, 2015 *Accepted*
- Danilo Pani, Alessia Dessì, Barbara Cabras, Luigi Raffo, *A real-time algorithm for tracking of foetal ECG sources obtained by block-on-line BSS techniques*, Computing in Cardiology Conference (CinC) 2012, 9 Sept 2012
- Danilo Pani, Gianluca Barabino, Alessia Dessì, Matteo Piga, Alessandro Mathieu ,Luigi Raffo, *An Optimized Infrastructure for Deferred Telemonitoring of Home Rehabilitation in Chronic Rheumatic Patients*, eTELEMED 2013, The Fifth International Conference on eHealth, Telemedicine, and Social Medicine, 24 Febb 2013
- Danilo Pani, Gianluca Barabino, Alessia Dessì, Luigi Raffo, *A collaborative approach to the telerehabilitation of patients with hand impairments*, International Conference on Collaboration Technologies and Systems (CTS) / IEEE, 20 May 2013
- Danilo Pani, Gianluca Barabino, Alessia Dessì, Alessandro Mathieu, Luigi Raffo, *A Portable Real-Time Monitoring System for Kinesitherapic Hand Rehabilitation Exercises*, BIOSTEC 2012, 5th International Joint Conference on Biomedical Engineering Systems and Technologies, 2012, pp. 82-89

Submitted papers

- Danilo Pani, Alessia Dessì, Jose F. Saenz-Cogollo, Gianluca Barabino, Beatrice Fraboni, Annalisa Bonfiglio, *Fully textile, PEDOT:PSS based electrodes for wearable ECG monitoring systems*, IEEE Transactions on Biomedical Engineering, *Under review*